

*IN VITRO* MUTAGENESIS OF  
*ESCHERICHIA COLI* CITRATE SYNTHASE

by

Deborah Helen Anderson

A Thesis

Submitted to

The Faculty of Graduate Studies

In Partial Fulfilment of

The Requirement for the Degree of

Doctor of Philosophy

Department of Chemistry

August, 1988.

Permission has been granted to the National Library of Canada to microfilm this thesis and to lend or sell copies of the film.

The author (copyright owner) has reserved other publication rights, and neither the thesis nor extensive extracts from it may be printed or otherwise reproduced without his/her written permission.

L'autorisation a été accordée à la Bibliothèque nationale du Canada de microfilmer cette thèse et de prêter ou de vendre des exemplaires du film.

L'auteur (titulaire du droit d'auteur) se réserve les autres droits de publication; ni la thèse ni de longs extraits de celle-ci ne doivent être imprimés ou autrement reproduits sans son autorisation écrite.

ISBN 0-315-47943-4

IN VITRO MUTAGENESIS OF  
ESCHERICHIA COLI CITRATE SYNTHASE

BY

DEBORAH HELEN ANDERSON

A thesis submitted to the Faculty of Graduate Studies of  
the University of Manitoba in partial fulfillment of the requirements  
of the degree of

DOCTOR OF PHILOSOPHY

© 1988

Permission has been granted to the LIBRARY OF THE UNIVER-  
SITY OF MANITOBA to lend or sell copies of this thesis, to  
the NATIONAL LIBRARY OF CANADA to microfilm this  
thesis and to lend or sell copies of the film, and UNIVERSITY  
MICROFILMS to publish an abstract of this thesis.

The author reserves other publication rights, and neither the  
thesis nor extensive extracts from it may be printed or other-  
wise reproduced without the author's written permission.

To my Husband, Kim Mysyk, for his patience and constant support.

And to my Parents, Don and Pat Anderson,  
for their high expectations and unending encouragement.

## ACKNOWLEDGEMENTS

I wish to express my gratitude to my Supervisor, Dr. Harry W. Duckworth, for his guidance and encouragement throughout the project, and for his critical reading of this Thesis.

Thanks also, to the other members of my advisory committee: Dr. J. C. Jamieson, Dr. P. C. Loewen, and Dr. J. G. Dodd.

Special appreciation to Dr. L. J. Donald for introducing me to recombinant DNA methodology.

Thanks are also extended to the University of Manitoba and the Natural Science and Engineering Research Council of Canada for financial support.

## TABLE OF CONTENTS

	Page
ACKNOWLEDGEMENTS . . . . .	i
TABLE OF CONTENTS . . . . .	ii
LIST OF FIGURES . . . . .	v
LIST OF TABLES . . . . .	x
ABBREVIATIONS . . . . .	xiii
ABSTRACT . . . . .	xv
INTRODUCTION	
Citrate Synthase	
The Central Role of Citrate Synthase	
in Cellular Metabolism . . . . .	1
Classes of Citrate Synthases . . . . .	6
Citrate Synthase Reaction Mechanism . . . . .	14
Alignment and Comparison of Citrate	
Synthase Sequences . . . . .	18
Evidence for the Same Basic Subunit	
for all Citrate Synthases . . . . .	26
A Structural Model for the Subunit of	
<i>E. coli</i> Citrate Synthase . . . . .	28
The History of Mutagenesis . . . . .	32
MATERIALS AND METHODS	
Bacterial Strains and Plasmids . . . . .	48
Construction of Mutants by <i>in vitro</i> Techniques .	
Oligonucleotide-Directed Methods . . . . .	51
Screening for Mutants . . . . .	54

## Table of Contents Continued...

	Page
Routine Procedures	
DNA Sequencing . . . . .	56
DNA Isolation and Purification . . . . .	56
Large Scale Protein Production and Purification . . . . .	58
Enzyme Assays . . . . .	59
Collection and Analysis of Kinetic Data . . . . .	61
Binding Measurements by ANS Displacement . . . . .	64
NADH Binding . . . . .	65
Physical Studies . . . . .	65
Media . . . . .	65
Reagents . . . . .	66
 RESULTS	
Active Site Mutants	
CS $\Delta$ (264-287) . . . . .	68
CS226 <sup>H<math>\rightarrow</math>Q</sup> and CS229 <sup>H<math>\rightarrow</math>Q</sup> . . . . .	79
CS305 <sup>H<math>\rightarrow</math>A</sup> and CS314 <sup>R<math>\rightarrow</math>L</sup> . . . . .	90
Attempts to Locate the NADH Binding Site	
CS188 <sup>R<math>\rightarrow</math>L</sup> , CS217 <sup>R<math>\rightarrow</math>L</sup> , CS221 <sup>R<math>\rightarrow</math>L</sup> and CS217 <sup>R<math>\rightarrow</math>L</sup> /221 <sup>R<math>\rightarrow</math>L</sup> . . . . .	97
Mutants which Affect the Allosteric Equilibrium of <i>E. coli</i> Citrate Synthase	
CS260 <sup>W<math>\rightarrow</math>A</sup> . . . . .	104
CS319 <sup>R<math>\rightarrow</math>L</sup> . . . . .	116

## Table of Contents Continued...

	Page
DISCUSSION	
Active Site Mutants	
CS $\Delta$ (264-287) . . . . .	125
CS226 <sup>H<math>\rightarrow</math>Q</sup> and CS229 <sup>H<math>\rightarrow</math>Q</sup> . . . . .	128
CS305 <sup>H<math>\rightarrow</math>A</sup> and CS314 <sup>R<math>\rightarrow</math>L</sup> . . . . .	132
Attempts to Locate the NADH Binding Site	
CS188 <sup>R<math>\rightarrow</math>L</sup> , CS217 <sup>R<math>\rightarrow</math>L</sup> , CS221 <sup>R<math>\rightarrow</math>L</sup>	
and CS217 <sup>R<math>\rightarrow</math>L</sup> /221 <sup>R<math>\rightarrow</math>L</sup> . . . . .	140
Mutants which Affect the Allosteric Equilibrium	
of <i>E. coli</i> Citrate Synthase	
CS260 <sup>W<math>\rightarrow</math>A</sup> . . . . .	148
CS319 <sup>R<math>\rightarrow</math>L</sup> . . . . .	153
Conclusions . . . . .	159
BIBLIOGRAPHY . . . . .	161

## LIST OF FIGURES

	Page
Figure 1. The Tricarboxylic Acid (TCA) cycle. . . . .	2
Figure 2. The Glyoxylate cycle. . . . .	3
Figure 3. The non-cyclic Tricarboxylic Acid pathway .	4
Figure 4. The allosteric nature of <i>E. coli</i> citrate synthase. . . . .	8
Figure 5. Fluorescence enhancement of NADH in the presence of <i>E. coli</i> citrate synthase. . . . .	10
Figure 6. The structures of various adenylic acid derivatives . . . . .	11
Figure 7. Citrate synthase reaction mechanism. (Shown for the pig heart enzyme). . . . .	15
Figure 8. Amino acid sequence alignment of the seven known citrate synthase sequences: pig heart, two yeast isozymes, <i>E. coli</i> , <i>A. anitratum</i> , <i>P. aeruginosa</i> and <i>R. prowazekii</i> . . . . .	20
Figure 9. Stereo drawings of the active site of pig heart citrate synthase. . . . .	23
Figure 10. Schematic diagram of the interactions between citrate and <i>E. coli</i> citrate synthase. . . . .	24
Figure 11. Model of one subunit of <i>E. coli</i> citrate synthase, showing the location of the active site, and the degree of sequence homology between the pig heart and <i>E. coli</i> enzymes .	29

## List of Figures Continued...

	Page
Figure 12. Basic oligonucleotide-directed <i>in vitro</i> mutagenesis method. . . . .	37
Figure 13. Hybridization method for mutant screening .	40
Figure 14. The "Winter" coupled priming technique, used for cyclic selection mutagenesis . . .	44
Figure 15. The "Eckstein" method of oligonucleotide-directed mutagenesis. . . . .	46
Figure 16. Making of pESgltA from pHSgltA. . . . .	50
Figure 17. Making p $\Delta$ FXgltA, which expresses mutant protein CSA(264-287). . . . .	52
Figure 18. Scheme for re-sequencing the M13cl15 coding strand after mutagenesis . . . . .	57
Figure 19. Reaction of DTNB with a sulfhydryl group . .	60
Figure 20. Kinetic constants for the citrate synthase reaction . . . . .	62
Figure 21. SDS-polyacrylamide gel and Ouchterlony double-diffusion plate of: wild type citrate synthase, CSA(264-287) and CS226 <sup>H</sup> →Q . . . .	69
Figure 22. Model of an <i>E. coli</i> citrate synthase subunit, showing location of the 24 amino acids deleted in CSA(264-287) . . . . .	72
Figure 23. Circular dichroism spectra of wild type citrate synthase and CSA(264-287) . . . . .	73
Figure 24. pH-dependence of NADH Binding for wild type citrate synthase and CSA(264-287). . .	75

	Page
List of Figures Continued...	
Figure 25. Effect of AcCoA and KCl on NADH binding for wild type citrate synthase and CSA(264-287) . . . . .	76
Figure 26. Displacement of ANS from ANS-citrate synthase complexes by various ligands, for wild type citrate synthase and CSA(264-287) . . . . .	77
Figure 27. Model of an <i>E. coli</i> citrate synthase subunit, showing the location of His-226, His-229, His-305, and Arg-314, residues involved in mutagenesis experiments . . . . .	80
Figure 28. Double reciprocal plots of reaction velocities as a function of the two substrates, oxaloacetate and acetyl-CoA, for wild type citrate synthase, CS226 <sup>H→Q</sup> and CS229 <sup>H→Q</sup> . . . . .	81
Figure 29. $\alpha$ -Ketoglutarate inhibition, measured as a competitive inhibitor of oxaloacetate, for wild type citrate synthase, CS226 <sup>H→Q</sup> and CS229 <sup>H→Q</sup> . . . . .	87
Figure 30. Model of an <i>E. coli</i> citrate synthase subunit, showing the location of Cys-206, Arg-188, Arg-217, and Arg-221 . . . . .	98
Figure 31. Sequence alignment of the seven known citrate synthase sequences in the region of Trp-260.	104

## List of Figures Continued...

	Page
Figure 32. Model of an <i>E. coli</i> citrate synthase subunit, showing the location of Trp-260 and Arg-319.	105
Figure 33. NADH saturation curves for crude and purified preparations of wild type citrate synthase and CS260 <sup>W→A</sup> . . . . .	106
Figure 34. Urea denaturation curves for wild type citrate synthase, and the two forms of CS260 <sup>W→A</sup> . . . . .	112
Figure 35. Effect of oxaloacetate concentration on the NADH saturation curves of wild type citrate synthase and CS319 <sup>R→L</sup> . . . . .	118
Figure 36. KCl saturation for wild type citrate synthase and CS319 <sup>R→L</sup> . . . . .	121
Figure 37. Apparent shift in the allosteric equilibrium of CS319 <sup>R→L</sup> . . . . .	122
Figure 38. Active site of <i>E. coli</i> citrate synthase, showing how oxaloacetate is bound (A), and how $\alpha$ -ketoglutarate is proposed to bind (B) . . . . .	137
Figure 39. Region of <i>E. coli</i> citrate synthase model near Cys-206, showing the location of various residues which may be important in NADH binding. . . . .	141

## List of Figures Continued...

	Page
Figure 40. Comparison of the sequence alignment of a portion of several nucleotide binding enzymes with that of <i>E. coli</i> citrate synthase in the region of Cys-206. . . . .	145
Figure 41. Stereodiagram of the model of <i>E. coli</i> citrate synthase, showing the projection of Trp-260 into the dimeric contact surface. . . . .	149
Figure 42. Close-up view of the interaction between Arg-319 and Glu-343 in the <i>E. coli</i> citrate synthase model . . . . .	158

## LIST OF TABLES

	Page
Table 1. List of residues involved in binding citrate and CoA in pig heart citrate synthase, and their homologous residues in the <i>E. coli</i> enzyme . . . . .	22
Table 2. Oligonucleotide sequences, and the location at which they prime to the <i>gltA</i> insert . . . .	49
Table 3. Oligonucleotide-directed <i>in vitro</i> mutagenesis methods and results. . . . .	55
Table 4. Steady-state kinetic data for wild type citrate synthase, CS226 <sup>H→Q</sup> and CS229 <sup>H→Q</sup> . . . .	84
Table 5. NADH binding data for wild type citrate synthase, CS226 <sup>H→Q</sup> and CS229 <sup>H→Q</sup> . . . . .	85
Table 6. ANS displacement data for wild type citrate synthase, CS226 <sup>H→Q</sup> and CS229 <sup>H→Q</sup> . . . . .	88
Table 7. Steady-state kinetic data for wild type citrate synthase, CS305 <sup>H→A</sup> and CS314 <sup>R→L</sup> . . . .	92
Table 8. NADH binding data for wild type citrate synthase, CS305 <sup>H→A</sup> and CS314 <sup>R→L</sup> . . . . .	94
Table 9. ANS displacement data for wild type citrate synthase, CS305 <sup>H→A</sup> and CS314 <sup>R→L</sup> . . . . .	96
Table 10. Steady-state kinetic data for wild type citrate synthase, CS188 <sup>R→L</sup> , CS217 <sup>R→L</sup> , CS221 <sup>R→L</sup> and CS217 <sup>R→L</sup> /221 <sup>R→L</sup> . . . . .	100

## List of Tables Continued

	Page
Table 11. NADH binding data for wild type citrate synthase, CS188 <sup>R→L</sup> , CS217 <sup>R→L</sup> , CS221 <sup>R→L</sup> and CS217 <sup>R→L</sup> /221 <sup>R→L</sup> . . . . .	101
Table 12. ANS displacement data for wild type citrate synthase, CS188 <sup>R→L</sup> , CS217 <sup>R→L</sup> , CS221 <sup>R→L</sup> and CS217 <sup>R→L</sup> /221 <sup>R→L</sup> . . . . .	102
Table 13. Addition of crude extract to purified CS260 <sup>W→A</sup> (I) restores normal NADH sensitivity.	107
Table 14. Steady-state kinetic data for wild type citrate synthase, CS260 <sup>W→A</sup> (I) and CS260 <sup>W→A</sup> (S)	109
Table 15. NADH binding data for wild type citrate synthase, CS260 <sup>W→A</sup> (I) and CS260 <sup>W→A</sup> (S). . . . .	111
Table 16. ANS displacement data for wild type citrate synthase, CS260 <sup>W→A</sup> (I) and CS260 <sup>W→A</sup> (S). . . . .	114
Table 17. Steady-state kinetic data, in the presence and absence of 0.1M KCl, for wild type citrate synthase and CS260 <sup>W→A</sup> (I) . . . . .	115
Table 18. NADH binding data for wild type citrate synthase and CS319 <sup>R→L</sup> . . . . .	117
Table 19. Steady-state kinetic data for wild type citrate synthase and CS319 <sup>R→L</sup> . . . . .	119
Table 20. ANS displacement data for wild type citrate synthase and CS319 <sup>R→L</sup> . . . . .	124

## List of Tables Continued

	Page
Table 21. Association and dissociation constants for oxaloacetate binding to wild type citrate synthase and mutant forms CS226 <sup>H→Q</sup> and CS229 <sup>H→Q</sup> . . . . .	130
Table 22. Kinetic parameters for wild type citrate synthase and two active site mutants, CS305 <sup>H→A</sup> and CS314 <sup>R→L</sup> . . . . .	134
Table 23. Homology between amino acid residues potentially involved in NADH binding, near Cys-206 of <i>E. coli</i> citrate synthase and the six other sequences of citrate synthase. . .	143
Table 24. Kinetic parameters for wild type citrate synthase and CS319 <sup>R→L</sup> . . . . .	154

## ABBREVIATIONS

AcCoA	Acetyl coenzyme A
<i>A. anitratum</i>	<i>Acinetobactor anitratum</i>
AMP(3'-)	Adenosine 3'-monophosphate
AMP(5'-), ADP ATP	Adenosine 5'-mono-, di-, and triphosphate, respectively
ANS	8-anilino-1-naphthalenesulfonate
CC-DNA	Covalently closed DNA
CoA(-SH)	Coenzyme A
dATP, A	Adenosine 5'-triphosphate
dCTP, C	Cytidine 5'-triphosphate
DEAE	diethylaminoethyl
dGTP, G	Guanidine 5'-triphosphate
DNA	Deoxyribonucleic acid
DTNB	5,5'-dithiobis-(2-nitrobenzoic acid)
dTTP, T	Thymidine 5'-triphosphate
dUMP	Uridine 5'-monophosphate
dUTP, U	Uridine 5'-triphosphate
<i>E. coli</i>	<i>Escherichia coli</i>
EDTA	Ethylenediaminetetraacetate
KCl	potassium chloride
$\alpha$ -KG	$\alpha$ -ketoglutarate
Klenow polymerase	DNA polymerase I, Klenow fragment
NAD <sup>+</sup> , NADH	Nicotinamide adenine dinucleotide in its oxidized and reduced forms, respectively
NADP <sup>+</sup> , NADPH	Nicotinamide adenine dinucleotide phosphate in its oxidized and reduced forms, respectively

NMR	nuclear magnetic resonance
OAA	oxaloacetate
<i>P. aeruginosa</i>	<i>Pseudomonas aeruginosa</i>
RF	replicative form
RNA	ribonucleic acid
<i>R. prowazekii</i>	<i>Rickettsia prowazekii</i>
SDS	Sodium dodecyl sulfate
TCA	Tricarboxylic Acid
TNB	3-carboxy-4-nitrothiophenolate anion
Tris	Tris(hydroxymethyl)aminomethane
U	Units

**ABSTRACT**

## ABSTRACT

*Escherichia coli* citrate synthase is an allosteric enzyme, a three-dimensional model of which has been constructed based on the known X-ray structure of pig heart citrate synthase and the sequence homology between the two enzymes. The pig heart active site residues are conserved in the *E. coli* sequence, and their roles in substrate binding and/or catalysis have been postulated. They are believed to play similar roles in the *E. coli* enzyme. A mutant was prepared in which 24 amino acid residues had been deleted near the acetyl-CoA binding site, including a catalytic residue His-264. This deletion mutant was inactive and unable to bind acetyl-CoA at the active site. It was however, still able to bind NADH, as well as acetyl-CoA, at the allosteric site.

In the remaining experiments, oligonucleotide-directed *in vitro* mutagenesis was used to mutate individual amino acid residues, at the level of the DNA. Mutation to glutamine of His-226, but particularly His-229, predicted to be involved in oxaloacetate binding, resulted in mutant enzymes which not only showed reduced affinity for that substrate, but also for the substrate analogue  $\alpha$ -ketoglutarate, thus proving the competitive nature of  $\alpha$ -ketoglutarate inhibition. Removal of the positive charges from the side chains of His-305 and Arg-314, residues predicted to be involved in the polarization of the carbonyl group of oxaloacetate, gave rise to mutant enzymes with extremely low turnover numbers, confirming their importance in catalysis.

Several arginine residues (Arg-188, Arg-217, Arg-221, and both Arg-217 and Arg-221) were mutated to leucine in an attempt to locate a specific interaction between the enzyme and the allosteric inhibitor NADH; however, none of these mutations had any effect on NADH inhibition or the ability of the enzyme to bind that nucleotide.

Trp-260 (a residue homologous between bacterial citrate synthases) was changed to alanine (the corresponding residue found in eukaryotic sequences), with widespread effects on the enzyme—affecting both its ability to bind the substrates, and the ability of NADH to inhibit the enzyme activity.

In the final mutant, Arg-319 was mutated to leucine, which resulted in a shift in the allosteric equilibrium of the enzyme towards R, the active state, with the corresponding increase in substrate affinities and reduction in KCl activation properties.

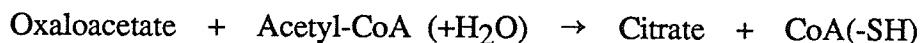
Not only do these experiments confirm the predicted roles of active site residues homologous to those in the pig heart enzyme, but they strongly support the idea that the basic subunits of the non-allosteric (pig heart) and allosteric (*E. coli*) citrate synthases are very similar.

## INTRODUCTION

## Citrate Synthase

### The Central Role of Citrate Synthase in Cellular Metabolism:

Citrate synthase is the first enzyme in the Tricarboxylic Acid (TCA) Cycle and catalyzes the following condensation reaction:



It facilitates the entry of carbon, in the form of acetyl units, into the cycle (Figure 1), and is the only enzyme within that cycle to catalyze the formation of a carbon to carbon bond. Because intermediates do not accumulate (Krebs & Lowenstein, 1960), the citrate synthase reaction may well be the rate limiting step of the TCA cycle, so that its control is likely to make a significant contribution to the overall regulation of the cycle.

The TCA cycle has a two-fold metabolic function. The first is to oxidize metabolites and generate NADH, which can be used either as a source of reducing power in biosynthesis, or for the production of ATP, through oxidative phosphorylation (Figure 1). The second role of the cycle is to supply precursors, in the form of various intermediates in the cycle, which are required for the biosynthesis of sugars, fatty acids and amino acids. In most plants and microorganisms, a modified form of the TCA cycle, the glyoxylate cycle, allows these organisms to utilize acetate or fatty acids as the sole source of carbon (Figure 2). The glyoxylate cycle produces succinate, from two molecules of acetyl-CoA, which is then used for the biosynthesis of new sugar molecules. Both the TCA cycle and the glyoxylate cycle may operate simultaneously, providing the cells' energy and biosynthetic needs, respectively.

During the anaerobic growth possible in some organisms, the enzyme  $\alpha$ -ketoglutarate dehydrogenase is absent; so that the TCA cycle becomes a branched, non-cyclic pathway (Amarasingham & Davis, 1965) (Figure 3). The reductive arm of this pathway is independent of the enzyme citrate synthase and leads to the production of succinyl-CoA, used in the biosynthesis of heme groups and some amino acids. The

## The Tricarboxylic Acid (TCA) Cycle:

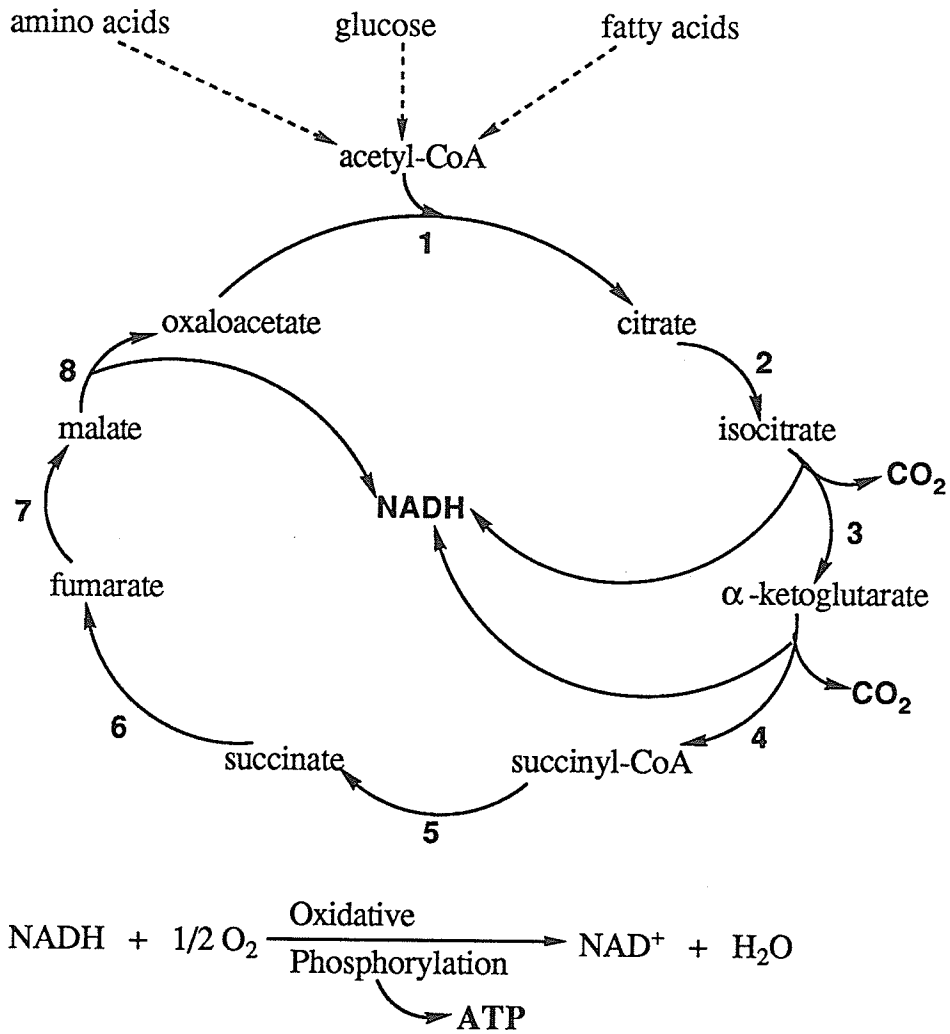


Figure 1. The Tricarboxylic Acid (TCA) Cycle. The enzymes in the TCA cycle are indicated by numbers, and are as follows:

1. Citrate Synthase
2. Aconitase
3. Isocitrate Dehydrogenase
4.  $\alpha$ -Ketoglutarate Dehydrogenase
5. Succinyl-CoA Synthetase
6. Succinate Dehydrogenase
7. Fumarase
8. Malate Dehydrogenase

## The Glyoxylate Cycle:

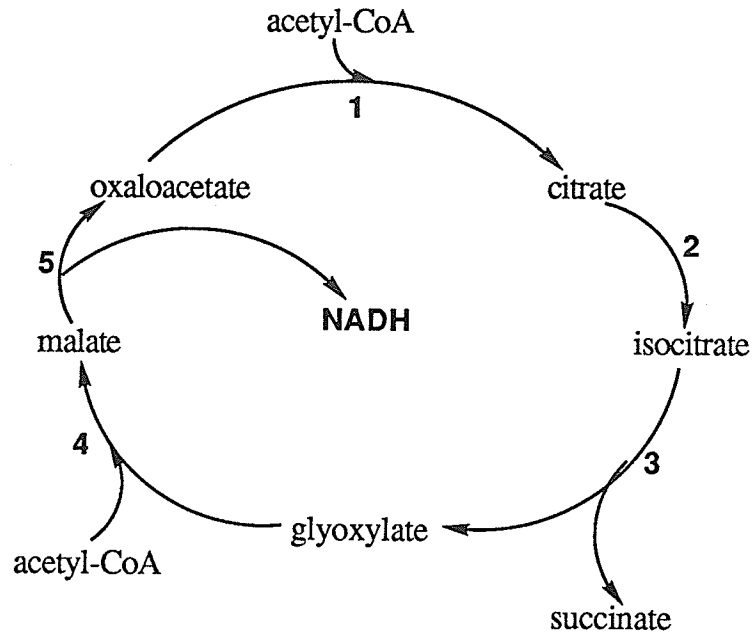


Figure 2. The Glyoxylate Cycle. The enzymes in the cycle are indicated by numbers, and are as follows:

1. Citrate Synthase
2. Aconitase
3. Isocitrate Lyase
4. Malate Synthase
5. Malate Dehydrogenase

## The Non-cyclic Tricarboxylic Acid Pathway:

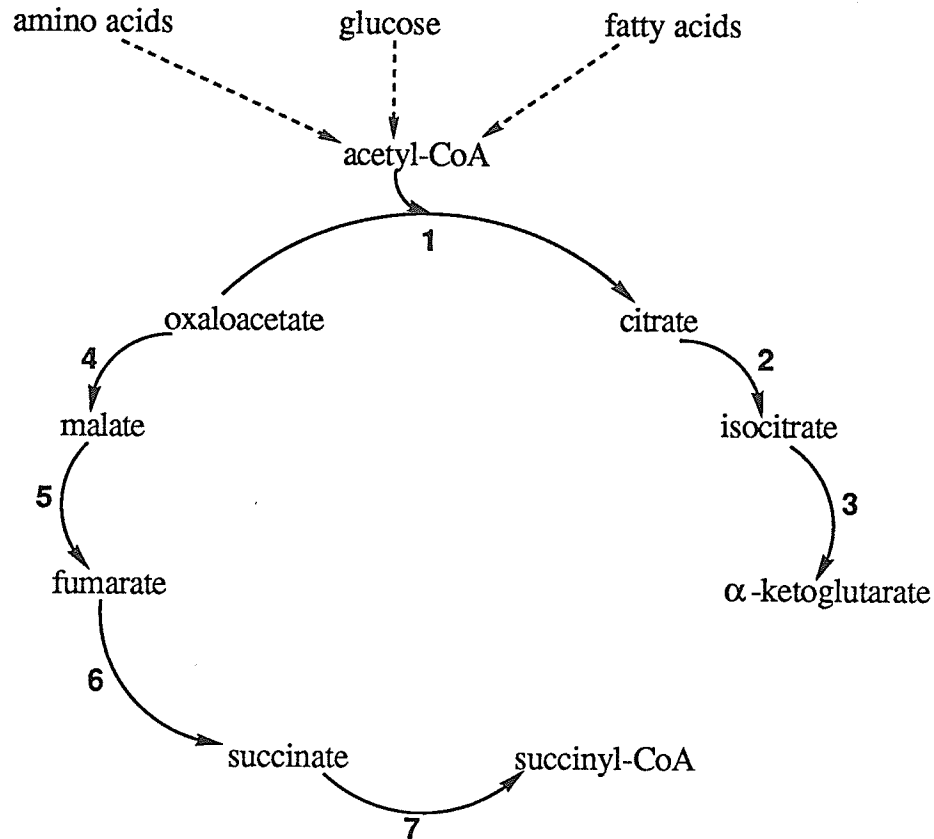


Figure 3. The Non-cyclic Tricarboxylic Acid pathway in facultative anaerobic bacteria, like *Escherichia coli*. The enzymes in the pathway are indicated by numbers, and are as follows:

1. Citrate Synthase
2. Aconitase
3. Isocitrate Dehydrogenase
4. Malate Dehydrogenase
5. Fumarase
6. Fumarate Reductase
7. Succinyl-CoA Synthetase

oxidative arm of the non-cyclic TCA pathway is simply the first three steps of the TCA cycle, including that catalyzed by citrate synthase, and results in the formation of  $\alpha$ -ketoglutarate, an important precursor in the biosynthesis of amino acids.  $\alpha$ -Ketoglutarate is enzymatically converted to glutamate by the direct incorporation of ammonia molecules; and glutamate, in turn, provides the cell with a source of  $\alpha$ -amino groups, for the biosynthesis of various amino acids. In *E. coli*, this non-cyclic TCA pathway operates under aerobic, as well as anaerobic, conditions (Amarasingham & Davis, 1965). Thus, citrate synthase is a key enzyme in the production of NADH, ATP, and in some cases,  $\alpha$ -ketoglutarate.

### Classes of Citrate Synthases:

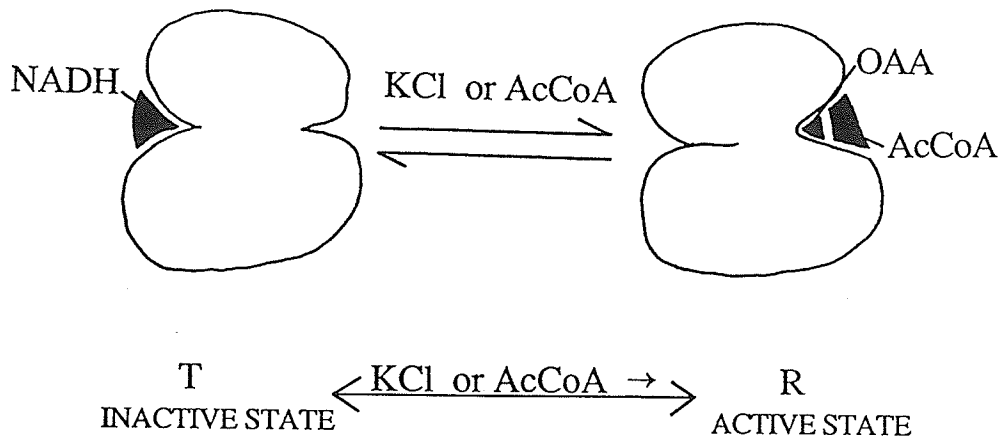
All citrate synthases which have been carefully examined are composed of a single type of polypeptide chain of about 430 amino acids, corresponding to a molecular weight of about 48,000 g/mole (Weitzman & Danson, 1976; Bloxham *et al.*, 1981, 1982; Suissa *et al.*, 1984; Rosenkrantz *et al.*, 1986; Tong & Duckworth, 1975; Ner *et al.*, 1983; Donald & Duckworth, 1987). Weitzman & Danson (1976) were the first to divide citrate synthases into two classes. The enzymes of eukaryotic and Gram-positive bacteria form one class of citrate synthases, and are composed of "small" non-allosteric dimers, of molecular weight about 100,000 g/mole. This class of enzymes is not inhibited by NADH, or  $\alpha$ -ketoglutarate, but is inhibited by ATP, which is competitive with the substrate, acetyl-CoA. This inhibition has been suggested as a plausible feedback mechanism, whereby ATP, the ultimate product of the TCA cycle, controls the activity of the first enzyme of that pathway (Weitzman & Danson, 1976). Pig heart citrate synthase, the best studied eukaryotic example, with a subunit molecular weight of 48,969 g/mole (Bloxham *et al.*, 1981, 1982), has been the subject of a very thorough X-ray crystallographic analysis (Remington *et al.*, 1982; Wiegand & Remington, 1986), so that its three-dimensional structure is well defined. A variety of other eukaryotic and Gram-positive citrate synthases have been partially characterized (e.g. Higa & Cazzulo, 1976; Porter & Wright, 1977; Koeller & Kindl, 1977; Juan *et al.*, 1977; Harmey & Neupert, 1979; and Alam *et al.*, 1982) and all seem to fit into the "small", non-allosteric class of enzymes.

The other class of citrate synthases are those of Gram-negative bacteria, like *E. coli*, which are "large" enzymes, of molecular weight about 280,000 g/mole, in which hexamers are prominent at pH 7.8 and 0.1M KCl (Tong & Duckworth, 1975). These "large" citrate synthases are not very sensitive to inhibition by ATP, but are subject to strong and specific allosteric inhibition by NADH (Weitzman, 1966; Weitzman & Danson, 1976). Since NADH can be considered a product of the TCA cycle, the role of

ATP, as a feedback inhibitor of citrate synthase, might be transferred to NADH in this class of enzymes. *E. coli* citrate synthase is the best studied example in this class. The gene encoding this enzyme, *gltA*, has been cloned (Guest, 1981) into the *Hind*III and *Sal*I restriction endonuclease sites of the plasmid vector, pBR322, yielding an ampicillin-resistant recombinant plasmid, pHS*gltA* (Duckworth & Bell, 1982). In the *E. coli* host cell line HB101, pHS*gltA* produces citrate synthase as about 8% of its total cellular protein, 14 times more citrate synthase than the cell would contain without the plasmid. Thus, the cloning of the *gltA* gene into pBR322 has provided a biological system for obtaining large quantities of *E. coli* citrate synthase, which are homogeneous upon purification and show normal allosteric properties.

The entire *E. coli gltA* gene has been sequenced (Ner *et al.*, 1983) and its inferred protein sequence matches that of the portions of the *E. coli* citrate synthase protein which have been sequenced (Bhayana & Duckworth, 1984). The protein is synthesized with 427 amino acid residues, but after the amino-terminal methionine is removed, the 426 amino acid subunit of citrate synthase has a molecular weight of 47,930 g/mole.

Since *E. coli* citrate synthase is an allosteric enzyme, it can exist in two conformational states. In terms of the Monod, Wyman and Changeux model (1965), the R, or active state of the enzyme binds substrates (like acetyl-CoA and oxaloacetate) and activators (like KCl), but not allosteric inhibitors (like NADH) (Figure 4); while the T, or inactive state does not bind substrates or activators, but has a high affinity for allosteric inhibitors. These two conformational states are presumed to be in equilibrium ( $T \leftrightarrow R$ ) and the resting state of the enzyme (conformation in the absence of ligands) can be deduced by the shape of its ligand saturation curves. *E. coli* citrate synthase shows hyperbolic saturation by NADH and, in the absence of KCl, sigmoid saturation by acetyl-CoA. In the presence of KCl (0.1M), acetyl-CoA saturation becomes hyperbolic. Therefore, in the absence of ligands, *E. coli* citrate synthase is in T state,



-does not bind substrates  
at active site  
-binds allosteric inhibitor,  
NADH

-binds substrates at active site  
-does not bind allosteric  
inhibitor, NADH

Figure 4. The allosteric nature of *E. coli* citrate synthase. The resting state of the enzyme (i.e. in the absence of ligands) is T state.

and the effect of KCl (0.1M) on the acetyl-CoA saturation curve indicates that KCl activates the enzyme by converting it from T to R state (Morse & Duckworth, 1980).

NADH fluorescence is enhanced by binding to *E. coli* citrate synthase, shifting the peak of emission of the coenzyme from 457 to 428nm. Thus, when measured at 428nm, the fluorescence of NADH bound to the enzyme is about 15-fold that for free NADH in solution (Figure 5). This fluorescence enhancement property may be used to measure the binding of NADH to the enzyme, alone or in the presence of various ligands (Duckworth & Tong, 1976; Talgoy & Duckworth, 1979).  $\text{NAD}^+$  and  $\text{NADP}^+$  are weak competitive inhibitors of NADH binding at pH 7.8, with  $K_i$  values greater than 1mM, but stronger inhibition is shown by 5'-AMP and 3'-AMP, with  $K_i$  values of  $83 \pm 5$  and  $65 \pm 4$   $\mu\text{M}$ , respectively (see Figure 6 for structures). Acetyl-CoA, one of the substrates, and KCl, an activator, also inhibit the binding in a weakly cooperative manner. This has been interpreted in terms of two types of binding sites for nucleotides on citrate synthase; an active site which binds acetyl-CoA, the substrate, and its competitive inhibitor, 3'-AMP; and an allosteric site which is found in both the T and R states (Talgoy & Duckworth, 1979), and can bind a number of adenylates at the same site ( $K_D = 40$  to  $200$   $\mu\text{M}$ ), but which has its characteristically high affinity for NADH ( $K_D = 1.6\mu\text{M}$ ), only in the T state. Active and allosteric sites cannot, therefore, be occupied at the same time by acetyl-CoA and NADH respectively, and the binding of one induces a specific conformational change which destroys the binding site of the other (Figure 4). In the absence of ligands, *E. coli* citrate synthase is in T state, so the effect of KCl may be to promote acetyl-CoA binding and enzyme activity by bringing the enzyme into R state, simultaneously abolishing NADH binding. NADH inhibits the enzyme presumably because it prevents this conformational change. The nucleotide, 5'-AMP, also inhibits the binding of NADH. Its similarity in structure to one-half of the NADH molecule (Figure 6) suggests that it might occupy part of the allosteric site. If this is the case, then it must be the dihydronicotinamide ring of the NADH that is

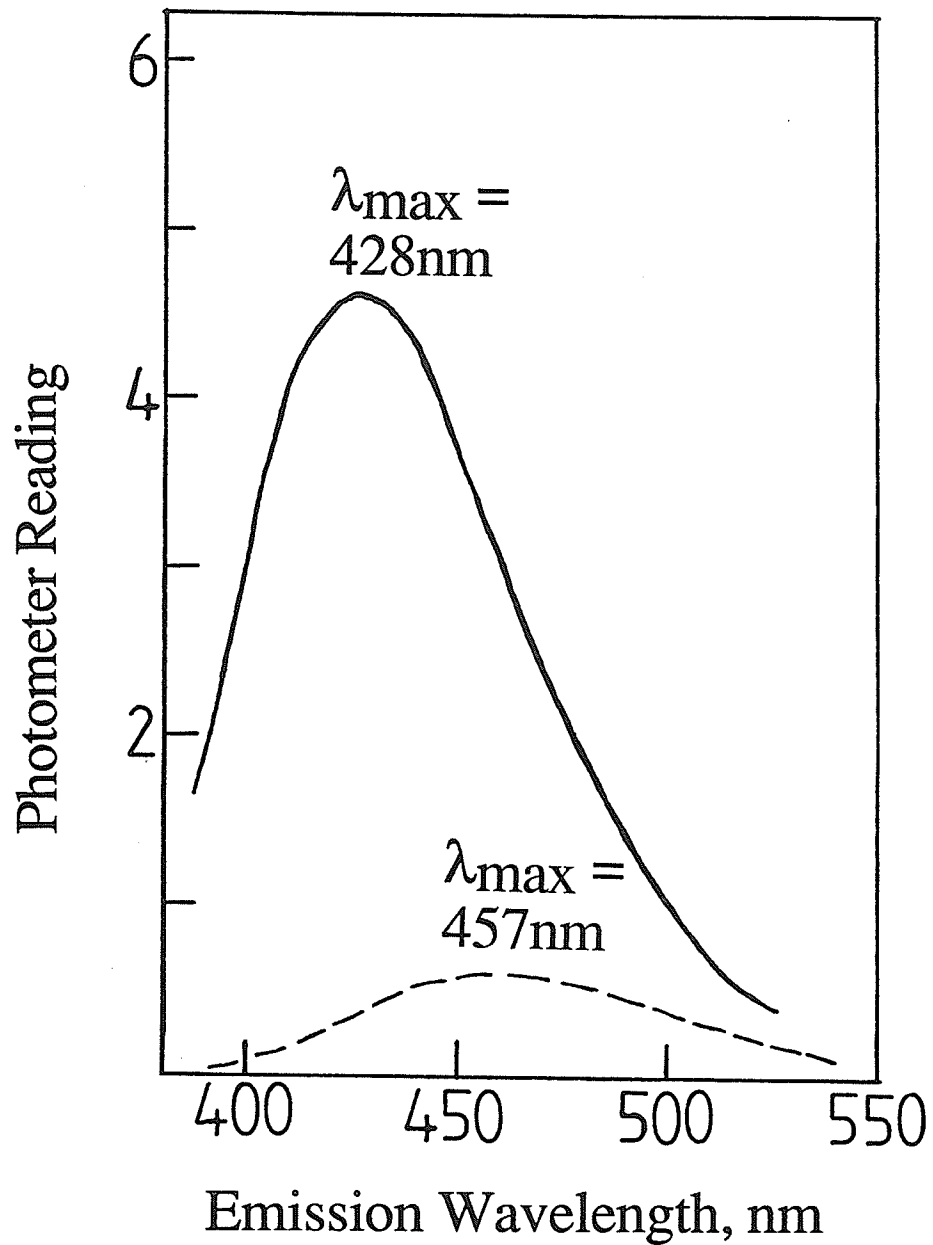


Figure 5. The effect of *E. coli* citrate synthase on the fluorescence emission of NADH. The broken line is for free NADH, 1.94 μM, in 0.015M sodium phosphate (pH 6.6), with excitation at 340nm. The solid line is for 1.94 μM NADH in the same buffer, plus 20 μM citrate synthase (subunit concentration), again with excitation at 340nm. (Taken from Duckworth & Tong, 1976.)

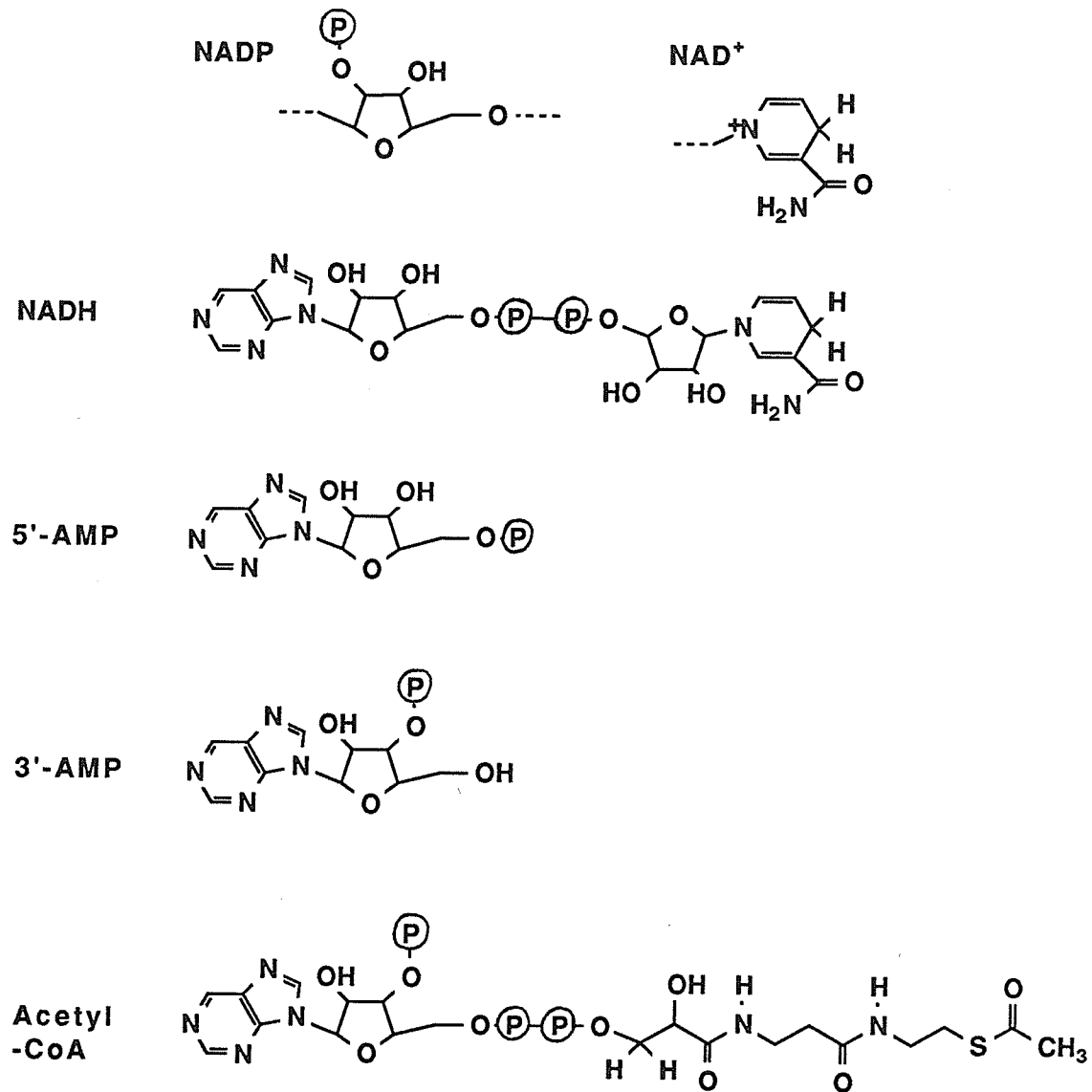


Figure 6. Structures of various adenylic acid derivatives.

involved in any allosteric conformational change, since 5'-AMP does not inhibit enzyme activity.

The inhibition of NADH binding by acetyl-CoA, a substrate, was originally explained using an allosteric mechanism. This explanation was however called into question by the later finding that both NADH and acetyl-CoA, besides various non-inhibitory adenylates, will protect a cysteine (Cys-206) of citrate synthase from reaction with 5,5'-dithiobis-(2-nitrobenzoic acid) (DTNB) (Talgoy *et al.*, 1979). Except for this effect by acetyl-CoA, all the evidence indicates that this cysteine is in or near the NADH binding site. Since acetyl-CoA itself is an adenylate, with a similar structure to that of NADH (Figure 6), the possibility exists that this substrate also binds at the allosteric site, where it would act not as an inhibitor, but perhaps as an allosteric activator. This effect, rather than the classical homotropic interaction among active sites, could also explain the sigmoid saturation curve observed at low salt concentrations (Faloona & Srere, 1969). Oxaloacetate, the second substrate, and  $\alpha$ -ketoglutarate, an inhibitor whose mode of action is uncertain, have no effect on NADH binding to citrate synthase at pH 7.8.

The allosteric properties of the Gram-negative citrate synthases have brought them under close examination, and have led to a further division of this class into two subclasses. The NADH inhibition observed for the citrate synthases of aerobic bacteria can be relieved by (5'-)AMP, but that of facultative anaerobic bacteria shows no such reactivation. Weitzman and Jones (1968) suggested a rationale for such a division based on the metabolic pathways of energy generation available to these two groups of bacteria. Strict aerobes, like *Acinetobacter anitratum* and *Pseudomonas aeruginosa*, are absolutely dependent on the TCA cycle for energy production; consequently, elevated AMP concentrations are an indication of low energy and the requirement for enhanced cycle activity within the cell. Facultative anaerobes, like *E. coli*, can generate energy by fermentation, so that they are not strictly dependent on the TCA cycle for energy

production, and this may be why their citrate synthase enzymes have no biological need to exhibit AMP reactivation. Under anaerobic conditions, the TCA cycle becomes a branched, non-cyclic pathway, as discussed previously, and simply leads to the production of succinyl-CoA and  $\alpha$ -ketoglutarate, used for biosynthesis. It is interesting to note that the citrate synthases of these anaerobically growing organisms are sensitive to inhibition by  $\alpha$ -ketoglutarate, demonstrating yet another example of a feedback control mechanism (Weitzman & Dunmore, 1969). Since this inhibition may be abolished by treatments with high pH and/or high salt concentration, which do not eliminate activity, it has been suggested that this  $\alpha$ -ketoglutarate inhibition, like that of NADH, is allosteric (Wright *et al.*, 1967; Wright & Sanwal, 1971). It is far from certain, however, that  $\alpha$ -ketoglutarate ( $\text{HOOC-CH}_2\text{-CH}_2\text{-CO-COOH}$ ) binds to a separate allosteric site and since it is very similar in structure to oxaloacetate ( $\text{HOOC-CH}_2\text{-CO-COOH}$ ), a substrate of citrate synthase, it is reasonable to expect that it would show some affinity for the oxaloacetate binding site. Since  $\alpha$ -ketoglutarate does not inhibit citrate synthase in the presence of 0.1M KCl, and does not strengthen NADH binding when KCl or acetyl-CoA are present, it seems unlikely that it could be stabilizing the T state, as NADH does. In fact,  $\alpha$ -ketoglutarate has been found to inhibit oxaloacetate binding to the enzyme-CoA complex, perhaps competitively, but at the same levels it will not inhibit binding of oxaloacetate to the enzyme itself if KCl is present (Talgoy & Duckworth, 1979). It may be that  $\alpha$ -ketoglutarate can bind to the oxaloacetate (active) sites, but that this site becomes more selective for oxaloacetate in the presence of KCl.

### Citrate Synthase Reaction Mechanism:

The structures of three crystal forms of pig heart citrate synthase have been determined using X-ray crystallography: an "open" form (crystallized in the absence of ligands), a "nearly closed" form (crystallized with bound citrate and coenzyme A), and a "fully closed" form (crystallized with bound oxaloacetate and the substrate analogue, S-acetyl-CoA) (Remington *et al.*, 1982; Wiegand & Remington, 1986). This three-dimensional information locates the active site at the interface of the large and small folding domains of a single subunit of the enzyme, with each domain making contributions to the active site. Each active site is formed primarily from the amino acid residues from a single subunit, with a few residues contributed by the second subunit of the dimer. X-ray data show that oxaloacetate and citrate are both deeply bound, at the heart of the active site. Their orientation indicates that pig heart citrate synthase follows an Ordered reaction mechanism, in which oxaloacetate binds to the enzyme first, followed by acetyl-CoA. Kinetic evidence also supports an Ordered mechanism, in which oxaloacetate binds first (Johansson & Pettersson, 1974). In the case of *E. coli* citrate synthase, oxaloacetate improves the binding of the acetyl-CoA analogue, coenzyme A (Talgy & Duckworth, 1979), and citrate, the product, is a competitive inhibitor with respect to oxaloacetate (Wright & Sanwal, 1971). Both of these facts indicate that with this enzyme, also, oxaloacetate binds first under catalytic conditions. Therefore, all kinetic data within this thesis have been interpreted in terms of the Ordered Bisubstrate mechanism and the equation which it predicts (Cleland, 1963). (See Methods section for more details.)

The reaction mechanism for citrate synthase is shown in Figure 7, where the numbering refers to amino acid side chains from the pig heart enzyme. Oxaloacetate is shown as plain text, while acetyl-CoA is shadowed, so that the contributions of each substrate can easily be followed through the reaction mechanism. His-274 abstracts a proton from the methyl group of acetyl-CoA, and in a concerted reaction His-320

## Citrate Synthase Reaction Mechanism:

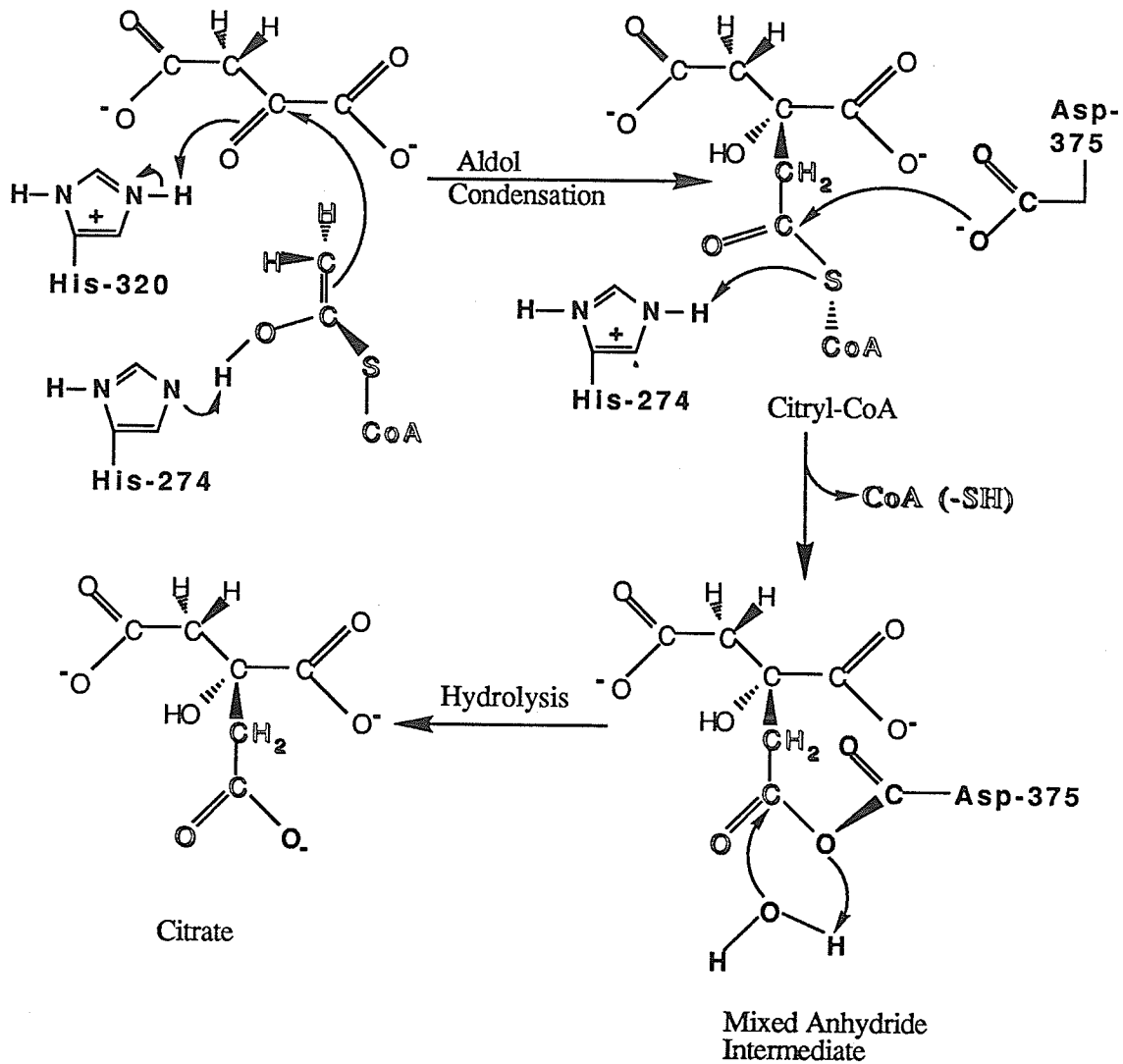
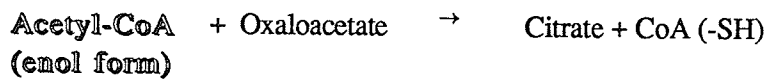


Figure 7. Citrate synthase reaction mechanism. The portions of citrate derived from oxaloacetate are shown as plain text, while those from acetyl-CoA are shadowed (numbering is shown for the pig heart enzyme). *E. coli* citrate synthase has residues equivalent to His-320, His-274 and Asp-375 of pig heart: His-305, His-264 and Asp-362, respectively. The details of the reaction mechanism are discussed in the text.

protonates the carbonyl of oxaloacetate. Acetyl-CoA attacks the si-face of the carbonyl group in an aldol condensation, forming a thioester, citryl-CoA. Asp-375 then attacks the thioester carbonyl group, displacing CoA, and forming a mixed anhydride intermediate, which upon hydrolysis yields citrate. Note that the presence of several bound water molecules in the immediate vicinity of the thioester bond, seen in the X-ray work, indicates that the final step of the hydrolysis could occur without the necessity of opening the active site to the solvent continuum. Note also that equivalent residues His-264, His-305 and Asp-362 are present in the *E. coli* sequence.

Wiegand and Remington (1986) proposed this model for catalytic activity based on the three conformational states observed crystallographically for the pig heart enzyme. The two closed forms obtained represent the ligase and hydrolase activities, which both require a highly specific three-dimensional environment isolated from solvent; and are the catalytically competent forms. The third conformational state is the open, or product-release form, which allows substrate entry, as well as product release. In this scheme, oxaloacetate binds to the enzyme, inducing the "nearly closed" conformation observed in one crystal form (that with bound oxaloacetate and the analogue, S-acetyl-CoA). This form strongly polarizes and orients oxaloacetate and provides a binding site for acetyl-CoA with a narrow channel leading to oxaloacetate. As acetyl-CoA enters, a proton is abstracted from the methyl group and condensation occurs in a concerted reaction that results in the inversion of the configuration of the hydrogens of the methyl group. The appearance of citryl-CoA on the enzyme induces the hydrolytic, fully "closed" form of the enzyme, observed in the crystals containing citrate and CoA. The hydrolysis reaction occurs via aspartate and bound water, leaving the enzyme free to open and release the products, citrate and CoA.

Thus, pig heart citrate synthase undergoes a conformational change during the catalytic mechanism. This conformational change involves small shifts and rotations of helices within the small and large folding domains of the enzyme, and at their interface.

These small shifts and rotations alter the packing of various amino acid side chains, and cumulatively give rise to larger movements of up to 15Å for more distant regions (Lesk & Chothia, 1984), and about an 18° rotation of the two domains relative to each other (Remington *et al.*, 1982; Wiegand & Remington, 1986). By adopting different conformations for each distinct step in catalysis, the enzyme maintains a high degree of control over the progress of the reaction, so that hydrolysis cannot occur until after the formation of the citryl-CoA intermediate.

### Alignment and Comparison of Citrate Synthase Sequences:

The amino acid sequences of three eukaryotic and three prokaryotic citrate synthases have now been determined. The enzyme from pig heart (Bloxham *et al.*, 1981, 1982) is especially important because, as mentioned previously, it was the subject of a very thorough X-ray crystallographic investigation by Robert Huber and co-workers (Remington *et al.*, 1982; Wiegand & Remington, 1986). The amino acid sequences of other eukaryotic citrate synthases, two yeast isozymes, were inferred from the DNA sequences of cDNA clones (Suissa *et al.*, 1984; Rosenkrantz *et al.*, 1986). These three citrate synthases are all inhibited by ATP, but do not show significant inhibition by  $\alpha$ -ketoglutarate, or NADH. As described previously, the gene for *E. coli* citrate synthase has been cloned and sequenced. It is about 28% homologous in amino acid sequence with the pig heart enzyme, showing identities for most of the active site residues (Bhayana & Duckworth, 1984) identified by Huber and colleagues, as will be discussed in detail later. More recently, the sequence of two other Gram-negative citrate synthase genes have also been determined, those of *Acinetobacter anitratum* (Donald & Duckworth, 1986, 1987) and *Pseudomonas aeruginosa* (L. J. Donald, unpublished work). Like the *E. coli* enzyme, these are allosterically inhibited by NADH, although they require about one hundred times more NADH to achieve the same inhibitory effect. These three Gram-negative bacteria show about 70% amino acid sequence homology between them.

The *Rickettsia prowazekii* citrate synthase gene has also been cloned and sequenced, and its protein sequence inferred (Wood *et al.*, 1987). *R. prowazekii* is an obligate intracellular parasitic bacterium, which multiplies within the cytoplasm of its eukaryotic host cell. Despite the fact that its morphology and cell wall are more typical of Gram-negative bacteria, the citrate synthase of this organism shows more functional similarity to the eukaryotic and Gram-positive class of enzyme. It is a "small" enzyme, whose activity is inhibited by ATP, but not by  $\alpha$ -ketoglutarate, or NADH, and yet its

amino acid sequence bears a striking resemblance to those of the Gram-negative bacteria, showing 59% sequence homology with the *E. coli* enzyme, as compared to only 20% homology with the functionally similar pig heart citrate synthase (Figure 7). Elucidation of the structure of this unusual enzyme, and comparison with the *E. coli* and pig heart enzymes, could help to establish the location and extent of changes required to convert one class of citrate synthase to the other (Wood *et al.*, 1987).

An alignment of the amino acid sequences of the seven citrate synthases of known primary structure is shown in Figure 8. The regions involved in  $\alpha$ -helical secondary structure are shown above two of the sequences. For the pig heart enzyme, this is direct three-dimensional information from X-ray data (Remington *et al.*, 1982); while for *E. coli* citrate synthase, the location of the  $\alpha$ -helical structures is speculation, based on model building, which will be discussed later. The three eukaryotic sequences show a very high degree of sequence homology between them, about 60%. Similarly, the three Gram-negative bacterial enzymes are approximately 70% identical in amino acid sequence to each other, and about 30% homologous to the eukaryotic sequences.

Regions of homology are scattered throughout the sequences and include most of the active site residues, as determined from the X-ray analysis of the pig heart citrate synthase data (Remington *et al.*, 1982; Wiegand & Remington, 1986). These active site residues are listed in Table 1, with the equivalent residues found in *E. coli* citrate synthase. Figure 9A is a diagram of the active site of the pig heart enzyme, from Wiegand and Remington (1986), showing the proximity of several active site residues to the product citrate. Upon comparison (Table 1), it is clear that equivalent residues are conserved in the *E. coli* enzyme. A schematic representation of those residues which form hydrogen bonds with citrate is shown in Figure 10. The strong homology exhibited in these active site residues, in all seven enzyme sequences, reflects the fact that these enzymes catalyze the same reaction and probably have similar tertiary structures in the region of the active site. Residues 314 to 320 in the pig heart sequence





Table 1. Active Site Residues in Pig Heart Citrate Synthase and the Equivalent Residues in the *E. coli* Enzyme.

<u>Residues Involved in Citrate Binding:</u>		<u>Residues Involved in CoA Binding:</u>	
Pig Heart <sup>a</sup> Citrate Synthase	<i>E. coli</i> Citrate Synthase	Pig Heart <sup>a</sup> Citrate Synthase	<i>E. coli</i> Citrate Synthase
• His-238	His-229	Arg-46	Thr-47
• His-274 <sup>b</sup>	His-264	Δ Arg-324	Lys-309
• His-320 <sup>b,e</sup>	His-305	§ Arg-164' <sup>c</sup>	Arg-157
• Arg-329	Arg-314	Val-314 <sup>e</sup>	Arg-299
• Arg-401	Arg-387	Δ Val-315 <sup>e</sup>	Leu-300
<sup>f</sup> Arg-421' <sup>c</sup>	Arg-407	Pro-316 <sup>e</sup>	Met-301
• Phe-397 <sup>d</sup>	Phe-383	• Gly-317 <sup>e</sup>	Gly-302
• Asp-375 <sup>b</sup>	Asp-362	Δ Tyr-318 <sup>e</sup>	Phe-303
		• Gly-319 <sup>e</sup>	Gly-304

<sup>a</sup> Residues identified by Wiegand and Remington (1986).

<sup>b</sup> Residues involved in catalysis.

<sup>c</sup> The ' indicates that these residues are provided for the active site by the second subunit.

<sup>d</sup> Forms an unusual edge-on interaction with the citrate molecule.

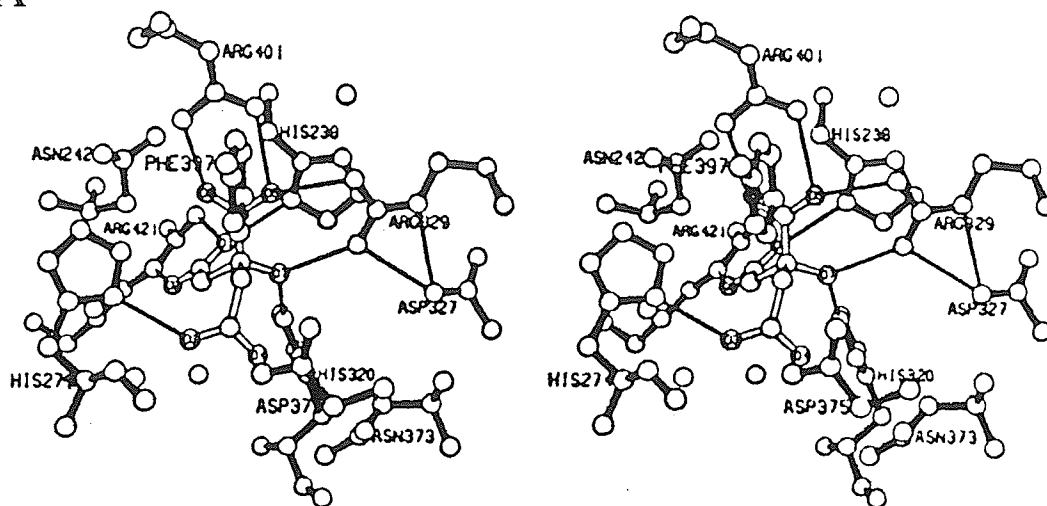
<sup>e</sup> Peptide backbone involved in binding of adenine portion of acetyl-CoA (Wiegand & Remington, 1986).

Homology symbols: • = absolutely conserved in all seven sequences; Δ = conservative replacements, as defined in Figure 12 (sequence alignment).

<sup>f</sup> Identical in 5 out of the 7 citrate synthase sequences; but is proline in the two yeast sequences.

<sup>g</sup> Identical in the pig heart, *E. coli*, *A. anitratum*, *P. aeruginosa*; lysine in the two yeast sequences, but no homologous residue is present in the *R. prowazekii* sequence (the alignment shows a deletion of this residue—see Figure 8).

A



B

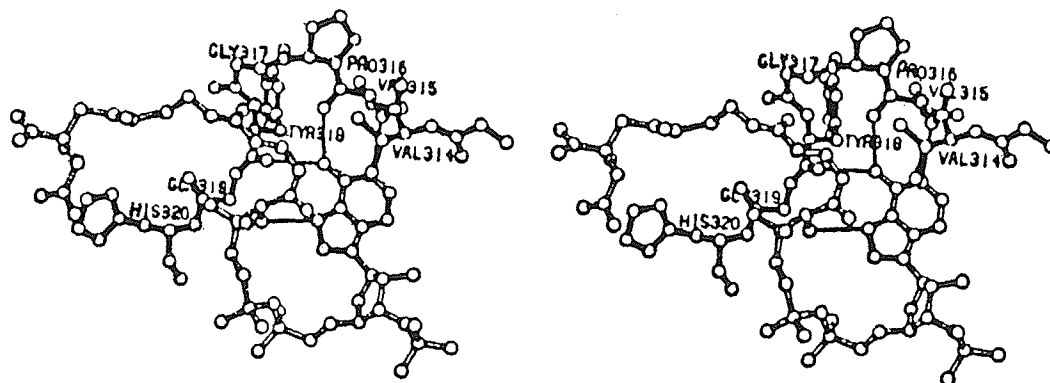


Figure 9. A) Stereo drawing of the citrate binding site in the fully "closed" form of pig heart citrate synthase. The citrate molecule is drawn with open bonds. Thin bonds represent the important hydrogen bonds or salt bridges. Arginine-421 is from the other subunit of the dimer.

B) Stereo drawing of a model-built citryl-CoA based on the crystallographic analysis of bound citrate and coenzyme A, and the adenine recognition loop 314-320. Citryl-CoA is indicated by open bonds while the thin bonds represent some of the important interactions. Note the main-chain hydrogen bonds to the adenine ring. (Both were taken from Wiegand & Remington, 1986.)

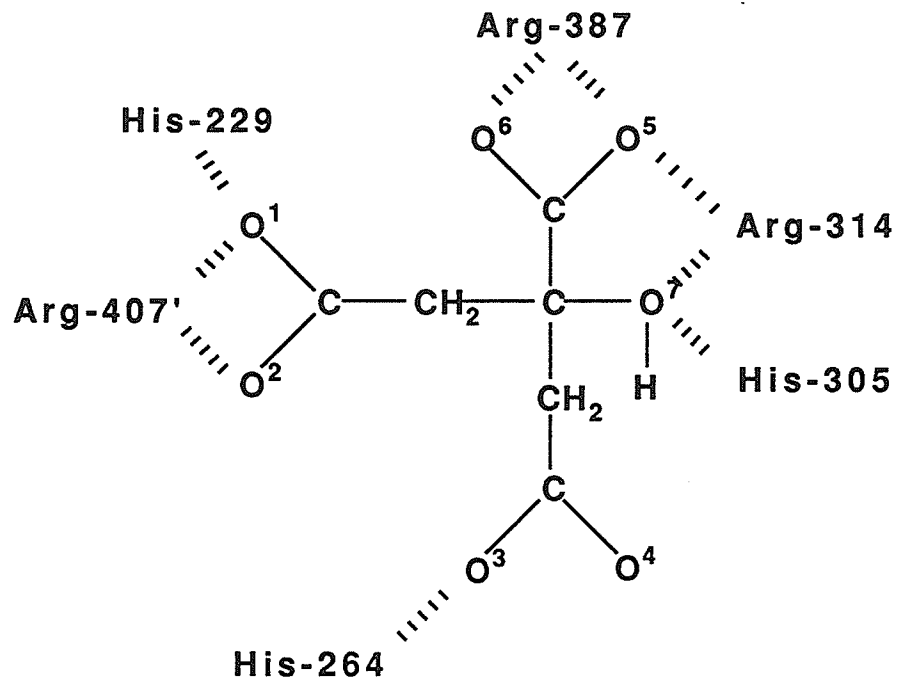


Figure 10. Schematic representation of the interactions between citrate and *E. coli* citrate synthase. The ' after Arg-407 indicates that it is contributed by the second subunit of the dimer.

are wrapped around the adenine ring of CoA and form hydrogen bonds with the peptide backbone rather than the amino acid side chains (Figure 9B), therefore the fact that there are few conserved amino acids in this region is not surprising (Table 1 and Figure 8). Note, however, that two glycine residues are conserved in all seven sequences, indicating their importance in the maintenance of the structure of the adenine recognition loop. In the pig heart enzyme, Arg-46 and Arg-324 form a salt bridge to the 5'-diphosphate group of CoA, while Arg-164 (from the other subunit) interacts with its 3'-phosphate. The other citrate synthase sequences have arginines or lysines in homologous positions to Arg-164 (except *R. prowazekii*) and Arg-324 (Figure 8), but there seems to be no residue equivalent to Arg-46 in any of the four bacterial sequences. It has been suggested that the loss of this ionic interaction in the *E. coli* enzyme explains the fact that this enzyme has a lower affinity for acetyl-CoA when compared to pig heart enzyme (Ner *et al.*, 1983); but the fact that the *R. prowazekii* citrate synthase also lacks this homologous residue, as well as an Arg-164 equivalent, and yet shows the same high affinity as the pig heart enzyme for that substrate (Wood *et al.*, 1987), casts some doubt on this explanation. It is possible that the tertiary structure of these bacterial proteins may bring another positively charged residue into the region of these phosphate groups, but given the lack of three-dimensional information for any of these enzymes, this is simply speculation.

Evidence for the Same Basic Subunit for All Citrate Synthases:

In spite of the obvious differences between the dimeric non-allosteric citrate synthases and their hexameric allosteric counterparts, the individual subunits of these enzymes are believed to be very similar (Morse & Duckworth, 1980; Bell *et al.*, 1983; Duckworth *et al.*, 1987). The sites of proteolytic cleavage have been identified in the *E. coli* enzyme (Bhayana & Duckworth, 1984) and are essentially homologous to the those in the pig heart enzyme (Bloxham *et al.*, 1981, 1982; Lill *et al.*, 1984).

Additional evidence that eukaryotic and Gram-negative citrate synthases have the same basic subunit comes from several studies of citrate synthase mutants. Danson *et al.* (1979) succeeded in reverting an *E. coli* mutant, lacking citrate synthase, to one with a native molecular weight and regulatory properties analogous to those of eukaryotic citrate synthases. They found that both the original, "large" allosteric enzyme, and the new, "small" non-allosteric enzyme were coded for by the same gene.

A wild type marine *Pseudomonas* has been shown to possess two interconvertible forms of citrate synthase: an NADH- and AMP-insensitive, ATP-inhibited form, of molecular weight about 100,000 g/mole, and a second form with molecular weight about 300,000 g/mole, which is strongly activated by AMP and KCl, and inhibited by NADH (Massarini & Cazzulo, 1974, 1975; Higa *et al.*, 1978). Another citrate synthase mutant, this one of *Pseudomonas aeruginosa*, was found to have the unusual property of containing both a "large" and a "small" citrate synthase at the same time (Solomon & Weitzman, 1983). At present, though, it is unclear whether the two citrate synthases in the *Pseudomonas aeruginosa* mutant are interconvertible forms of the same gene product, as in the marine *Pseudomonas*, or if this particular strain of *P. aeruginosa* has two separate citrate synthase genes.

The resemblances between these mutationally generated enzymes and the types of naturally occurring citrate synthases are striking, and raise the possibility that the marked changes in subunit compositions and regulatory behavior may result from only

small genetic alterations of amino acid sequence (Morse & Duckworth, 1980; Weitzman, 1987). Like the oxygen-binding proteins, where myoglobin is a monomeric version of hemoglobin and the allosteric properties of hemoglobin arise from the subunit interactions (Perutz, 1970), the allosteric nature of the hexameric citrate synthases is proposed to result from the additional subunit contacts formed by the bringing together of three enzyme dimers (Duckworth *et al.*, 1987).

The pig heart enzyme has been shown to assume different conformations during the various stages of catalysis, yet it is non-allosteric, since no allosteric inhibitor has been found to stabilize the inactive (product release) form of the enzyme. In view of the high degree of sequence homology between pig heart and *E. coli* citrate synthase around the active site, the *E. coli* enzyme probably shows the same catalytic mechanism. Therefore, the acquisition of allosteric properties by *E. coli* citrate synthase may simply be related to the ability of NADH to stabilize the product release form of this enzyme. The fact that only hexameric enzyme forms show allosteric properties, may in turn reflect the possibility that the NADH sites are formed when three enzyme dimers come together.

### A Structural Model for the Subunit of *E. coli* Citrate Synthase:

In order to make wise choices for mutagenesis experiments, designed to answer specific structure-function questions about a protein, it is essential to have some three-dimensional information. There have been at least three separate attempts to obtain good quality crystals of *E. coli* citrate synthase, suitable for high resolution X-ray crystallographic studies, with no success (Duckworth *et al.*, 1987). The more recent cloning, sequencing, and expression of the citrate synthase genes from *Acinetobacter anitratum* (Donald & Duckworth, 1986, 1987) and *Pseudomonas aeruginosa* (L. J. Donald, unpublished), has led to the prospect that crystals of one or both of these enzymes may have better properties than those of *E. coli*. Since these two enzymes are also allosterically inhibited by NADH, any three-dimensional information that may become available for either enzyme, should provide specific details about the NADH binding site present in all Gram-negative citrate synthases, including *E. coli*.

In the meantime, a working model of the *E. coli* enzyme has been constructed by Ansel Chu, in Gary Brayer's research group at the University of British Columbia, by building the *E. coli* sequence into the pig heart coordinates, available from X-ray crystallography (Remington *et al.*, 1982). This model, of one subunit of *E. coli* citrate synthase, is shown in Figure 11. Most of the protein takes on  $\alpha$ -helical secondary structure, represented in the figure as cylinders. There are twenty  $\alpha$ -helices, labeled from A to T, and one section of anti-parallel  $\beta$ -sheet. Active site residues are indicated as black dots, all conserved in the *E. coli* enzyme. Those contributed from the second subunit are shown as black squares—recall that the active form of pig heart citrate synthase, on which this model is based, is a dimer, where both subunits make contributions to the active site contained primarily on one subunit. Each subunit can be further divided into a small (helices N–R) and a large (helices A–M, S and T) folding domain, both of which contribute residues to the active site. The relative motion of these two domains is thought to accompany catalysis, and the conformational change between

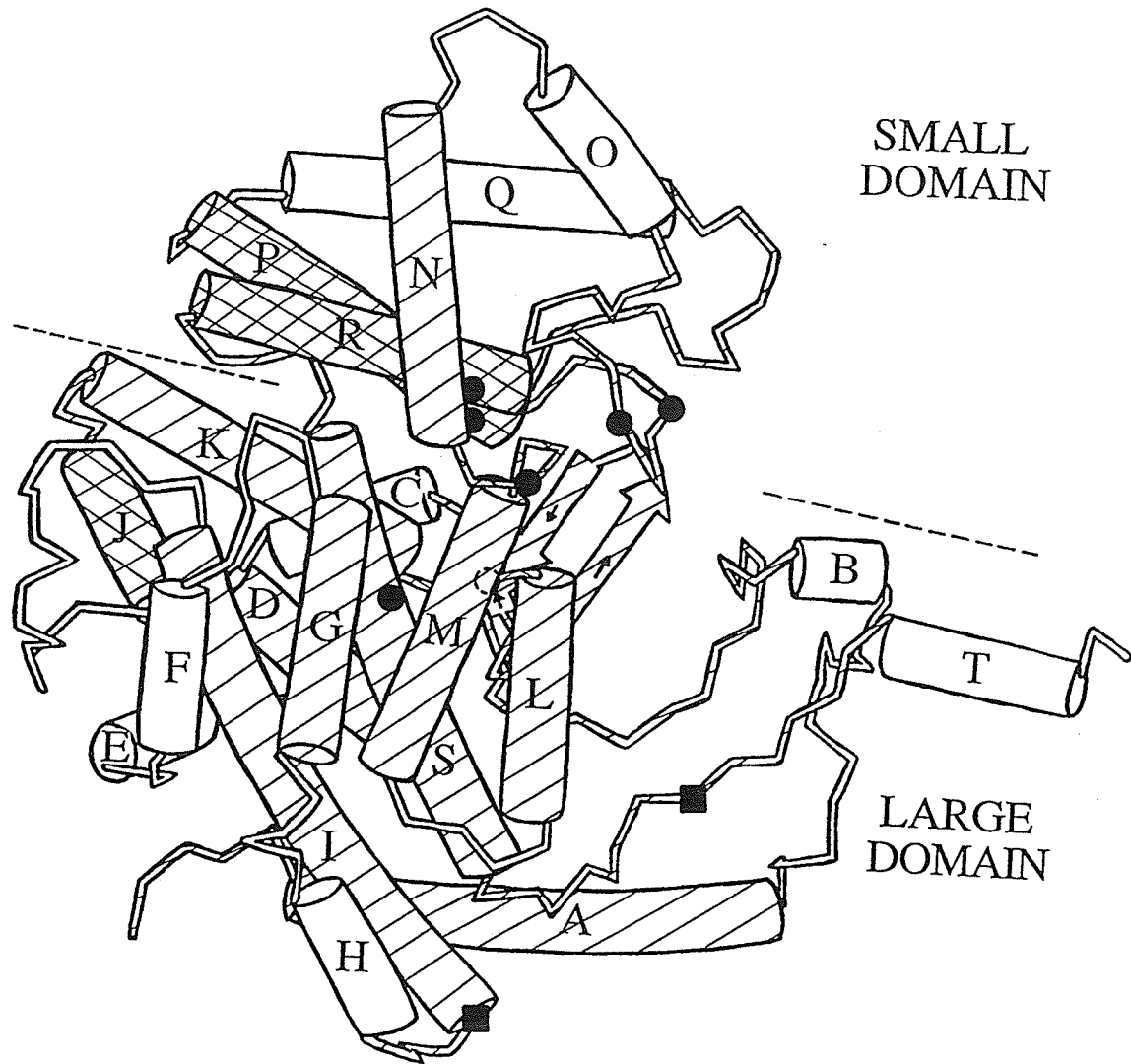


Figure 11. Model of one subunit of *E. coli* citrate synthase. There are 20  $\alpha$ -helices, labeled A through T, indicated by cylinders, and one section of anti-parallel  $\beta$ -sheet, shown as wide arrows. Active site residues are shown as filled in circles, except His-229, which is concealed in the diagram behind the M helix, on the section of random coil between the K and L helices, and is shown as a dashed circle. Those residues contributed to the active site by the other subunit in the dimer are shown as filled in squares. The subunit can be divided into a small and large folding domain, each of which contributes residues to the active site. The shading indicates the degree of sequence homology between the pig heart and *E. coli* enzymes, where doubly shaded regions have greater than 50% homology, singly shaded regions have between 25 and 50% homology, and unshaded regions have less than 25% homology.

the inactive and active states, as discussed previously (Remington *et al.*, 1982; Wiegand & Remington, 1986; Lesk & Chothia, 1984). The shading (Figure 11) indicates the degree of sequence homology between the pig heart and *E. coli* enzymes. Doubly shaded regions have greater than 50% homology and are highly conserved regions, which include the active site. Singly shaded regions have between 25 and 50% homology and show moderate similarities. These include the I and S helices, which form the core of the monomer, as well as the G, M and L helices, three out of the four helices (helix F is the fourth) involved in making up the dimeric contact surface, across the front of the model. The unshaded regions have less than 25% homology and could be involved in the features unique to the *E. coli* enzyme—the additional subunit contacts required to form the hexameric structure, and the binding of the allosteric inhibitor, NADH—since these properties are not present in the pig heart enzyme.

Using the model for *E. coli* citrate synthase as a guide, together with the alignment of the various citrate synthase amino acid sequences, experiments can be chosen to establish what structural features account for its active and allosteric properties, namely:

- i) What parts of the subunit provide the new subunit interactions needed to maintain the hexameric structure found in the *E. coli* enzyme?
- ii) Where does the NADH bind to the enzyme, and how does it cause inhibition?
- iii) Where does  $\alpha$ -ketoglutarate bind to the enzyme, and how does it inhibit? (Recall that  $\alpha$ -ketoglutarate is an inhibitor whose mode of action is unclear. Suggestions have been made that it is allosteric, like NADH (Wright *et al.*, 1967); however, its obvious structural similarity to the substrate, oxaloacetate, would lead one to speculate a competitive mechanism of inhibition.)
- iv) To fine-tune predictions (as determined for the pig heart enzyme from X-ray information) about the functions and relative importance of various active site residues which are conserved in the *E. coli* enzyme.

Mutagenesis experiments, discussed in this thesis, will be concerned with points ii), iii) and iv).

## The History of Mutagenesis

The idea of using mutations to find out more about the structural features important for specific functions of an enzyme is not new. Naturally occurring mutations have provided valuable information about amino acid residues which are absolutely essential to the normal functioning of an enzyme; but spontaneous mutation rates are very low, of the order of  $10^{-6}$  to  $10^{-7}$  per gene per generation (Tamarin, 1982). The actual number of spontaneous mutations occurring in a population of cells is substantially higher than this, but most of the mutations are detrimental to the cell, and result in retarded growth or cell death. These lethal mutations remain undetected in a sample population, significantly reducing the apparent spontaneous mutation rate. To a lesser extent, these low rates can also be attributed to the redundancy of the genetic code. Although all amino acids are specified by a triplet codon, many only require the first two bases to be precisely defined; while the third can be any of the four possible bases. Some amino acids are coded for by semi-specific codons, where the third base is required to be a pyrimidine, or in other cases, a purine. In fact all but two amino acid residues, methionine and tryptophan, are coded for by more than one triplet codon. In addition to this redundancy, the tendency for like amino acids (i.e. non-polar, hydrophobic, polar, acidic and basic) to be represented by related codons, minimizes the effects of mutations. This ensures that a single random base change has an increased probability, compared with the random assignment of codons, of resulting in no amino acid substitution or in one involving amino acids with similar properties. Thus, the low frequency of naturally occurring mutations is a formidable problem which makes their isolation and characterization a laborious task.

These low mutation rates can be increased through the use of *in vivo* mutagenesis techniques (Tamarin, 1982) like X-rays, ultraviolet light and treatment with various chemical mutagens. Large doses of X-rays cause the DNA to break apart in several locations and its mutagenic effect is cumulative, regardless of whether it is given in a large dose all at once, or spread out in smaller doses over a period of time.

Ultraviolet light introduces covalent bonds between adjacent pyrimidine nucleotides, creating dimers—usually thymine-thymine, but also thymine-cytosine or cytosine-cytosine. Dimerization distorts the double helix and this interferes with both DNA replication and RNA transcription. Repair mechanisms in most cells break these dimers or remove the fragment containing the dimer and repair the DNA by filling in the correct nucleotides, using the second strand as a guide; but, if the damaged regions are missed, the presence of a dimer will result in breaks and mutations in newly synthesized DNA, once replication occurs.

Numerous chemical mutagens have also been used to increase the frequency of mutations in DNA, by growing the cells in the presence of base analogues, or treating whole cells with nitrous acid, hydroxylamine, alkylating agents or acridine dyes. These mutagens have been widely used over the years and a useful summary of their effects can be found in Tamarin (1982), the highlights of which will be described herein. Two of the more commonly used base analogues are 5-bromouracil and 2-aminopurine. Because 5-bromouracil resembles thymine, it may be inserted in its place during DNA replication. The keto form of 5-bromouracil, which pairs with adenine, may undergo tautomerization to the enol form, which readily pairs with guanine, causing a T-A to C-G mutation. Like adenine, 2-aminopurine forms two hydrogen bonds with thymine, but it can also form a single hydrogen bond with cytosine. Therefore, it can replace either adenine or guanine, producing an A-T to G-C transition. Nitrous acid oxidatively deaminates cytosine to uracil, and hydroxylamine converts cytosine to N<sup>4</sup>-hydroxycytosine. Both treatments result in C-G to T-A mutations. Alkylating agents, like ethyl methane sulfonate and ethyl ethane sulfonate remove the purine rings of adenine and guanine nucleotides through a multistep process which results in the hydrolysis of the purine-deoxyribose bond. When DNA replication or repair takes place, any of the four possible bases can be inserted into the new strand as a complement to the gap created when these alkylating agents remove a purine. The gap

remains to continue to generate new mutations each generation, unless it is repaired. Acridine dyes are planar heterocyclic molecules, like acridine orange and proflavin, which become non-covalently inserted, or intercalated, between two successive bases in DNA, physically separating them. This leads to the addition or deletion, usually of a single base pair per molecule intercalated, during DNA replication, and results in a shift in the reading frame of the gene. Thus, the mutagenic effects of acridine dyes begin at the point of insertion or deletion and continue through to the end of the gene; which may be considerably longer or shorter, since the normal stop codon will not be recognized in the new reading frame.

Although these *in vivo* techniques significantly increase the frequency of mutation, they have some serious limitations as well. Since the mutagenesis is carried out on whole cells, it is difficult to determine if several changes are produced in the same organism; so that the observed differences from the normal, or wild type, organism may be due to more than one change. As well, although most genes show more or less similar rates of mutation, whether spontaneous or induced (which depend on the size of the gene, or target for mutation), some base pairs gain far more than the number of mutations expected from a random distribution (Lewin, 1983). They may have ten or even one hundred times more mutations than predicted by random hits; these sites are called hotspots. Conversely, there are sites in which only a rare mutation is found. Interestingly enough, spontaneous point mutations and mutations induced by some mutagens have been found to give rise to one set of hotspots, while other mutagens give rise to a different set of hotspots. Although the reason behind their existence is not clear, one possible explanation has been found in the *lac I* gene of *E. coli*, where hotspots for spontaneous point mutations all occur at sites at which the wild type sequence contains a 5-methylcytosine, a cytosine which has been modified by a methylase enzyme (Lewin, 1983). Spontaneous oxidative deamination converts 5-methylcytosine to thymine, and cytosine to uracil. The uracil, however, is recognized

by an enzyme in the cell, uracil-DNA-glycosidase, as not belonging in DNA; and so it is removed and replaced by cytosine. Since thymine is a normal component of DNA, this system does not operate to correct that change, and a mutation results. In strains of *E. coli* unable to perform the methylation reaction, these hotspots do not exist.

Another factor which imposes serious limitations on the usefulness of *in vivo* mutagenesis methods is that of selectivity; often only certain base changes are produced, making it difficult to obtain specific desired mutations. In addition, isolation of mutations in a gene of special biochemical interest, by simple assay, requires not only exhaustive amounts of labor to screen thousands of mutagenized organisms, but also major, even lucky, assumptions about what properties a mutant may or may not possess relative to the wild type organism. Moreover, such methods do not permit the isolation of organisms with only minor variations in phenotype which may go undetected, or those which contain lethal mutations, since these cells do not survive. Classical *in vivo* mutagenesis therefore, allows the study of only certain aspects of the function of a given gene and only certain genes in a given genome.

With the advent of recombinant DNA technology, genes can be moved from their normal environment, in an intact genome, to cloning vectors, where the mutated DNA is non-essential. The availability of purified genes *in vitro*, in microgram quantities, has dramatically expanded the potential for inducing mutations. In the controlled environment of the test tube, it is now possible to alter, efficiently and systematically, the sequence of nucleotides in a segment of DNA. This allows these same mutagens to be directed at the gene of interest specifically, and also provides new opportunities for the development of more advanced mutagenesis techniques which address some of the other problems with the *in vivo* methods. But, unlike classical *in vivo* mutagenesis, in which all mutations were studied inside a living cell, *in vitro* mutagenesis invariably yields gene mutations out of their normal context. This can create some problems depending on the system under investigation. For example, the

physiological effect of a mutation in a regulatory protein, native to a mouse cell, can hardly be determined if this mutant protein is expressed in an *E. coli* cell. In a mouse cell, this regulatory protein may be expressed differently than in an *E. coli* cell, and interact with other mouse proteins or mouse DNA. Since none of these normal environmental molecules are present in an *E. coli* cell, it would be very difficult to assess the effect of mutations on this type of protein. However, if instead mutations were created in an enzyme to study the catalytic roles of certain amino acid residues, the context in which the enzyme is studied is less of a problem. The fact that this enzyme may be expressed at a different level, or be isolated from its normal cellular environment, would have little effect on the determination of which residues were important for catalysis.

Perhaps the most important advantage of *in vitro* mutagenesis is the ability to introduce mutations efficiently and predictably into a gene of interest. Localized random mutagenesis uses the *in vivo* methods discussed previously to create mutations in isolated segments of DNA which are then returned to the cloning vector in place of the same unmutagenized fragment. This type of mutagenesis yields a variety of mutants scattered over the region of interest and is often a first step in the characterization of a previously unstudied enzyme, especially in the absence of any three-dimensional information; so that more judicious and/or precise mutations may then be chosen. Ultimately, the investigator would want to change specific nucleotides in the DNA sequence to produce the corresponding mutations in the resulting protein.

The recent availability of commercial automated DNA synthesizers, which can readily make short pieces of DNA, called oligonucleotides, has made oligonucleotide-directed *in vitro* mutagenesis the method of choice, for creating specific mutations in cloned and sequenced genes. The basic strategy (Zoller & Smith, 1982) for this method is illustrated in Figure 12 and involves the formation of a heteroduplex between a single-stranded template DNA and the mutagenic oligonucleotide at the site of interest. The

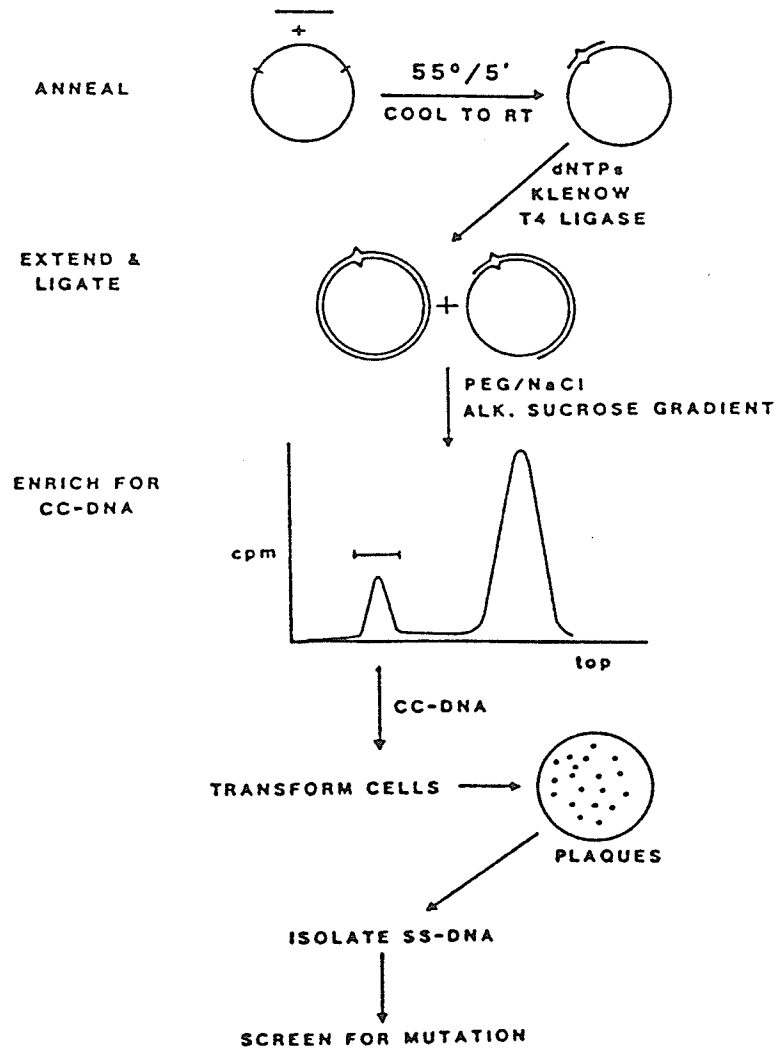


Figure 12. Basic oligonucleotide-directed *in vitro* mutagenesis method. CC-DNA is covalently closed DNA. (Taken from Zoller & Smith, 1982.) See text for details of method.

mutagenic oligonucleotide is complementary to the template, except for the mismatch that will induce the mutation, usually roughly in the center of the oligonucleotide. After the mutagenic oligonucleotide is annealed onto the wild type single-stranded template DNA, it is extended by *E. coli* DNA polymerase I, Klenow fragment (which lacks a 5' to 3' exonuclease activity) and covalently closed DNA molecules (CC-DNA) are formed by ligation of the newly synthesized strand with T4 DNA ligase. The conversion of single-stranded molecules into covalently closed double-stranded molecules is incomplete, so the CC-DNA is separated from unligated and incompletely extended molecules by alkaline sucrose gradient centrifugation. The CC-DNA enriched fraction is then neutralized and used to transform cells and obtain a population of mutant and wild type clones. This method requires that the DNA of interest be cloned, ideally into an M13 bacteriophage vector (Messing, 1983), which contains a multiple cloning site, and, whose life cycle provides the opportunity to obtain both double-stranded (or RF, for replicative form) DNA for cloning, and single-stranded template DNA, both for mutagenesis and sequencing. The insert DNA must also be of known sequence (the sequence of the M13 vector is already known), so that the sequence of the single-stranded template DNA can be searched, usually by computer, for sequences similar to that of the chosen oligonucleotide, thus determining if the oligonucleotide is likely to prime at any location other than that desired to create the mutation. After synthesis, the oligonucleotide is tested as a sequencing primer, just to be certain that it primes only in the desired location. If second or multiple site priming occurs, a new oligonucleotide must be synthesized, usually one that is longer to make it more specific for the desired priming site.

Once the mutagenesis procedure is complete, the resulting M13 clones must be screened (Zoller & Smith, 1983) to determine which are mutant and which are wild type. If the mutation either creates or destroys a restriction endonuclease site, then this can be used to distinguish between wild type and mutant clones. By digesting

replicative form (RF) phage DNA with the appropriate restriction endonuclease, a mutant with a restriction pattern different from the wild type, can be identified by examining the digests on an agarose gel. This method of screening is not often useful though, since most mutations do not create or destroy restriction endonuclease sites. The more commonly used method of hybridization screening uses the radioactively labeled mutagenic oligonucleotide as a probe for mutant clones. The principle behind this procedure is that the mutagenic oligonucleotide will form a more stable duplex with a mutant clone, which matches exactly, than with a wild type clone, which has a mismatch. Mutant clones are detected by forming a duplex at a low temperature where both mutant and wild type DNA interact, then carrying out washes at increasingly higher temperatures until only mutant molecules continue to bind the radioactive mutagenic oligonucleotide (Figure 13). Another method, which is becoming more widely used as mutagenesis procedures yield a larger proportion of mutants, is that of single-track sequencing (Zoller & Smith, 1983). In this method single-stranded DNA from each clone is subjected to single-channel chain-termination sequencing using the dideoxynucleotide that would differentiate wild type from mutant clones (Sanger *et al.*, 1977). For example, if a G to T mutation is being induced, A-tracking the single-stranded DNA from the clones would show an A complementary to mutant clones containing the desired T change; but wild type clones, with a G at this position, would not show an A at the corresponding position.

In order to show conclusively that the mutation induced by the oligonucleotide is the only mutation in the clone to be studied, the entire segment of DNA which was present in the mutagenesis experiment, and is also present in the expressed mutant clone, must be resequenced. This insures that any variation in observed phenotype is due to the single known mutation.

In any mutagenesis experiment, it is important to maintain a high yield of mutants to minimize the need for mutant screening. The relationship between these two

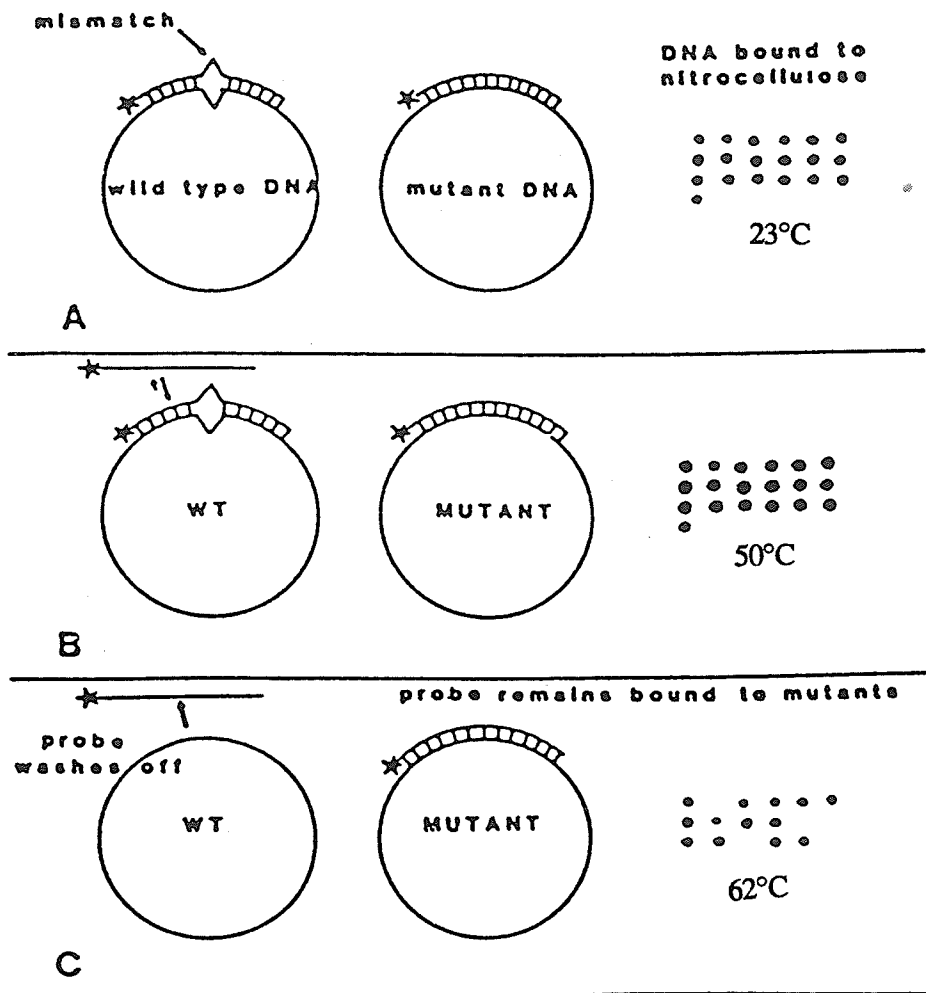


Figure 13. Screening for mutants using the mutagenic oligonucleotide as a hybridization probe. Example of 18 clones + 1 wild type clone assayed by dot blot. Hybridization was conducted at  $37^{\circ}\text{C}$ , washes were carried out at  $23^{\circ}\text{C}$ ,  $50^{\circ}\text{C}$ , and  $62^{\circ}\text{C}$ . (Taken from Zoller & Smith, 1984.)

factors is logarithmic, and so as the frequency of mutation drops, the number of clones which must be screened rises dramatically (Amersham, 1987). Although the theoretical yield of mutants is 50%, it is usually considerably less than this. By far the most serious problem which causes a reduction in the mutant yield is the strand-displacing helicase activity of DNA polymerase I, Klenow fragment, which tends to lift off the mutagenic primer when the synthesis of the DNA circle approaches completion. This allows the wild type template strand to direct the sequence of the newly synthesized strand of DNA, and results in both copies matching the wild type. This problem can be somewhat lessened by adjusting the relative concentrations of Klenow polymerase and T4 DNA ligase, so that as soon as the DNA circle is complete, the ligase seals the nick in the sugar-phosphate backbone of the new strand of DNA before the primer can be displaced (Smith, 1985). The yield of mutants may also be reduced by *in vivo* repair of the 5'-end of the mutagenic oligonucleotide or repair mechanisms in the cell which can distinguish between the wild type strand and the newly synthesized mutant strand, selecting against the mutant strand. For example, a small concentration of contaminating dUTP, present in the primer-extension step, can cause the newly synthesized strand to be more susceptible to repair since dUTP is not a normal constituent of DNA. Also, newly synthesized DNA strands which have not yet been methylated are preferentially repaired at the position of a mismatch. These factors can reduce the yield of mutants substantially, to less than 5%, so that even though the oligonucleotide-directed method allows us to choose precisely the change we want to make from one nucleotide to another, at a specific location, the yield of mutants may make screening a major problem. For this reason, modifications have been made to the basic method to improve the yield of mutants.

One modified method simply includes a second primer upstream of the mutagenic primer in the primer-extension step; typically the M13 universal sequencing primer is used (Zoller & Smith, 1984). Extension of this additional primer promotes the

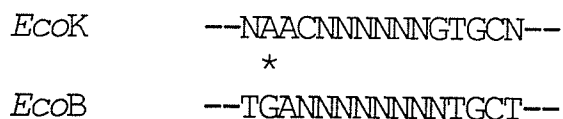
incorporation of the mutagenic primer into the newly synthesized sequence, forming a gapped duplex bearing a mismatch. In this method, enrichment of the extended DNA is not required, probably due to the protection from *in vivo* repair of the 5'-end of the mutagenic oligonucleotide, by ligation to the extended DNA from the sequencing primer. In the single primer method, equivalent protection occurs only when complete extension and ligation occur.

The Kunkel (1985) method uses a specialized host for growing the phage before mutagenesis. This host cell is deficient in the enzymes dUTPase (*dut*<sup>-</sup>) and uracil glycosylase (*ung*<sup>-</sup>). The *dut*<sup>-</sup> mutation causes an increase in the intracellular dUTP levels, because the enzyme which converts dUTP to dUMP, dUTPase, is inactive. The *ung*<sup>-</sup> designation indicates that the cell has a defective uracil-DNA-glycosidase enzyme, whose normal function is the removal of dUTP bases from DNA. This defect allows dUTPs which are incorporated into the DNA in place of dTTP to remain, and these two mutations result in dUTPs taking the place of dTTPs about 1% of the time. After the mutagenesis procedure, an *ung*<sup>+</sup> host is used to select against the dUTP containing strand. This method yields about 40% mutants.

Another modified method, the gapped duplex method (Kramer *et al.*, 1982), improves the yield of CC-DNA, and therefore mutants, by starting the mutagenesis procedure with a partial duplex of DNA, in which only a small segment of single-stranded DNA is available for the oligonucleotide to prime. The Klenow polymerase then has only a short region to fill in with nucleotides in order to complete the circle, and provide CC-DNA for transformation. Yields of up to 50% have been observed with this method.

The Winter coupled priming cyclic selection method (Carter *et al.*, 1985) depends on the sequence similarity between *EcoK* and *EcoB* restriction endonuclease sites. *EcoK* and *EcoB* are restriction endonucleases which recognize a target site, but then travel 1000-5000 bases along the DNA strand before cutting at an apparently

random site (Amersham, 1987). The sequences which *EcoK* & *EcoB* recognize differ at only one site:



The method uses two primers, one mutagenic, and one complementary to the *EcoK/EcoB* strand selection site. Both primers are used in the mutagenesis procedure, making two mutations, one to alter the DNA sequence at the desired location, and the other to change restriction site specificity, so that the host cell will cleave only the undesired wild type strand (Figure 14). This modification permits repeated rounds of mutagenesis without recloning. For example, an *EcoB* selection primer could be incorporated into the newly synthesized strand with the mutagenic oligonucleotide (Figure 14). After selection in an *EcoK*-restricting host, an *EcoB* specific clone containing the single mutation can be isolated. The DNA from this clone can then be used as the template in the next mutagenesis experiment, if a second mutation is desired. In this second mutagenesis procedure, the selection primer used is that of *EcoK*, and the double mutant is selected with an *EcoB*-restricting host (Figure 14). This method results in up to 60% mutants and the cycle can be repeated many times, to obtain clones with multiple mutations.

There are new problems with the methods which include second primers and the gapped duplex method. Because filling in is able to occur in the absence of the mutant oligonucleotide, by priming to the large double-stranded DNA region in the gapped duplex method or to the second oligonucleotide in the two primer methods, a background of non-mutant CC-DNA molecules is generated. This is especially troublesome in cases where the mutant oligonucleotide binds poorly to the single-stranded template DNA and may result in very low mutant yields.

In the case of the Eckstein method (Taylor *et al.*, 1985a, 1985b; Nakamaye & Eckstein, 1986), unwanted priming and the generation of a non-mutant strand is not a

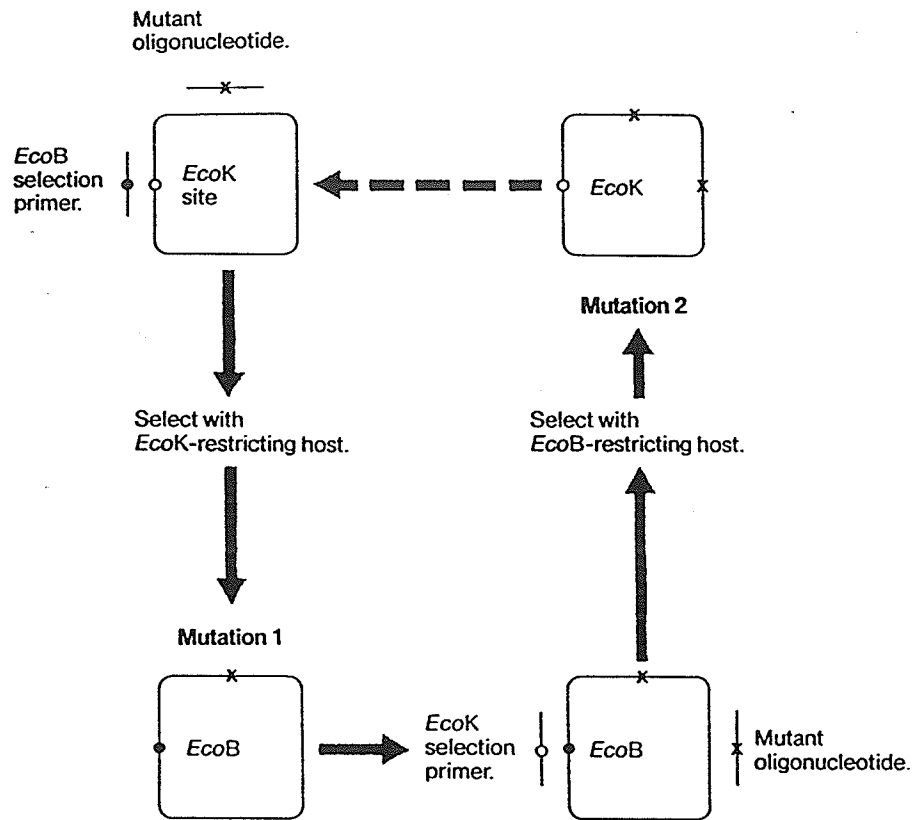


Figure 14. The "Winter" coupled priming technique, used for cyclic selection mutagenesis. (Taken from Amersham, 1987.) See text for details of method.

problem, because the only primer used is the mutagenic one. The mutagenic primer is annealed onto the single-stranded template and extended by Klenow polymerase in the presence of T4 DNA ligase to generate a mutant heteroduplex (Figure 15A). Selective removal of the non-mutant strand is made possible by the incorporation of a thionucleotide (Figure 15B) into the mutant strand during *in vitro* synthesis (Amersham, 1987). Nitrocellulose filtration (Figure 15A) then removes any contaminating single-stranded template DNA, significantly reducing the non-mutant background. Eckstein observed that certain restriction endonucleases cannot cleave phosphorothioate DNA (Taylor *et al.*, 1985a). As a result, single-strand nicks are generated in DNA containing one phosphorothioate and one non-phosphorothioate strand. Such nicks present sites for Exonuclease III, which can then be used to digest away all or part of the non-mutant (non-phosphorothioate) strand of the cloned target sequence. The mutant strand is then used as a template to reconstruct the double-stranded closed circular molecule, thus creating a homoduplex mutant molecule, and resulting in up to 95% mutants, upon transformation.

Several of these methods were used in this thesis to create mutations in the citrate synthase gene of *Escherichia coli*, mainly the two primer method, which includes the M13 universal sequencing primer, and the Eckstein method.

These mutagenesis procedures allow biochemists to study the precise functions of selected amino acid side chains, by changing specific amino acid residues, at the DNA level, and comparing the properties of the resulting mutant enzymes to those of the wild type. With well chosen experiments, protein chemists and enzymologists can learn the function of amino acid residues which are conserved in the corresponding enzymes of different organisms. They can also determine the importance of each residue in the binding of substrates at the active site, or inhibitors at active and allosteric locations. Further experiments may also be designed to determine which residues are catalytically

A

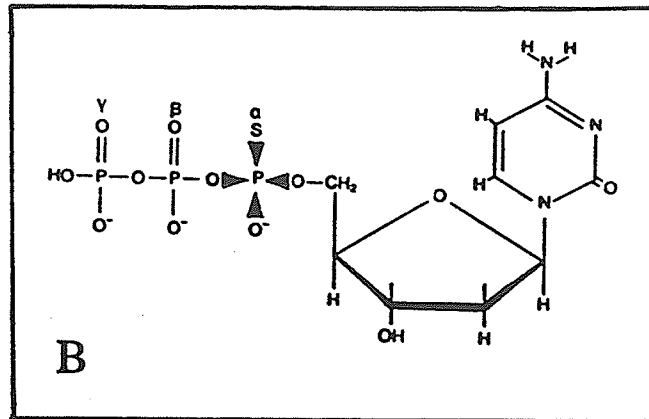
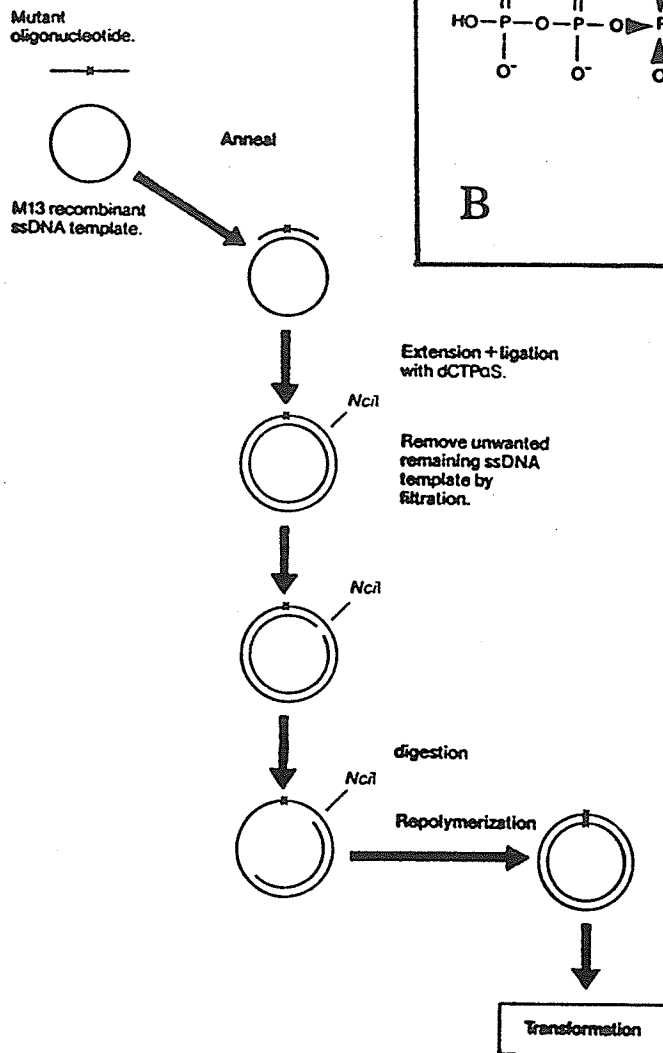


Figure 15 A The "Eckstein" method of oligonucleotide-directed mutagenesis.

B The structure of dCTP $\alpha$ S nucleotides, used in the "Eckstein" method.  
(Both taken from Amersham, 1987.) See text for details of method.

important for the normal functioning of the enzyme and those involved in the stabilization of the different conformations associated with allosteric enzymes.

## **MATERIALS AND METHODS**

## Bacterial Strains and Plasmids

All mutant versions of the *E. coli* citrate synthase gene *gltA*, prepared using an oligonucleotide-directed method as described later, were expressed in the plasmid pES*gltA*, which was derived from pHS*gltA*, the clone previously used to obtain large amounts of wild type enzyme (Duckworth & Bell, 1982), as follows. The 733-base pair *Hind*III–*Bam*HI fragment of pHS*gltA*, which contains most of the natural *gltA* promoter but none of the citrate synthase coding sequence, was cloned into M13mp19, and a synthetic oligonucleotide, designated oligo Eco (see Table 2), was used in the procedure of Zoller and Smith (1983) to introduce a new *Eco*RI site into this fragment by mutating T–319 in the sequence of Ner *et al.* (1983) to A (Figure 16). In the work-up of the reaction, JM103 cells were used and the sucrose gradient step was omitted. Mutants were screened by digesting the replicative form of the resulting phage DNA with *Eco*RI and running the samples on an agarose gel. Replicative form of the desired mutant was digested with *Eco*RI and *Bam*HI, and the new shorter *Eco*RI–*Bam*HI fragment was isolated by agarose gel electrophoresis, and ligated with the gel-purified large fragment from the *Eco*RI–*Bam*HI digest of pHS*gltA* (Figure 16). The product of this ligation, pES*gltA* (6233 base pairs), is 294 base pairs smaller than pHS*gltA* but still expresses wild type and mutant versions of the citrate synthase gene efficiently. The sequence absent in pES*gltA* contained several restriction endonuclease sites (for *Bcl*II, *Cla*I, *Hind*III, *Kpn*I and *Hpa*I), so that the *Hpa*I site within the *gltA* coding sequence of pES*gltA* is now unique. This unique *Hpa*I site has been used, in conjunction with the unique *Sal*I site, to cut out and replace the small wild type *Hpa*I–*Sal*I fragment with each corresponding *Hpa*I–*Sal*I fragment containing a mutation, in order to express mutant forms of *E. coli* citrate synthase. Therefore after mutagenesis, only the region between this *Hpa*I site and the end of the coding sequence

Table 2. Oligonucleotide sequences, and the location at which they prime to the *gltA* insert.

Designation of oligonucleotide	Sequence of oligonucleotide, where "•" is above the mismatched nucleotide(s)	Complementary to bases <sup>e</sup> :
oligo Eco <sup>a</sup>	5' -GGAAGGAATTCCCGACG-3' •	-327→-311
oligo 188 <sup>a</sup>	-TCGTTGAGCGGGTAAAC- •	861→877
oligo 217 <sup>b</sup>	-CCATAGCAAGTTCCAGA- •	950→966
oligo 221 <sup>b,c</sup>	-ATCAGAATAAGGTCCAT- •	963→979
oligo 226 <sup>d</sup>	-GGTCAGCCTGCAGGATC- •	977→993
oligo 229 <sup>a</sup>	-TTCTGTTCCCTGGTCAGC- •	987→1003
oligo 260 <sup>b,c</sup>	-AGGTCCCGCCAGTGAAG- ••	1078→1094
oligo 305 <sup>b</sup>	-CACGCGGGCACC GAAGC- ••	1213→1229
oligo 314 <sup>b</sup>	-CGGTGGCGAGCGGGTCG- •	1241→1257
oligo 319 <sup>b</sup>	-AGGTTTCAAGCATTACG- •	1256→1272
oligo 329 <sup>b,c</sup>	-TCATCCTTCGTGCCCAG- •	1293→1309
oligo 387 <sup>a,c</sup>	-TCCAGCCAACGGTACGT- •	1466→1482
oligo term <sup>a,c</sup>	-GCCATATGAACGGCGGG- •	1621→1637

<sup>a</sup> Synthesized at the Institute of Cell Biology, University of Manitoba, in an Applied Biosystems 380B DNA Synthesizer.

<sup>b</sup> Synthesized by the DNA Custom Synthesis Centre, University of Calgary.

<sup>c</sup> Used as a sequencing primer (see text for details).

<sup>d</sup> Custom-synthesized by Pharmacia (Canada) Ltd.

<sup>e</sup> Numbering according to Ner *et al.* (1983).

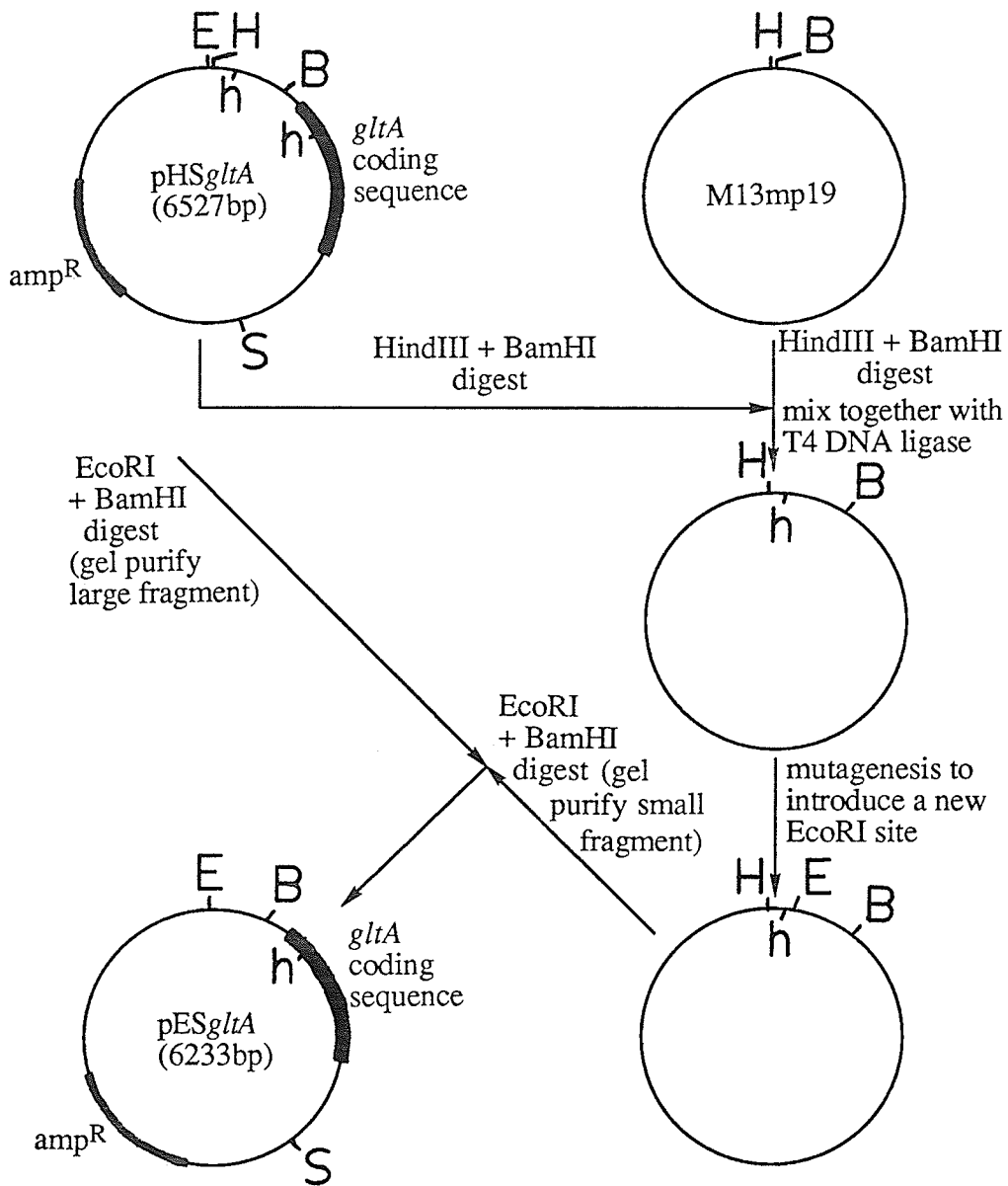


Figure 16. Making pESgltA. (E = EcoRI, H = HindIII, B = BamHI, S = Sall, h = HpaI and bp = base pairs).

needed to be re-sequenced, since only this segment of DNA was present in both the mutagenized DNA and the expressed citrate synthase clone.

Mutant plasmids were expressed in the *E. coli* host strain MOB154, and mutant proteins were purified from extracts of this strain harboring the appropriate mutant plasmid. MOB154, a gift from Dr. D. O. Wood (University of Alabama, Mobile), has a stable mutation in the *gltA* gene and lacks any detectable citrate synthase as judged by both enzyme assay and immunological methods (Anderson & Duckworth, 1988). It is a *recA* derivative of MOB147 (described in Wood *et al.*, 1983).

### Construction of Mutants by *in vitro* Techniques

The first mutant described in this thesis, designated CS $\Delta$ (264–287) because the codons for amino acids 264 through 287 have been deleted, was created by purifying the *Bam*HI–*Sal*I fragment of pHS*gltA* by agarose gel electrophoresis, digesting it with *Fsp*I and *Xmn*I, and re-ligating the blunt ends (Figure 17). Recutting the ligation product with *Bam*HI and *Sal*I, as well as with *Xmn*I to select against reassembled wild type sequence, and ligating the resulting fragment to the gel-purified large fragment from *Bam*HI–*Sal*I-digested pHS*gltA*, gave the mutant gene in expressible form. This construction was verified by DNA sequencing (Sanger *et al.*, 1977) of the appropriate *Sau*3AI fragment cloned into M13mp18.

#### Oligonucleotide-Directed Methods:

The remaining mutants were all made using some form of the oligonucleotide-directed *in vitro* mutagenesis method of Zoller and Smith (1983). In each experiment the single-stranded template DNA used was an M13mp8 clone of the *Bam*HI–*Sal*I fragment of pHS*gltA*, called M13cl15 (prepared by Dr. L. J. Donald of this laboratory), which contains the entire citrate synthase coding region. The oligonucleotides used to

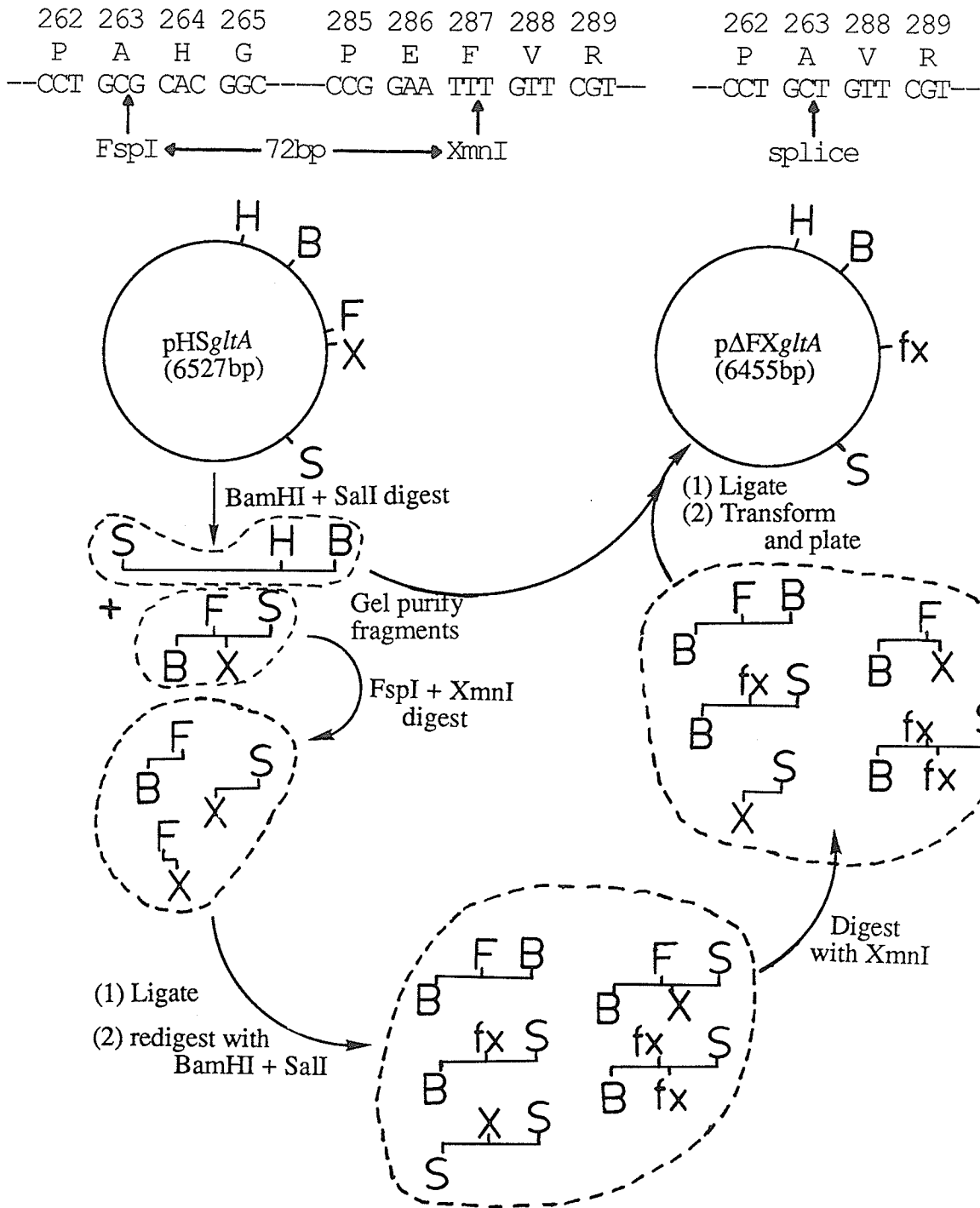


Figure 17. Making  $p\Delta FXgltA$ , which expresses mutant protein  $CS\Delta(264-287)$ . (B =  $BamHI$ , F =  $FspI$ , S =  $SalI$ , X =  $XmnI$ ,  $fx$  = non-palindrome produced by ligation of  $FspI$  and  $XmnI$  fragments, and  $bp$  = base pairs).

create the mutations have each been given a designation and are listed in Table 2. Each of these oligonucleotides was complementary to a region in the insert of the coding strand of M13cl15 also shown in Table 2 (numbering according to Ner *et al.*, 1983). Most oligonucleotides were delivered lyophilized, and had been purified by the laboratory which performed the synthesis, including all of the oligonucleotides prepared by the DNA Custom Synthesis Centre at the University of Calgary, as well as oligo 226, synthesized by Pharmacia (Canada) Ltd. Several oligonucleotides were synthesized in Manitoba, in the Applied Biosystems Synthesizer at the Institute of Cell Biology, University of Manitoba, and purified by Dr. L. J. Donald in this laboratory. The published procedure of Sanchez and Urdea (1984), as modified in an Applied Biosystems Bulletin (Issue #30, dated February 5, 1986), was used to purify these oligonucleotides after synthesis, as follows. The crude oligonucleotide preparation was dissolved in water, extracted with n-butanol, evaporated, and resuspended in water. It was then electrophoresed on a 20% polyacrylamide gel containing 7.5M urea, in TBE buffer (10.8g Tris, 5.5g boric acid, 0.93g EDTA per liter, pH 8.4). The oligonucleotide band was located by ultraviolet light shadowing, using an Eastman Chromagram Sheet, 13181 Silica Gel with Fluorescent Indicator (No. 6060), under the gel. The oligonucleotide band was excised and eluted with gentle shaking, overnight at room temperature, into 0.5M ammonium acetate/10mM magnesium acetate. After filtration, the oligonucleotide solution was passed through a Waters C-18 Sep-pak column which had been pre-washed with acetonitrile, followed by water, and equilibrated with 0.5M ammonium acetate. Elution with 60% methanol/40% water and evaporation to dryness yielded the oligonucleotide in pure form.

Prior to use in a mutagenesis experiment, each oligonucleotide was tested as a sequencing primer (Sanger *et al.*, 1977), using wild type M13cl15 as the single-stranded template DNA, to ensure that each primed only in the desired location.

Three different oligonucleotide-directed mutagenesis methods were used in this thesis, and all have been discussed in detail in the Introduction. Oligo Eco was used in the basic single primer mutagenesis method of Zoller and Smith (1983) to create a new EcoRI site upstream from the *gltA* coding sequence in pHS*gltA*, in order to make the plasmid pES*gltA* as described above. Three of the mutagenesis experiments included the M13 universal sequencing primer (Duckworth *et al.*, 1981; a gift from Dr. M. L. Duckworth, University of Manitoba) as a second primer, during the primer extension step (Zoller & Smith, 1984). Again, as in the single primer method, JM103 host cells were used and the sucrose gradient step was omitted. Table 3 specifies which experiments were performed with each method. The remaining mutants, by far the majority in this thesis, were constructed using the Eckstein method (Taylor *et al.*, 1985a, 1985b; Nakamaye & Eckstein, 1986), with a kit supplied by Amersham (Canada) Ltd.

#### Screening for Mutants:

After the mutagenesis procedures, transformants were screened to determine which clones were mutant and which were wild type. The frequency of mutants obtained in each experiment is given in Table 3. Two of the mutagenesis experiments created new restriction endonuclease sites; oligo Eco created an EcoRI site, as discussed above, and oligo 226 created a PstI site. These clones were screened by preparing replicative form DNA, digesting it with the appropriate restriction endonuclease, and comparing the restriction patterns on an agarose gel, with that obtained from a wild type clone.

The remaining mutants were screened using single-channel chain-termination (Sanger *et al.*, 1977), as discussed in the Introduction. The oligonucleotide used as the sequencing primer and the dideoxy-nucleotide included to distinguish mutant from wild type clones are listed in Table 3. Table 3 also shows the precise base changes produced

Table 3. Oligonucleotide-directed *in vitro* mutagenesis results.

Mutagenic oligo-nucleotide	Method used for mutagenesis (see text for details)	Frequency of mutants produced	For single-channel chain-termination screening method (if applicable):				Location <sup>d</sup> , and resulting base change(s) in coding strand	Resulting mutant protein, indicating the amino acid mutation produced
			Oligonucleotide used as primer	Dideoxynucleotide included in reaction to distinguish mutant from wildtype clones	N/A <sup>c</sup>	N/A <sup>c</sup>		
oligo Eco	1 primer	1 in 24	N/A <sup>c</sup>	N/A <sup>c</sup>	-319T→A	N/A <sup>c</sup>		
oligo 188	Eckstein	1 in 30	oligo 221	A	871G→T	CS188R→L		
oligo 217	2 primer <sup>b</sup>	3 in 24	oligo 260	A	958G→T	CS217R→L		
oligo 221	2 primer <sup>b</sup>	1 in 36	oligo 260	A	970G→T	CS221R→L		
oligo 221 <sup>a</sup>	Eckstein	1 in 12	oligo 260	A	958G→T, 970G→T	CS217R→L/221R→L		
oligo 226	2 primer <sup>b</sup>	3 in 24	N/A <sup>c</sup>	N/A <sup>c</sup>	986C→G	CS226H→Q		
oligo 229	Eckstein	1 in 11	oligo 260	C	995T→G	CS229H→Q		
oligo 260	Eckstein	2 in 11	oligo 329	G	1086T→G, 1087G→C	CS260W→A		
oligo 305	Eckstein	3 in 5	oligo 329	C	1221C→G, 1222A→C	CS305H→A		
oligo 314	Eckstein	1 in 11	oligo 329	A	1249G→T	CS314R→L		
oligo 319	Eckstein	1 in 7	oligo 329	A	1264G→T	CS319R→L		

<sup>a</sup> The double mutant CS217R→L/221R→L was made using oligo 221 and single-stranded M13cl15 template DNA already containing the 217R→L mutation.

<sup>b</sup> The 2 primer method included the M13 universal sequencing primer as the second primer.

<sup>c</sup> Not applicable. These mutations were screened by digesting replicative form phage DNA, as explained in the text, since the mutations both create a restriction endonuclease site.

<sup>d</sup> Numbering according to Ner *et al.* (1983).

in the coding strand of the *gltA* gene and the designations of the resulting mutant proteins, indicating the amino acid mutations produced.

## Routine Procedures

### DNA Sequencing:

To confirm each mutation and to ensure that no other mutations had arisen within the coding sequence (during the *in vitro* strand synthesis step of the oligonucleotide-directed methods), the sequence of the coding strand between bases 759 and 1589 was redetermined by the method of Sanger *et al.* (1977), using five custom-made sequencing primers (see Table 2 and Figure 18 for sequences of oligonucleotides and their priming sites). The first two primers had one- and two-base mismatches, respectively, because they had been synthesized for mutagenesis experiments, while the other three were exact matches. Each primed only at the expected site, as judged by DNA sequencing. The region which was re-sequenced corresponded to the C-terminal 278 amino acids of the coding sequence, between the unique *HpaI* site and the end of the coding sequence (Figure 18). After verification, this region was then cut out with *HpaI* and *SalI*, gel-purified, and ligated to the gel-purified large fragment from an *HpaI* and *SalI* digest of pES*gltA*. To be absolutely certain that the mutation was in fact present in the pES*gltA* studied, the *BamHI-SalI* fragment of pES*gltA* was cloned into M13mp18 and resequenced through the region containing the mutation.

### DNA Isolation and Purification:

Plasmid and replicative form phage DNA were routinely prepared using the alkaline-SDS method of Birnboim and Doly (1979), except that after the phenol extraction step a series of precipitation steps was employed to remove most of the RNA present. Addition of 0.6 volumes of isopropanol precipitated all nucleic acid and protein. The resulting pellet was then resuspended in TE buffer (20mM Tris-Cl, 1mM

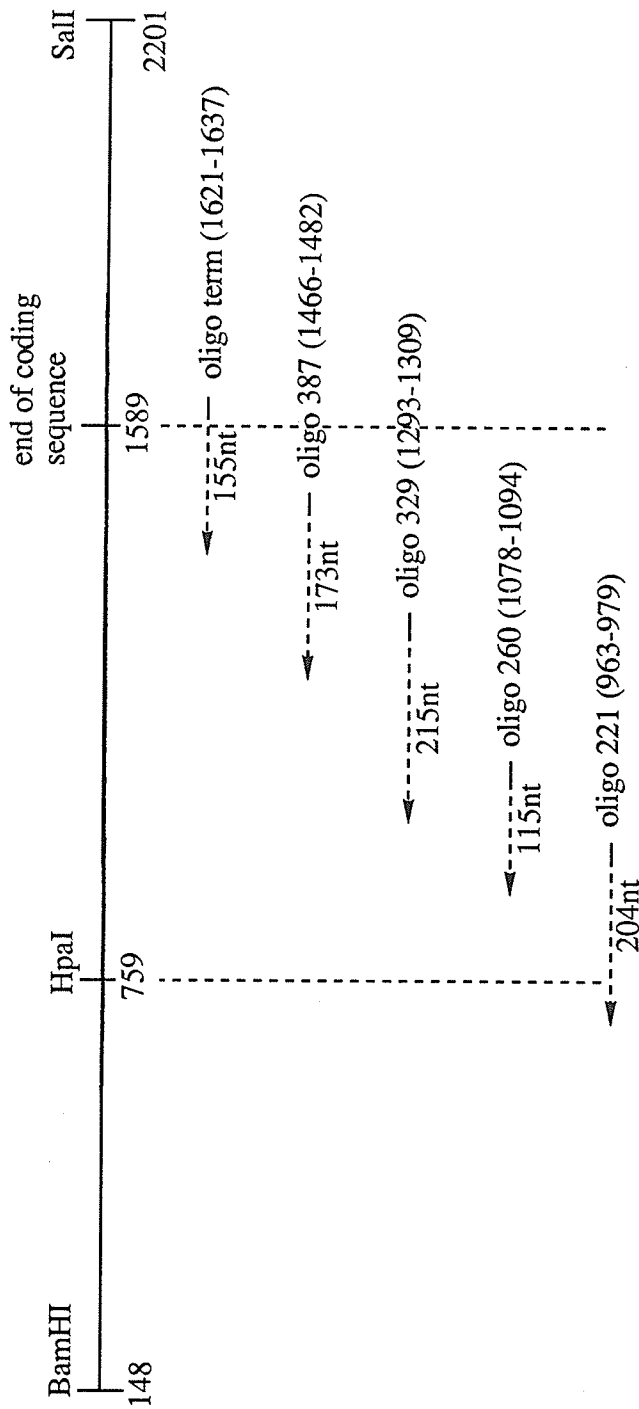


Figure 18. Scheme for re-sequencing the mutagenized M13cl15 coding strand between bases 759 and 1589 (Numbering according to Ner *et al.*, 1983). Five custom-made sequencing primers (see Table 2 for sequences) were used in the method of Sanger *et al.* (1977). The location of their priming sites, as well as the number of nucleotides (nt) read to obtain overlapping sequence information is shown.

EDTA, pH 8) and the RNA plus protein selectively precipitated by addition of an equal volume of LiCl (10M). After centrifugation, 0.6 volumes of isopropanol was added to the supernatant to precipitate the desired DNA. Single-stranded M13 phage DNA for mutagenesis and sequencing was prepared according to the method of Sanger *et al.* (1981). The remaining routine manipulations of DNA (including: electrophoresis of DNA on agarose gels, cloning, and transformation of competent cells with DNA) were as described in Maniatis *et al.* (1982).

#### Large Scale Protein Production and Purification:

MOB154, harboring the appropriate mutant form of pES*gltA*, was grown in a Lab-Line Incubator-Shaker at 37°C for 24 hours in twelve-two liter baffled flasks, each containing one liter of LB and 5mL ampicillin (20mg/mL). A further 5mL ampicillin (20mg/mL) was added after about 8 hours. Mutant enzymes were purified according to Duckworth and Bell (1982), except that the DNase treatment and ammonium sulfate precipitation steps were omitted. Since mutant CSA $\Delta$ (264–287) was inactive, it could not be followed through the purification procedure using the usual enzyme assay. It did cross-react, however, with rabbit antiserum raised against wild type *E. coli* citrate synthase and thus could be purified like the other enzymes, locating citrate synthase protein in fractions by the Ouchterlony double diffusion method (Ouchterlony, 1953) as described in Morse and Duckworth (1980), except at a temperature of 37°C.

After purification each protein was tested for purity by electrophoresis through an SDS polyacrylamide gel as described by Laemmli (1970) in an LKB-2001 vertical slab gel electrophoresis unit. Each gel was then stained overnight, and destained the following day, according to Fairbanks *et al.* (1971). In addition, an absorption spectrum was taken of each preparation to determine the amount of non-specific light scattering in the sample and its precise concentration. The protein concentration of CS260<sup>W→A</sup>(I) was determined using the method of Lowry *et al.* (1951), using wild

type citrate synthase as the protein standard, in order to measure the molar extinction coefficient for CS260<sup>W→A</sup>(I) and accurately determine its concentration.

Solutions of NADH were made fresh daily, and the concentrations were determined by measuring absorption at 340nm ( $\epsilon_m = 6220$ ).

#### Enzyme Assays:

Citrate synthase catalyzes the reaction of acetyl-CoA and oxaloacetate to form citrate and CoASH. The production of CoASH was measured using 5,5'-dithiobis-(2-nitrobenzoate) (DTNB). DTNB reacts very quickly with sulfhydryl groups producing a yellow mercaptide ion (see Figure 19), which absorbs strongly at 412nm ( $\epsilon_m = 13,600$ ). This property allowed the reaction catalyzed by citrate synthase to be followed on a Gilford 2400-2 single beam spectrophotometer by the method of Srere *et al.* (1963).

Since DTNB reacts with sulfhydryl groups, it can also react with sulfhydryl groups on proteins. Normally the concentration of protein in an assay is so low that the reaction with protein is negligible. However, two of the mutants described in this thesis, CS305<sup>H→A</sup> and CS314<sup>R→L</sup>, had extremely low specific activities, so that very large quantities of enzyme were required to obtain measurable activities. For this reason, kinetic measurements for these two mutants were always run with blanks, in which oxaloacetate was omitted from the reaction. It has been previously found that oxaloacetate has no effect on the reactivity of citrate synthase thiols (Talgy & Duckworth, 1979).

One unit (U) of citrate synthase activity is defined as the amount of enzyme required to produce 1  $\mu\text{mol}$  of product in one minute, at room temperature, in the standard assay as defined below.

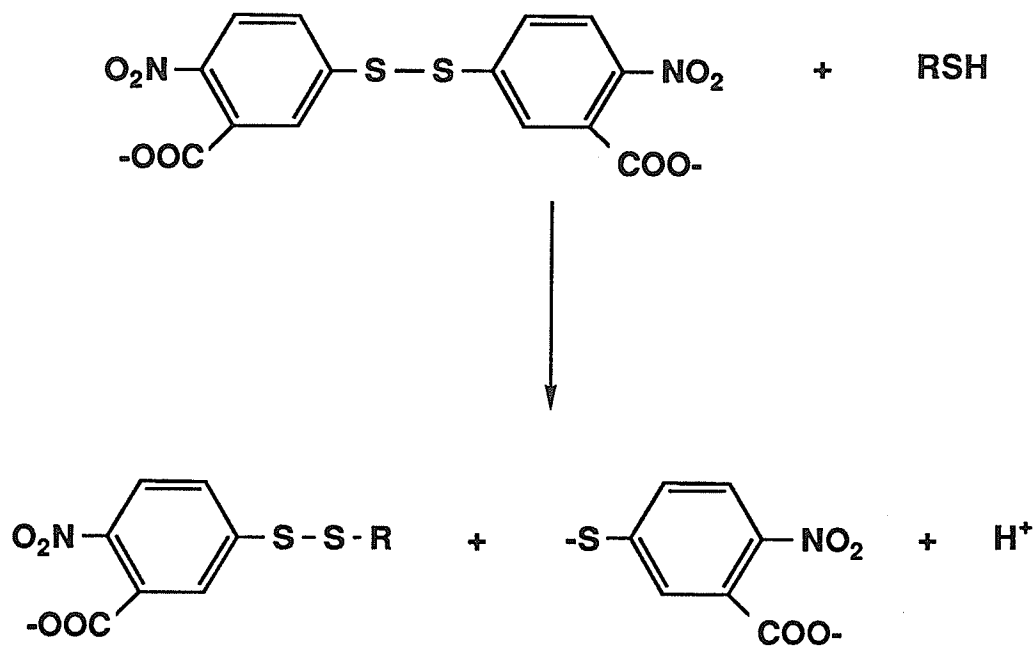


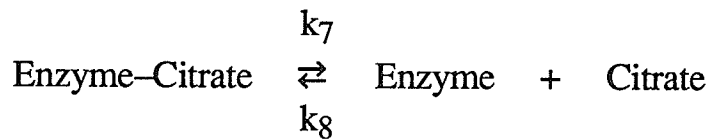
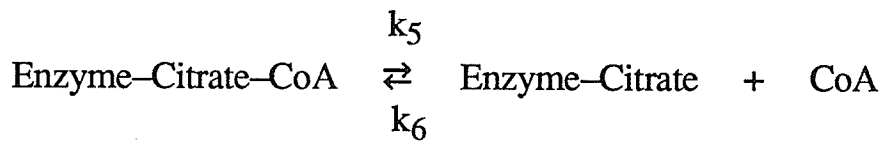
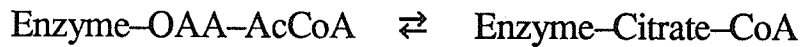
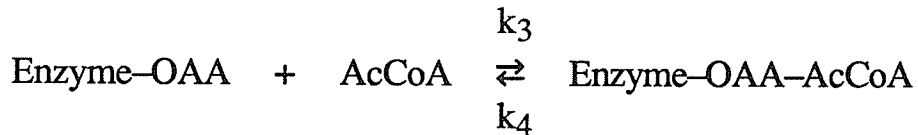
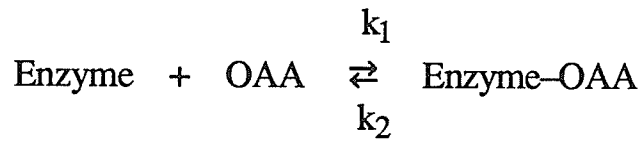
Figure 19. Reaction of DTNB with a sulfhydryl group to produce a mercaptide ion, which absorbs strongly at 412nm ( $\epsilon_m = 13600$ ).

## Collection and Analysis of Kinetic Data

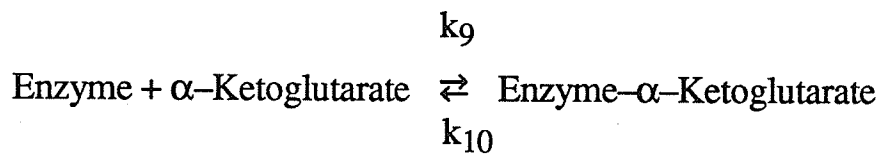
All kinetic studies were performed by the method of Srere *et al.* (1963) at 20°C. Standard buffer was 20mM Tris-Cl, pH 7.8, containing 1mM disodium EDTA, hereafter called Tris buffer. The standard citrate synthase assay solution contained 0.1mM each of acetyl-CoA and oxaloacetate, in Tris buffer containing 0.1M KCl. For studies of NADH or  $\alpha$ -ketoglutarate inhibition, the KCl was omitted. For measurements of NADH inhibition for CS305<sup>H→A</sup> and CS314<sup>R→L</sup>, the extent of inhibition was checked in a discontinuous assay, in which reaction mixtures not containing DTNB (including blanks lacking oxaloacetate), were incubated with enzyme for 10 minutes, and the amount of coenzyme A thiol measured by addition of DTNB at that point.

All kinetic data in this thesis have been interpreted in terms of the Ordered Bisubstrate mechanism and the equation which it predicts (Cleland, 1963). Accordingly, definitions for the various kinetic constants for citrate synthase are given in Figure 20.  $K_{iOAA}$  is the dissociation constant for oxaloacetate, the first substrate to bind to the enzyme.  $K_{OAA}$  is the Michaelis-Menten constant for the binding of oxaloacetate to the enzyme in the presence of saturating acetyl-CoA.  $K_{AcCoA}$  is the corresponding Michaelis-Menten constant for acetyl-CoA in the presence of saturating oxaloacetate. Finally,  $K_{i,\alpha-KG}$  is the dissociation constant for the inhibitor  $\alpha$ -ketoglutarate, measured as a competitive inhibitor of oxaloacetate, in the absence of KCl. Unless otherwise specified, the full steady state kinetic studies on the wild type and missense mutants were all performed in the presence of 0.1M KCl. All data from these studies were initially plotted in double-reciprocal form, points which showed a systematic deviation from the Ordered Bisubstrate equation (Cleland, 1963) were discarded, and the remaining data were fitted to that equation by the GENLSS program of DeTar (1972). This program finds the best values for all four parameters of the

According to the Ordered Bisubstrate equation (Cleland, 1963):



For the competitive inhibitor  $\alpha$ -Ketoglutarate:



The rate equation in the absence of products is:

$$\frac{1}{v} = \frac{1}{V_{\max}} \left( 1 + \frac{K_{\text{OAA}}}{[\text{OAA}]} + \frac{K_{\text{AcCoA}}}{[\text{AcCoA}]} + \frac{(K_{\text{iOAA}}) \cdot (K_{\text{AcCoA}})}{[\text{OAA}] \cdot [\text{AcCoA}]} \right)$$

where

$$V_{\max} = k_{\text{cat}} \cdot [\text{E}]_{\text{total}} = \frac{k_5 k_7}{(k_5 + k_7)} \cdot [\text{E}]_{\text{T}}$$

$$K_{\text{OAA}} = \frac{k_5 k_7}{k_1 \cdot (k_5 + k_7)} = \frac{k_{\text{cat}}}{k_1}$$

$$K_{\text{AcCoA}} = \frac{k_7 \cdot (k_4 + k_5)}{k_3 \cdot (k_5 + k_7)} = \frac{k_{\text{cat}}}{k_3} (1 + k_4/k_5)$$

and

$$K_{\text{iOAA}} = \frac{k_2}{k_1}$$

where  $k_{\text{cat}}$  is the turnover number for citrate synthase; that is, the number of condensations one enzyme molecule catalyzes per second,

and where  $K_{\text{i},\alpha\text{-KG}}$  (the dissociation constant for  $\alpha$ -ketoglutarate to the enzyme) =  $\frac{k_{10}}{k_9}$

Figure 20. Steady state kinetic constants for citrate synthase.

Ordered Bisubstrate equation ( $k_{cat}$ ,  $K_{OAA}$ ,  $K_{AcCoA}$ , and  $K_{iOAA}$ ; as defined above) and assigns an error to each which is approximately equivalent to standard error; for the exact definition of the error see DeTar (1972).

Data illustrated in the form of graphs are typical measurements and not result of averaging several measurements.

### Binding Measurements by ANS Displacement

Binding of acetyl-CoA and other ligands to wild type and mutant citrate synthases was measured by the ANS displacement technique, in which fluorescence is measured as a citrate synthase-ANS complex is titrated with the appropriate ligand. Details of the method, including its theoretical justification, are given by Talgoy and Duckworth (1979). Absolute numbers of binding sites cannot be obtained by this technique unless very tight binding occurs, but the method is a rapid and sensitive way of measuring relative strengths of binding and shapes of binding curves for a variety of ligands and conditions. Data, in the form of changes in fluorescence,  $\Delta F_{obs}$ , as a function of ligand concentration,  $[L]$ , were initially plotted as Scatchard plots ( $\Delta F_{obs}/[L]$  versus  $\Delta F_{obs}$ ), and data sets which gave linear plots were then fitted to the equation for a rectangular hyperbola, using the GENLSS program of DeTar (1972). Data sets whose Scatchard plots were concave down, indicating sigmoid saturation, were fitted to the equation  $\Delta F_{obs} = A[L]^2/(K + [L]^2)$ , where  $A$  is the value of  $\Delta F_{obs}$  which would be attained at saturating  $[L]$ , and  $K$  is a constant whose square root gives the value of  $[L]$  needed to achieve  $\Delta F_{obs} = A/2$ . There is no profound justification for fitting sigmoid saturation curves to this equation (it is simply the Hill (1910) equation with  $n = 2$ ), but it described almost all the sigmoid data well and therefore was a useful way to estimate parameters which empirically described the data, with their errors.

## NADH Binding

NADH binding was measured using the fluorescence enhancement technique of Duckworth and Tong (1976). Measurements were made both in the presence and absence of various ligands (acetyl-CoA, KCl, NAD<sup>+</sup> and oxaloacetate), to determine their effect on NADH binding to wild type citrate synthase and several mutants. For the studies of pH dependence, 15mM sodium phosphate was used for pH values of 7.4 or lower and 20mM Tris-Cl for values of 7.4 or higher; a measurement was made with each buffer at pH 7.4 to test for buffer dependence.

## Physical Studies

Sedimentation equilibrium measurements of molecular weight were as described previously (Tong & Duckworth, 1975). Circular dichroism spectra were determined with a JASCO Model J-500A spectropolarimeter, and  $\alpha$ -helix content was calculated according to Chen *et al.* (1972). Urea denaturation studies were performed as in Morse and Duckworth (1980), in the absence and presence of either NADH (0.5mM) or KCl (0.1M). Modification of citrate synthase with DTNB, both in the presence and absence of 0.1M KCl, has been described previously (Talgoy *et al.*, 1979).

## Media

All media were autoclaved immediately after preparation. JM103 host cells were grown on minimal plates (6g Na<sub>2</sub>HPO<sub>4</sub>, 3g KH<sub>2</sub>PO<sub>4</sub>, 1g NH<sub>4</sub>Cl, 0.5g NaCl per liter) containing 1mM MgSO<sub>4</sub>, 0.1mM CaCl<sub>2</sub>, 1mM thiamine HCl, 0.4% glucose, and 1.5g agar. M13 phage were grown in JM103 host cells in TY liquid culture medium (16g Bacto-tryptone, 10g yeast extract, 5g NaCl per liter, adjusted with NaOH to pH 7.2).

M13 phage were plated in top agar (10g Bacto-tryptone, 8g NaCl, 8g agar per liter) on TYE plates (20g Bacto-tryptone, 10g yeast extract, 16g NaCl, 1.5% agar per liter, adjusted with NaOH to pH 7.2). MOB154 host cells which had been transformed with a plasmid expressing an active citrate synthase enzyme (e.g. pES*glTA*), were selected on minimal plates (as above) containing 1mM cytosine, 1mM thiamine HCl, 0.4% glucose, and 1.5% agar. MOB154 was grown in liquid LB medium (10g Bacto-tryptone, 5g yeast extract, 10g NaCl per liter, adjusted with NaOH to pH 7.2), and plated on the same medium with the addition of 1.5% agar. Large scale MOB154 cultures containing wild type and mutant versions of plasmid pES*glTA*, were grown and plated as the MOB154 cultures above, with the addition of 0.1g ampicillin per mL of medium.

## Reagents

The following reagents were purchased from Boehringer Mannheim (Canada) Ltd: 5-Bromo-4-chloro-3-indolyl- $\beta$ -D-galactopyranoside (X-gal or BCIG), T4 DNA ligase, DNA polymerase I Klenow fragment, and some restriction enzymes. The restriction enzymes FspI and XmnI were obtained from New England Biolabs. Sephadex G-200, agarose NA (specially purified for gel electrophoresis of nucleic acids), coenzyme A (lithium salt), acetyl-CoA (lithium salt), dideoxy- and deoxy-nucleotides, T4 polynucleotide kinase and some restriction enzymes were from Pharmacia (Canada) Ltd. The radioactive nucleotides, [ $\alpha$ -<sup>32</sup>P]dCTP and [ $\alpha$ -<sup>32</sup>P]dATP, were purchased from Du Pont-New England Nuclear. The kit for oligonucleotide-directed *in vitro* mutagenesis was from Amersham Corp. Difco Laboratories supplied the Bacto-tryptone, yeast extract and Bacto-agar (agar). Whatman supplied the DE 52 (DEAE cellulose) and Eastman Organic Chemicals, the N, N, N', N'-Tetramethylenediamine (TEMED). The DTNB, oxaloacetate, formamide and ANS were from Aldrich Chemical Company. The ammonium sulfate (ultra pure)

was from Schwarz/Mann. The bromophenol blue was purchased from Matheson, Coleman and Bell, while the magnesium chloride was from J. T. Baker Chemical Company. Acrylamide, urea and methylene bisacrylamide (BIS) were obtained from both Bio-Rad Laboratories and Serva Feinbiochemica. Dimethyldichlorosilane solution (about 2% in 1,1,1-trichloroethane), magnesium sulphate and glucose were from The British Drug Houses (Canada) Ltd. Xylene cyanol and the Eastman Chromagram Sheet, 13181 Silica Gel with Fluorescent Indicator (No. 6060) were from Kodak. Numerous reagents were purchased from Sigma, including: Trizma base, sodium dodecyl sulfate, glutamic dehydrogenase, egg white lysozyme, bovine serum albumin, Coomassie Brilliant Blue R250, ampicillin, chloramphenicol, ethidium bromide,  $\alpha$ -ketoglutarate, NADH, NAD<sup>+</sup>, adenosine 5'-triphosphate, thiamine HCl, cytosine, isopropyl- $\beta$ -D-thiogalactopyranoside (IPTG), dithiothreitol and some DEAE cellulose. The following reagents were obtained from Fisher Scientific: potassium chloride, sodium chloride, lithium chloride, cesium chloride, calcium chloride, ammonium chloride, ammonium acetate, magnesium acetate, sodium acetate, potassium phosphate (dibasic), sodium phosphate monobasic, cupric sulfate, sodium potassium tartrate, Phenol Reagent 2N Solution (Folin Reagent), glycine, 2-mercaptoethanol, boric acid, ammonium persulfate, EDTA (disodium salt), agarose, polyethylene glycol-6000, acetonitrile, ether, chloroform, N,N-dimethyl formamide, isopropanol, methanol, n-amyl alcohol, ethanol, acetic acid, hydrochloric acid, and sodium hydroxide. Phenol was also purchased from Fisher Scientific, but was redistilled before use.

## **RESULTS**

## Active Site Mutants

## CS $\Delta$ (264-287)

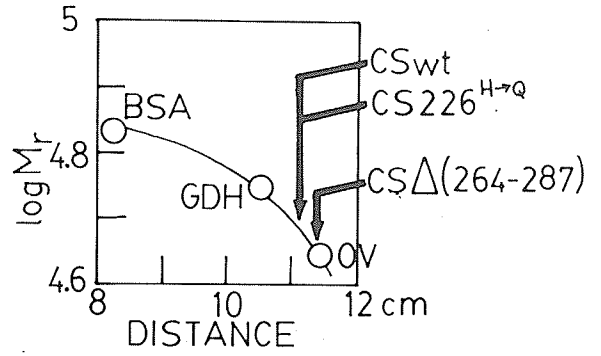
This mutant lacks 24 amino acids including the residue His-264, which is homologous to pig heart citrate synthase residue His-274, vitally involved in catalysis at the active site (Wiegand & Remington, 1986). The plasmid encoding CS $\Delta$ (264-287) did not support growth in the *gltA* defective *E. coli* host strain MOB154, under conditions selective for an active citrate synthase enzyme. Further, this mutant enzyme showed no activity in crude extracts of cultures grown in rich medium, or after purification. It did however, cross-react with rabbit antiserum raised against wild type *E. coli* citrate synthase and thus could be purified like the wild type enzyme, locating citrate synthase protein in fractions by the Ouchterlony double diffusion method (Ouchterlony, 1953) (Figure 21). Since this mutant protein tended to tail severely during passage through the Sephadex G-200 column, the final step in the purification procedure, individual fractions from this column were also monitored by SDS-polyacrylamide gel electrophoresis and the purest fractions pooled. This mutant protein has been prepared three times, and each final preparation consisted of one major band of apparent molecular weight about 45,000 g/mole (expected subunit molecular weight: 45,343 g/mole), plus five minor bands (Figure 21). These preparations are estimated to be about 80% pure. An absorption spectrum of the purified CS $\Delta$ (264-287) protein showed a large amount of light scattering. Protein concentrations, determined by measuring absorbance at 278nm ( $\epsilon_m = 46,780$ ), were then corrected for this effect by assuming the standard linear relationship between the inverse fourth power of the wavelength and absorbance.

High speed sedimentation equilibrium measurements on purified CS $\Delta$ (264-287) indicated that its weight-average molecular weight under native conditions was 240,000  $\pm$  10,000 g/mole while that of the wild type enzyme was 260,000  $\pm$  10,000 g/mole. The fact that the deletion mutant, and to a lesser extent, the wild type protein, were

Figure 21. **A)** SDS–polyacryamide gel showing the subunit size of CSA(264–287), as compared to wild type citrate synthase (CSwt) and a point mutant, CS226<sup>H→Q</sup>. **B)** Ouchterlony double-diffusion plate to demonstrate immunological identity between CSA(264–287), wild type citrate synthase (CSwt) and, CS226<sup>H→Q</sup>. The center well contained 5μL of undiluted rabbit anti–wild type *E. coli* citrate synthase antiserum. The upper right well contained 5μL of CSA(264–287) protein (0.21mg/mL); while the upper center well contained 5μL of CSwt enzyme (0.19mg/mL), and the upper left well contained 5μL of CS226<sup>H→Q</sup> enzyme (0.17mg/mL). Diffusion proceeded at 37°C and the photograph was taken after 20 hours.

A) SDS GEL

CSwt  
 CS226<sup>H→Q</sup>      CSΔ(264-287)



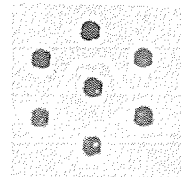
BSA (68000)

GDH (56000)

OV (44000)

B) OUCHTERLONY PLATE

CS226<sup>H→Q</sup>      CSwt      CSΔ(264-287)



somewhat dissociated, may explain why these values were both 10–12% lower than expected from amino acid sequence information. This indicates that CSA(264–287) is still able to form a species of similar quaternary structure to the wild type enzyme, so that the deletion of 24 amino acids does not appear to prevent aggregation of the subunits into hexamers. The tailing observed in the Sephadex G–200 gel filtration, however, suggests that this aggregation is not completely normal.

The part of the sequence deleted is predicted, from homology between *E. coli* citrate synthase and the pig heart enzyme, to include all of the N helix, plus the N–O corner and a few residues of the O helix (Figure 22). If the model is correct, the mutant is expected to contain 18 less residues (of the 275 in the wild type subunit) involved in  $\alpha$ -helical secondary structure, or about 6.5%, simply as a result of the deleted residues; but the probable distortion of the remainder of the O helix may well increase this value to as much as 9.8% (27 out of 275). When circular dichroism was used to compare the secondary structure of CSA(264–287) with that of the wild type enzyme, the  $\alpha$ -helix content whose contribution is most pronounced at 222 nm (Chen *et al.*, 1972) was about 9% lower for the deletion mutant (Figure 23). It should be noted though, that this method of determination gave values for the  $\alpha$ -helical content for the two proteins of 35% and 26%, for wild type and mutant respectively, when the model predicts values in the range of 66% and 63–65%. As well, it was quite difficult to determine the concentration of the poorly behaved mutant protein solution with any amount of accuracy because of the light scattering problem discussed previously. Nevertheless, the obvious shape difference between the two circular dichroism spectra shown in Figure 23, especially at 222 nm, confirms that the deletion mutant has significantly less  $\alpha$ -helical secondary structure than the wild type protein.

Since CSA(264–287) was inactive, no kinetic studies were possible, but NADH binding was measured by the fluorescence enhancement method of Duckworth and Tong (1976). CSA(264–287), like the wild type citrate synthase, bound NADH in a



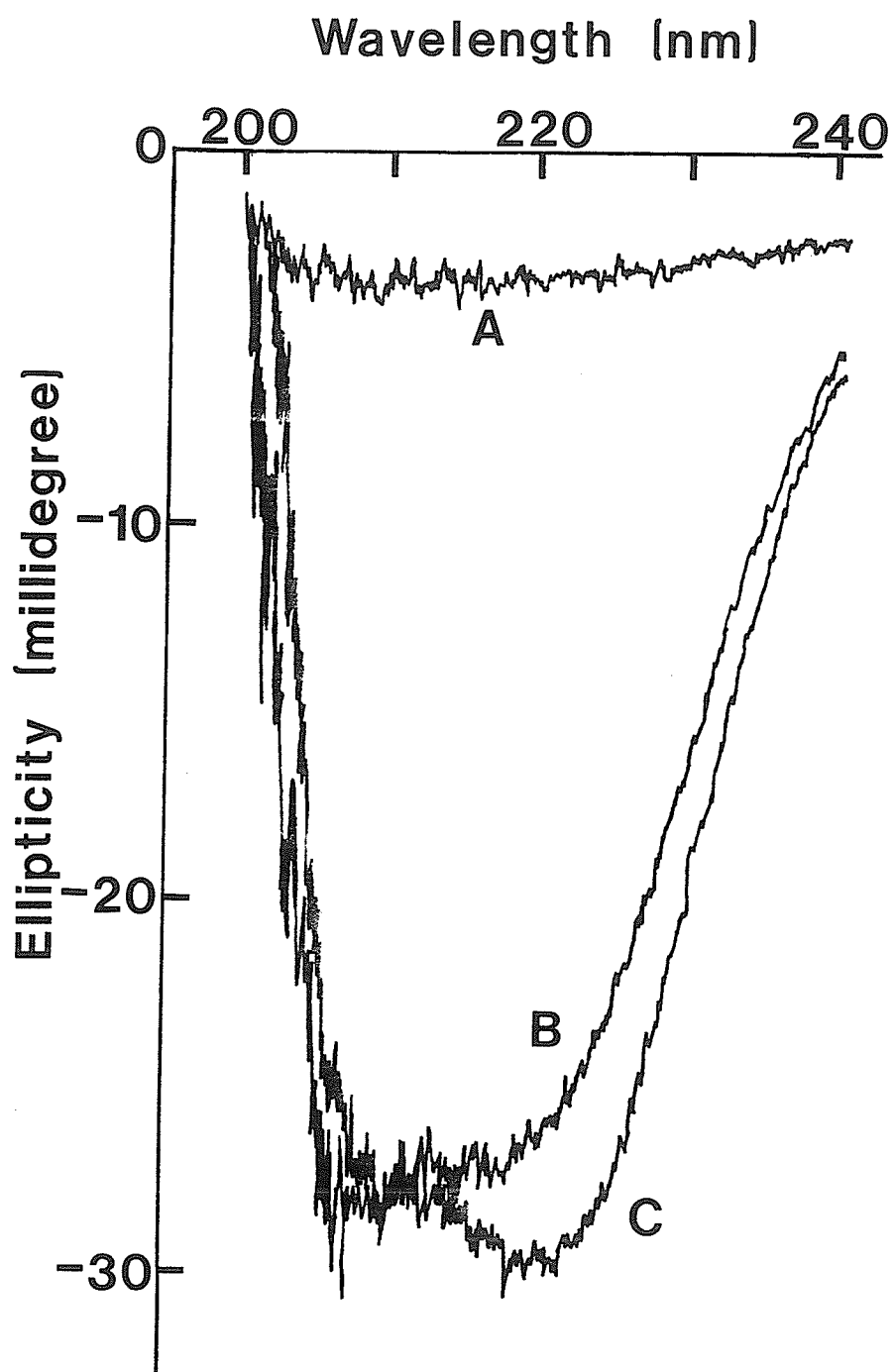


Figure 23. Circular dichroism spectra of wild type citrate synthase and deletion mutant, CS $\Delta$ (264-287), in Tris buffer. A) buffer blank; B) CS $\Delta$ (264-287), 0.25mg/mL; C) wild type, 0.24mg/mL.

pH-dependent manner (Figure 24). The dissociation constant was smallest at low pH, and the number of sites occupied at saturation decreased as pH was raised. In the case of the wild type enzyme, it has previously been shown that the change in the number of sites with pH is not an artifact of the binding method used (Duckworth & Tong, 1976); it may be the result of the changing degree of aggregation of subunits as the pH is changed (Tong & Duckworth, 1975). Less NADH was bound to CSA(264–287) than to the wild type citrate synthase, and the binding was tighter throughout the pH range (Figure 24), but detection of strong, pH-dependent binding of NADH indicates that the basic features of the sites are essentially normal.

Both the substrate, acetyl-CoA, and the activator, KCl weakened NADH binding, in the case of the deletion mutant as with the wild type enzyme (Figure 25). The inactive CSA(264–287) appeared less sensitive to the effect of KCl, by this criterion, but the difference may not be significant. Acetyl-CoA was equally effective with both proteins.

#### Binding of Coenzyme A Derivatives to CSA(264–287):

The binding of acetyl-CoA and coenzyme A to CSA(264–287) was measured by the ANS-displacement method of Talgoy and Duckworth (1979). The basis for this method has been explained under Methods. For the wild type enzyme, acetyl-CoA and coenzyme A each caused a saturable decrease in the fluorescence of ANS-citrate synthase mixtures (Figure 26, Panel A), from which values of  $L_{0.5}$ , the concentration of ligand needed to achieve half the maximal decrease, were calculated. These  $L_{0.5}$  values were about 270  $\mu$ M for wild type citrate synthase and were decreased by 0.1M KCl, a known activator of *E. coli* citrate synthase, which has previously been shown to shift the substrate saturation curve for acetyl-CoA to lower concentrations (Faloona & Srere, 1969). Oxaloacetate (0.2mM) also decreased the  $L_{0.5}$  value for coenzyme A, and the combination of oxaloacetate and KCl decreased the parameter still further

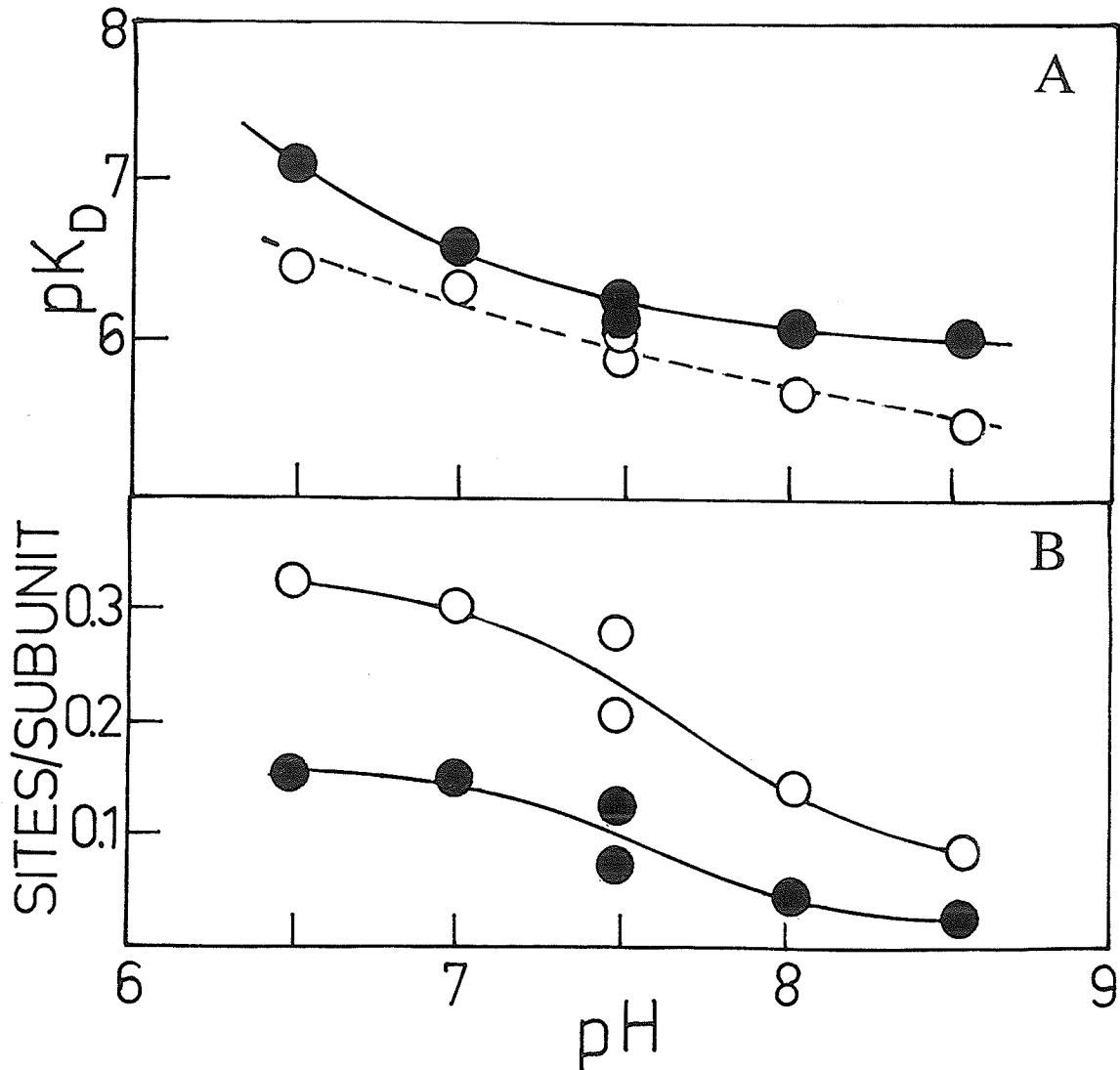


Figure 24. The pH dependence of binding parameters for the NADH-citrate synthase complex. A)  $pK_D$  versus pH; B) number of binding sites per subunit. Data are shown for wild type enzyme (O) and CSA(264-287) (●).

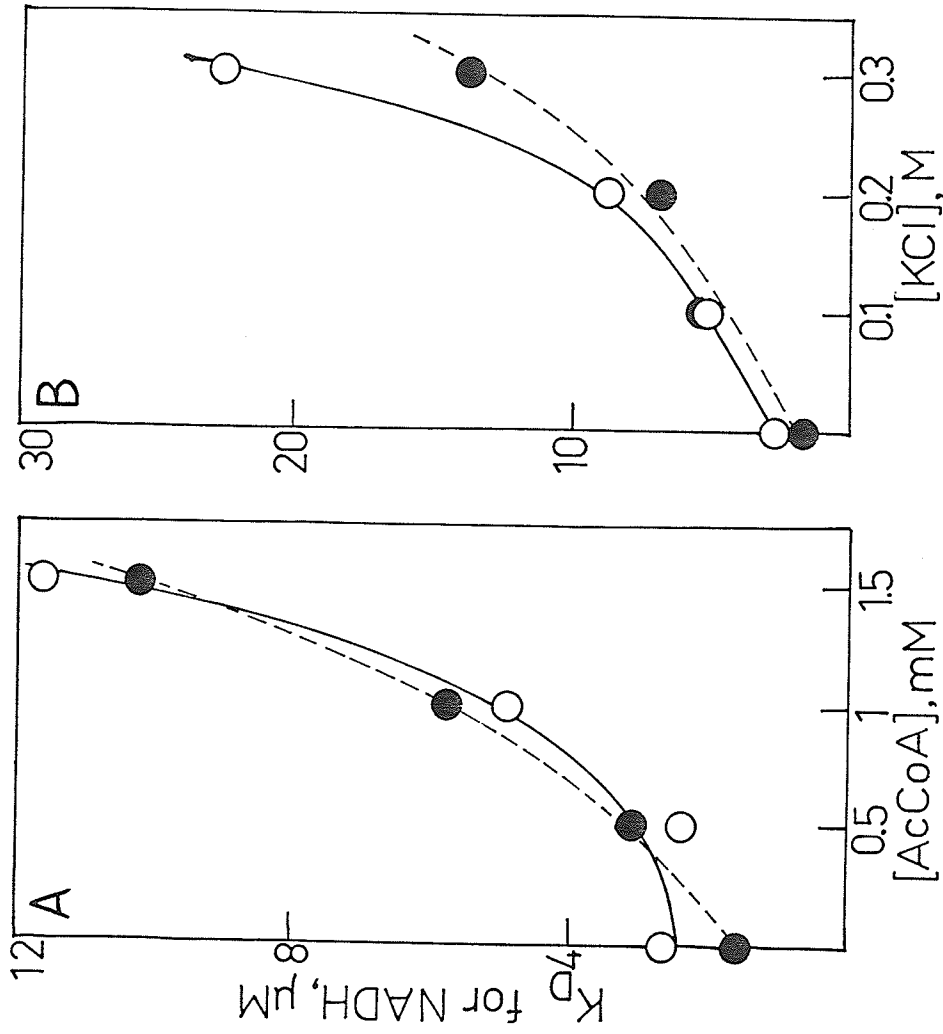


Figure 25. Effects of acetyl-CoA (AcCoA) (A) and KCl (B) on dissociation constant for the NADH-citrate synthase complex in Tris buffer at pH 7.8. Data are shown for wild type enzyme (O) and CSA(264-287) (●).

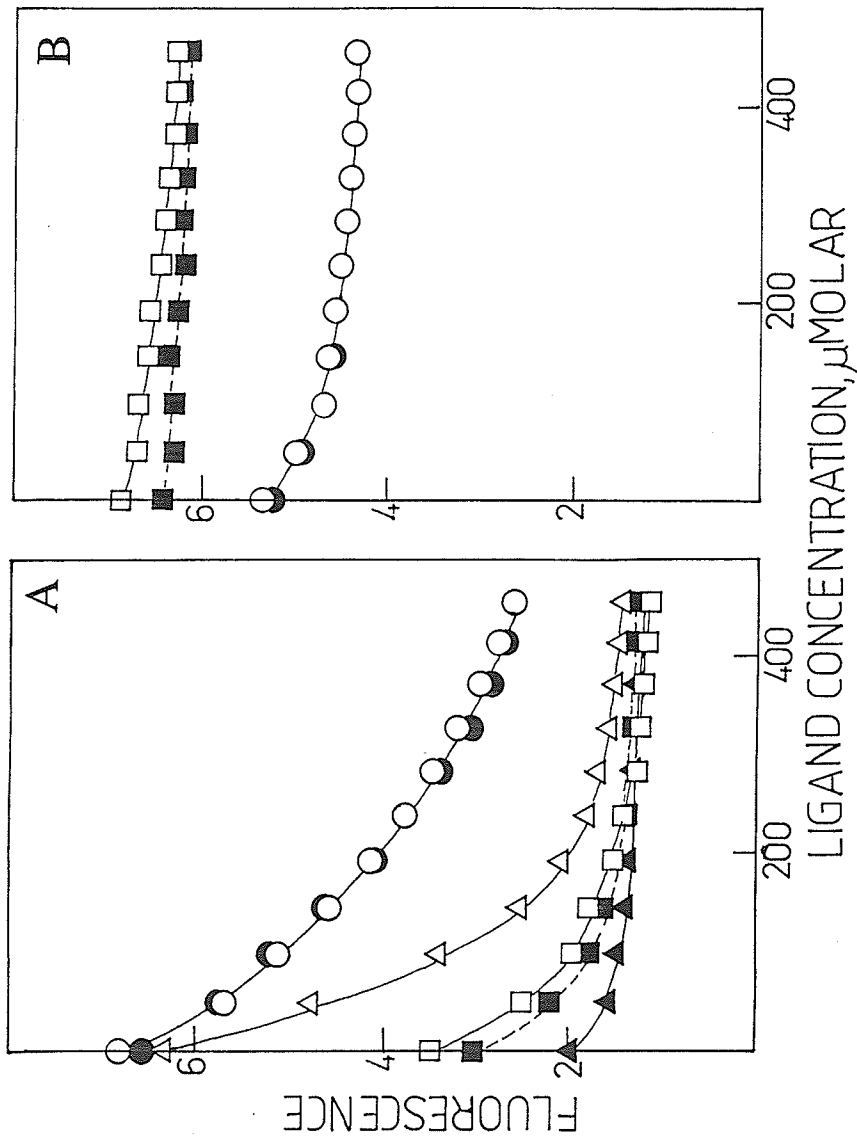


Figure 26. Measurement by ANS displacement of binding of ligands to wild type citrate synthase (A) and CSA(264-287) (B). Data are shown for titration of the ANS-citrate synthase complex with coenzyme A (●) or acetyl-CoA (○) in Tris buffer, pH 7.8; with coenzyme A (■) or acetyl-CoA (□) in the same buffer containing 0.1M KCl; with coenzyme A in the same buffer containing 0.2mM oxaloacetate (Δ); and in the same buffer containing 0.2mM oxaloacetate plus 0.1M KCl (▲). In B, only the first four titrations are shown, since oxaloacetate made no difference to the coenzyme A titrations involving CSA(264-287).

(Figure 26A). In contrast to the situation with the wild type enzyme, the deletion mutant showed relatively tight binding of both coenzyme A ligands, with an  $L_{0.5}$  value of about  $100\mu\text{M}$ , which was slightly weakened by  $0.1\text{M}$  KCl (Figure 26, Panel B). The total amount of fluorescence decrease induced by these ligands was much smaller than that observed with the wild type protein. Oxaloacetate,  $0.2\text{mM}$ , had no effect on coenzyme A saturation and so is not shown in Figure 26B for the sake of clarity. A further difference between  $\text{CS}\Delta(264-287)$  and the wild type protein was the effect of KCl alone on the fluorescence of the ANS-citrate synthase complex. In the case of the wild type citrate synthase, the fluorescence obtained for the same ANS-citrate synthase mixture was about 50% as great in the presence of  $0.1\text{M}$  KCl as in its absence (Figure 26A). With  $\text{CS}\Delta(264-287)$ ,  $0.1\text{M}$  KCl actually increased this fluorescence about 25%. Note that the total fluorescence observed with the deletion protein, in the absence of KCl, was approximately the same as that for wild type citrate synthase (Figure 26B).

## CS226<sup>H→Q</sup> and CS229<sup>H→Q</sup>

Originally, X-ray diffraction data from pig heart citrate synthase had implicated the residues equivalent to His-226 and His-229 of *E. coli*, in the binding of citrate and probably oxaloacetate at the active site (Remington *et al.*, 1982). The location of these two histidine residues is shown in Figure 27. The more recent refinement of the pig heart enzyme structure by Wiegand and Remington (1986), has led to the conclusion that the His-226 equivalent is not directly involved in binding, while the His-229 equivalent is believed to form either a hydrogen bond or an ion pair with a carboxylate anion of citrate and oxaloacetate. To determine if these conserved histidines play the same role in the *E. coli* enzyme, each has been mutated to glutamine.

### Steady State Kinetic Studies:

Double reciprocal plots of reaction velocities as a function of concentrations of the two substrates, oxaloacetate and acetyl-CoA, are shown in Figure 28 for wild type *E. coli* citrate synthase and the two missense mutants. As explained in the Introduction, the catalytic mechanism is probably Ordered bisubstrate, with oxaloacetate binding first. The data in Figure 28 conform in general to the steady state rate equation for this mechanism (Cleland, 1963), except that, for both mutants, acetyl-CoA saturation curves are sigmoid, not hyperbolic, at all but the highest substrate concentrations (Figure 28, Panels E & F). Interpretation of the data in Figure 28 in terms of the steady state equation for this mechanism (Cleland, 1963) yields the parameters in Table 4.

The CS226<sup>H→Q</sup> protein behaved like the wild type enzyme during purification, and gave a single band of molecular weight about 48,000 g/mole on an SDS gel (Figure 21). Its specific activity in the standard assay (0.1M KCl; 0.1mM each of acetyl-CoA and oxaloacetate; pH 7.8) was 17U/mg, compared with 36U/mg for the

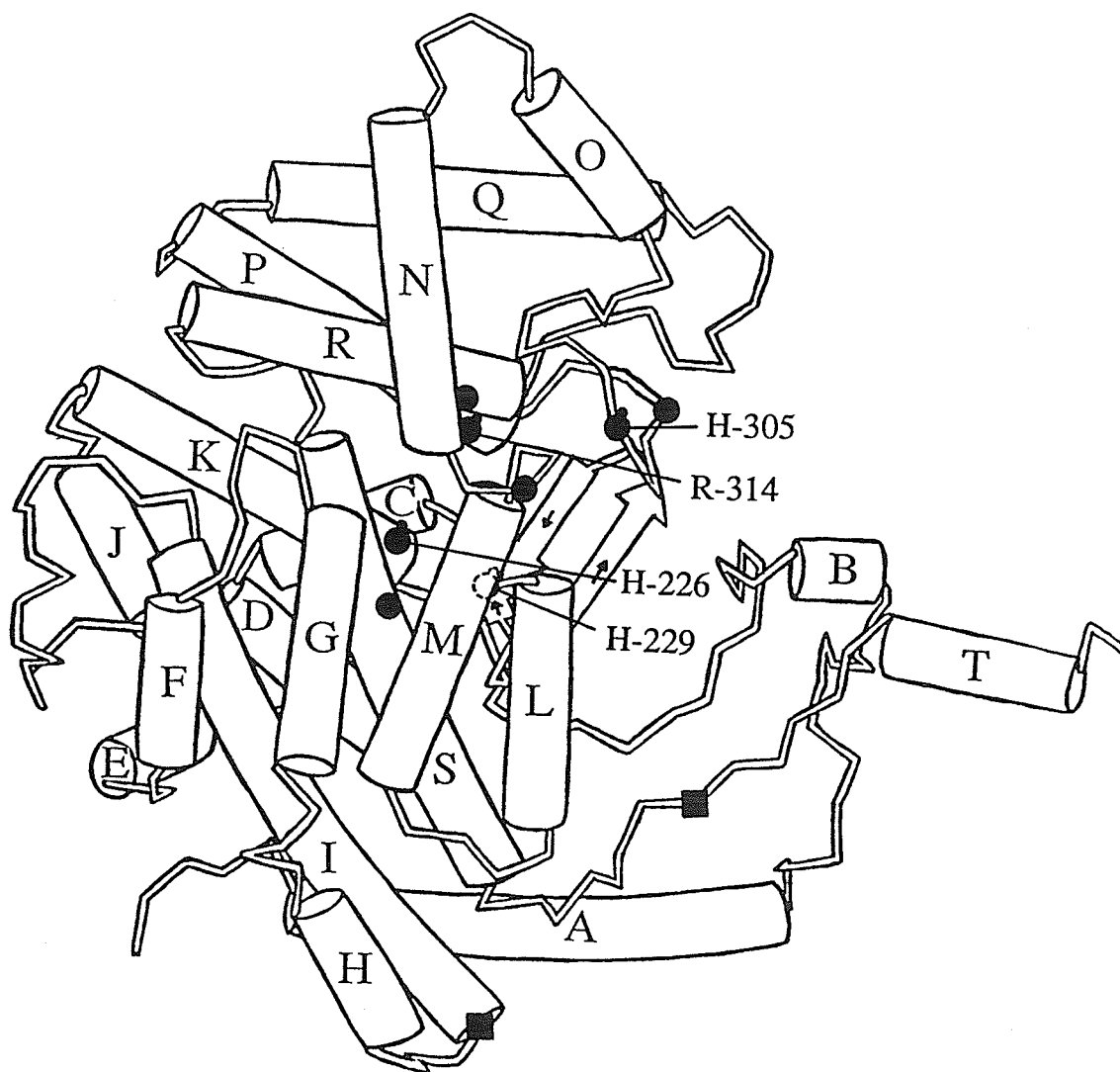
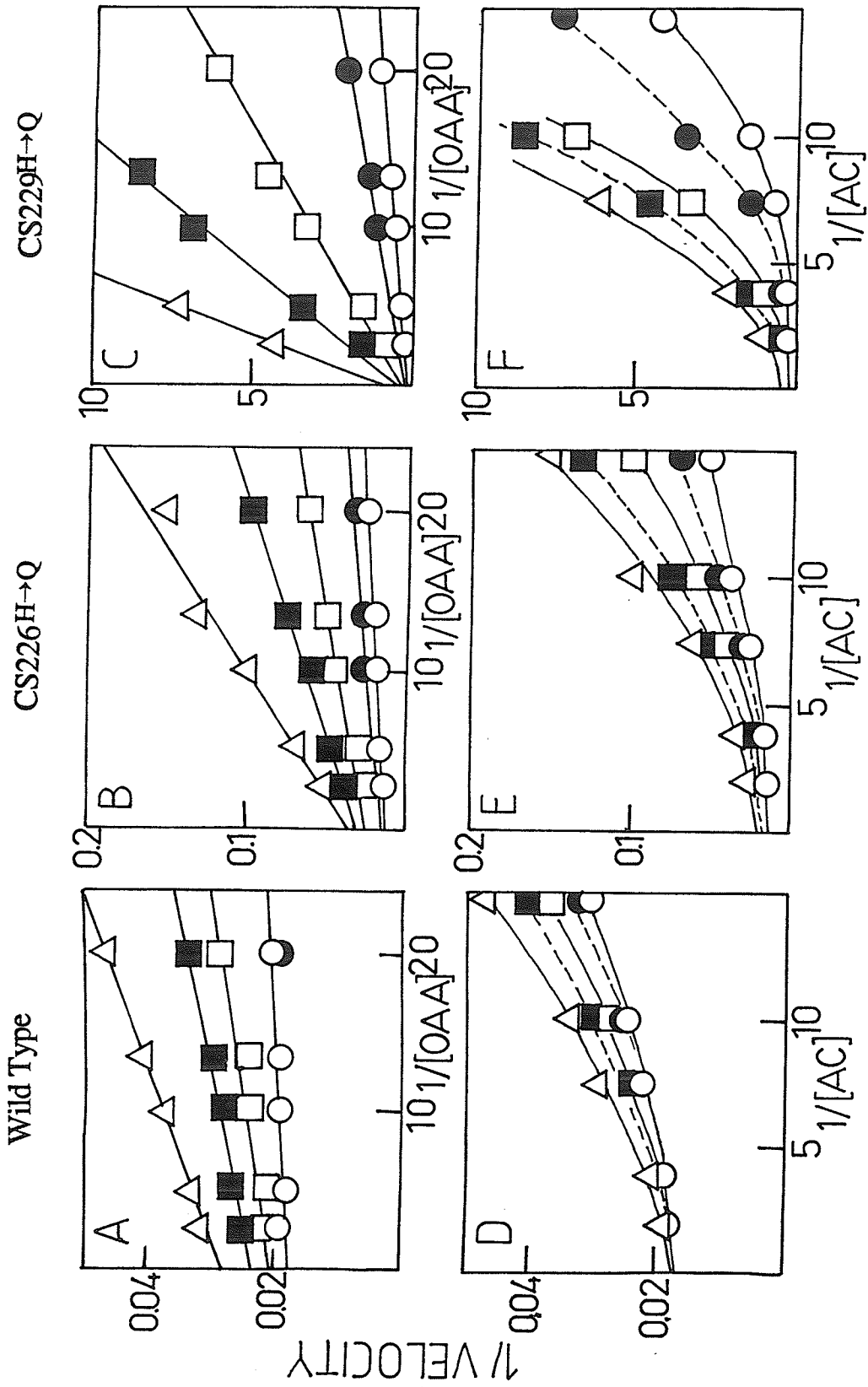


Figure 27. Model of an *E. coli* citrate synthase subunit showing the location of His-229, His-305 and Arg(R)-314. Each one of these is an active site residue. In addition, another conserved histidine, His-226, is also shown. His-229 is concealed in the diagram behind Helix M, on the section of random coil between Helices K and L, and is shown as a dashed circle. Each of these residues (indicated by a small dot) have been mutated separately, in a mutagenesis experiment.

Figure 28. Steady state kinetics of wild type citrate synthase and mutants, CS226H $\rightarrow$ Q and CS229H $\rightarrow$ Q. Double reciprocal plots. Velocity is expressed as moles of product produced per second per mole of citrate synthase subunit; substrate concentrations are in mM, and measurements were made in Tris buffer, pH 7.8 with 0.1M KCl also present. Panels A and D are for wild type enzyme, panels B and E for CS226H $\rightarrow$ Q, and panels C and F for CS229H $\rightarrow$ Q. For panels A, B and C, oxaloacetate (OAA) levels were varied at 0.07 (○), 0.1 (●), 0.133 (□) and 0.3 (■) and 0.5 (Δ) mM acetyl-CoA. For panels D, E and F, acetyl-CoA (AC) levels were varied at 0.05 (○), 0.075 (●), 0.1 (□), 0.2 (■) and 0.4 (Δ) mM oxaloacetate. Many points were omitted for clarity, in particular a number near the vertical axis in panels C and F, used to define the intercepts on that axis more accurately.



wild type enzyme. Its sensitivity to activation by KCl, and the amount of KCl needed to achieve half-maximal activation were similar, although not identical, to wild type values (Table 4). CS226<sup>H→Q</sup> showed normal sensitivity to NADH inhibition (measured kinetically), and its binding of NADH (measured by fluorescence enhancement), both in the presence and absence of various ligands, was normal (Table 5). It was however, less sensitive to inhibition by  $\alpha$ -ketoglutarate. This point is shown clearly in Figure 29, Panel B, where  $\alpha$ -ketoglutarate was tested as a competitive inhibitor with respect to oxaloacetate. The  $K_i$  for  $\alpha$ -ketoglutarate under these conditions was 840 $\mu$ M for CS226<sup>H→Q</sup> and 93 $\mu$ M for the wild type citrate synthase (Table 4).  $K_{OAA}$ , the true  $K_M$  for oxaloacetate (determined by extrapolation to saturating acetyl-CoA) was the same for the His-226 mutant as for the wild type, but perhaps a better measure of the strength of interaction of oxaloacetate with the free enzyme is obtained by determining  $K_{iOAA}$ , the dissociation constant for the binary complex. This parameter may be extracted readily from substrate saturation data for enzymes whose kinetics follow the Ordered bisubstrate mechanism and give linear replots (Cleland, 1963); but the appropriate replots of data from CS226<sup>H→Q</sup> were curved. By working with data at the highest concentrations of acetyl-CoA used, however, and assuming that the Ordered mechanism is a good approximation at these concentrations, a  $K_{iOAA}$  value of 140 $\pm$ 30 $\mu$ M was obtained for the His-226 mutant, 4 times that of the wild type enzyme.

Mutant protein CS229<sup>H→Q</sup> was also active and could be purified like the wild type enzyme; the purified enzyme again gave a single band, of molecular weight about 48,000 g/mole on an SDS gel. The specific activity of this enzyme was only 0.14U/mg, about 0.4% of the wild type value, in the standard assay. The parameters for activation by KCl were similar to those for wild type enzyme, and most of the reduced activity could be traced to the fact that the mutant enzyme had a substantially lower affinity for oxaloacetate;  $K_{OAA}$  was some 18 times and  $K_{iOAA}$  more than 50 times the wild type values (Table 4). The  $k_{cat}$  for this mutant was about one-tenth that

Table 4. Steady State Kinetic Parameters for Wild Type Citrate Synthase and Mutants CS226<sup>H→Q</sup> and CS229<sup>H→Q</sup>.

Parameter	Wild Type	CS226 <sup>H→Q</sup>	CS229 <sup>H→Q</sup>
$k_{\text{cat}}$ , sec <sup>-1</sup>	81±6 <sup>b</sup>	98±14	9.3±1.0
$K_{\text{AcCoA}}$ , μM	120±20	260±70	190±30
$K_{\text{OAA}}$ , μM	26±5	17±13	460±260
$K_{\text{iOAA}}$ , μM	33±7	140±30	1800±500
$K_{\text{i, } \alpha\text{-KG}}$ , μM	93±18	840±380	>2000
KCl Activation Ratio <sup>a</sup>	39±3	57±11	56±14
$K_{\text{M}}^{\text{a}}$ , KCl, mM	28±4	57±19	67±26
$K_{\text{i}}$ , NADH, μM	3.3±0.1	1.97±0.04	1.4±0.1
Maximum % Inhibition by NADH	99±1	96±1	92±5

<sup>a</sup> KCl activation data, expressed as increases in reaction rate as a function of [KCl], were fitted to the Michaelis-Menten equation by the GENLSS program (See Methods section). Parameters quoted are  $K_{\text{M}}$  (the apparent Michaelis constant for KCl) and "Activation Ratio", the ratio of the limiting catalytic rate at saturating KCl to the rate obtained without KCl. All measurements were in Tris buffer, pH 7.8, with oxaloacetate and acetyl-CoA each at 0.1 mM. Data at [KCl] up to 100 mM were used, because of inhibition at concentrations higher than this.

<sup>b</sup> For the method of calculation and the significance of the errors see the Methods section.

Table 5. NADH Binding for Wild Type Citrate Synthase and Mutants CS226<sup>H→Q</sup> and CS229<sup>H→Q</sup>.

K <sub>D</sub> measured in the presence of:	Wild Type	CS226 <sup>H→Q</sup>	CS229 <sup>H→Q</sup>
—	1.94±0.07 <sup>a</sup> (0.42-0.74) <sup>b,c</sup>	2.34±0.01 (0.77±0.01) <sup>b</sup>	2.14±0.18 (0.70±0.02) <sup>b</sup>
0.1M KCl	3.68±0.05 (0.53±0.03)	3.57±0.18 (0.65±0.02)	3.56±0.13 (0.53±0.01)
0.2M KCl	6.87±0.16 (0.49±0.01)	7.23±0.48 (0.62±0.23)	5.32±0.21 (0.50±0.01)
0.3M KCl	11.8±0.5 (0.43±0.01)	19.1±1.6 (0.56±0.04)	11.5±0.6 (0.52±0.02)
0.5mM AcCoA	3.09±0.16 (0.50±0.01)	2.89±0.17 (0.74±0.02)	3.81±0.08 (0.63±0.01)
1.0mM AcCoA	6.69±0.41 (0.57±0.02)	6.08±0.25 (0.81±0.18)	7.5±1.6 (0.65±0.05)
1.5mM AcCoA	6.79±0.33 (0.54±0.02)	10.33±0.43 (0.85±0.02)	9.57±0.44 (0.51±0.02)
0.1mM OAA	1.91±0.17 (0.56±0.02)	2.24±0.11 (0.79±0.01)	1.99±0.06 (0.70±0.01)
1 mM NAD <sup>+</sup>	5.47±0.54 (0.65±0.03)	3.57±0.01 (0.74±0.01)	4.50±0.06 (0.67±0.01)

<sup>a</sup> For the method of calculation and the significance of the errors see the Methods section.

<sup>b</sup> Quantities in brackets are the numbers of NADH sites occupied per enzyme subunit at saturation.

<sup>c</sup> Range of values found with different preparations.

for the wild type enzyme. Most strikingly, Panel C of Figure 29 shows that  $\alpha$ -ketoglutarate did not inhibit CS229<sup>H→Q</sup> at all, at concentrations as high as 0.8mM. The data actually show a slight activation by  $\alpha$ -ketoglutarate, which may perhaps be attributed to the increase in ionic strength when buffered  $\alpha$ -ketoglutarate was added to the assay solutions. Inhibition of the His-229 mutant by NADH (Table 4) and binding of that nucleotide (Table 5) were normal.

#### Measurements of Ligand Binding by ANS-Displacement:

Because of the instability of oxaloacetate at pH values above 7, conventional methods of measuring the binding of this ligand to citrate synthase and its mutants were not attempted, but the ANS displacement technique did allow indirect measurements of binding constants. Both mutants and the wild type enzyme showed a saturable decrease in the fluorescence of ANS-citrate synthase mixtures upon addition of acetyl-CoA and coenzyme A, from which  $L_{0.5}$  values were calculated (Table 6). Each enzyme showed a decrease in its respective  $L_{0.5}$  value in the presence of 0.1M KCl. Oxaloacetate (0.2mM) also decreased the  $L_{0.5}$  value for coenzyme A, in the case of the wild type enzyme and CS226<sup>H→Q</sup>, and the combination of oxaloacetate and KCl decreased the parameter still further (Table 6). For CS229<sup>H→Q</sup>, 0.2mM oxaloacetate had no effect on the  $L_{0.5}$  value for coenzyme A, in the presence or the absence of 0.1M KCl. This is not unexpected in light of the weak affinity of this mutant for oxaloacetate, already demonstrated by the steady state kinetic studies above.

As found previously (Talgy & Duckworth, 1979), oxaloacetate alone did not cause an appreciable decrease in the fluorescence of ANS-citrate synthase mixtures, but did so if 0.2mM coenzyme A was also present, because of the fact that oxaloacetate tightens coenzyme A binding. From this indirect effect, oxaloacetate saturation of wild type enzyme and the His-226 mutant could be measured, in the presence and absence of  $\alpha$ -ketoglutarate. As expected,  $\alpha$ -ketoglutarate was a competitive inhibitor of the

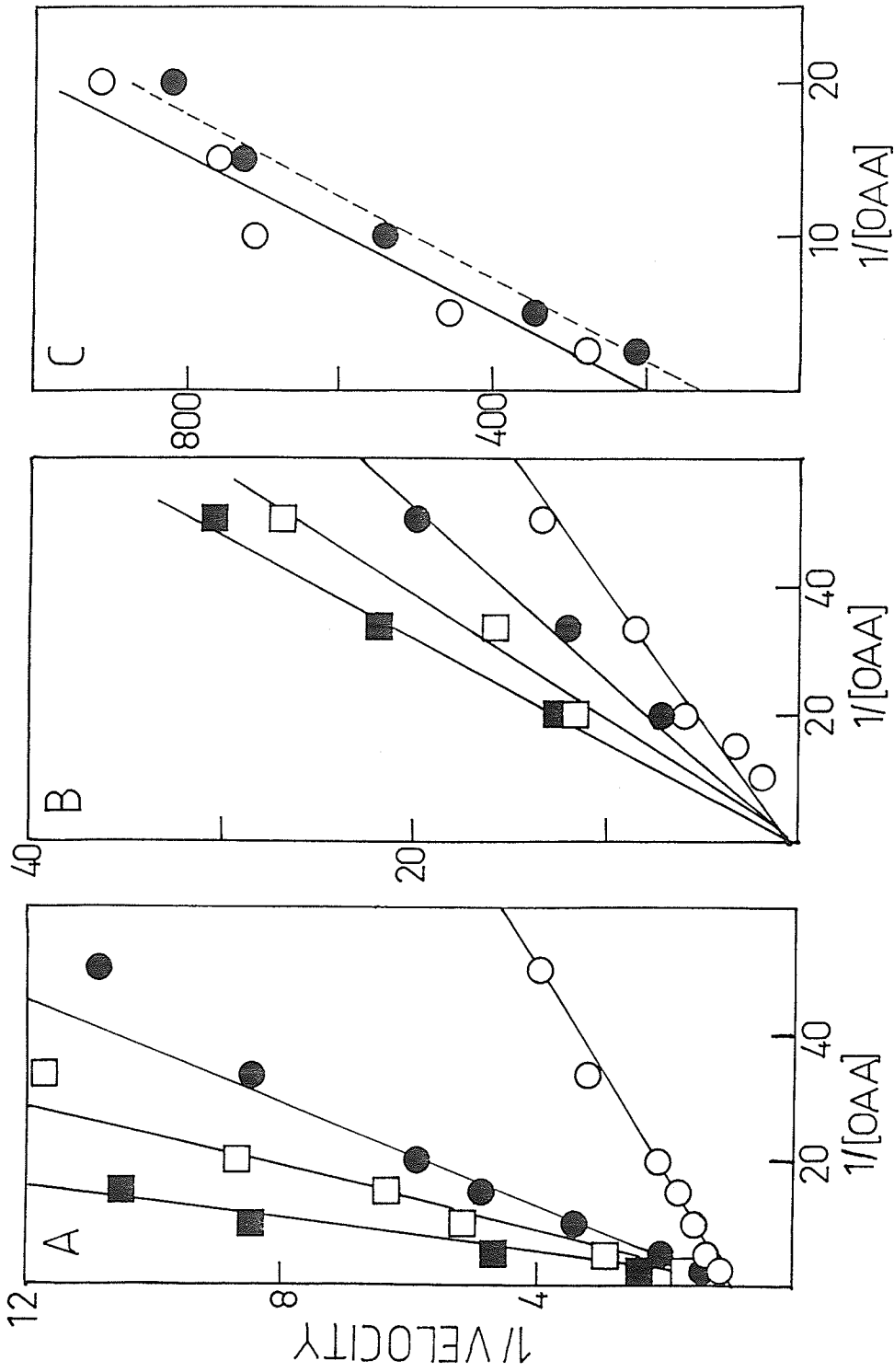


Figure 29. Inhibition of wild type citrate synthase, CS226H→Q and CS229H→Q by  $\alpha$ -ketoglutarate. Double reciprocal plots. Units of velocity and oxaloacetate concentration were as in Figure 28, but no KCl was added. For panel A (wild type) and panel B (CS226H→Q),  $\alpha$ -ketoglutarate concentrations were zero (○), 0.2mM (●), 0.4mM (□) and 0.8mM (■); for panel C (CS229H→Q),  $\alpha$ -ketoglutarate concentrations were zero (○) and 0.8mM (●).

Table 6. Parameters for Ligand Binding to Wild Type Citrate Synthase and Mutants CS226H $\rightarrow$ Q and CS229H $\rightarrow$ Q, as Measured by ANS-Displacement.

Parameter	Wild Type		CS226H $\rightarrow$ Q		CS229H $\rightarrow$ Q	
	no KCl	0.1M KCl	no KCl	0.1M KCl	no KCl	0.1M KCl
L <sub>0.5</sub> , AcCoA, $\mu$ M	260 $\pm$ 40 <sup>a</sup> (* <sup>b</sup> )	60 $\pm$ 3 (0.64)	410 $\pm$ 50 (0.69)	115 $\pm$ 3 (0.63)	230 $\pm$ 20 (0.69)	120 $\pm$ 1 (0.61)
L <sub>0.5</sub> , CoA, $\mu$ M	270 $\pm$ 40 (* <sup>b</sup> )	53 $\pm$ 3 (0.57)	380 $\pm$ 30 (0.69)	106 $\pm$ 3 (0.61)	240 $\pm$ 20 (0.69)	120 $\pm$ 2 (0.58)
L <sub>0.5</sub> , CoA, $\mu$ M <sup>c</sup>	73 $\pm$ 3 (0.78)	47 $\pm$ 5 (0.38)	137 $\pm$ 8 (0.69)	52 $\pm$ 1 (0.59)	190 $\pm$ 10 (0.67)	123 $\pm$ 1 (0.57)
K <sub>D</sub> , OAA, $\mu$ M <sup>d</sup>	25 $\pm$ 1 (0.54)	ND <sup>e</sup>	60 $\pm$ 10 (0.67)	ND	>200	ND
K <sub>D</sub> , $\alpha$ -KG, $\mu$ M <sup>f</sup>	76 $\pm$ 11	ND	1000 $\pm$ 300	ND	>4000	ND

<sup>a</sup> For the method of calculation and the significance of the errors see the Methods section.

<sup>b</sup> Quantities in brackets are the fractions of initial fluorescence of ANS-citrate synthase complex quenched by saturating amounts of ligand; in all cases the uncertainties are no more than  $\pm 0.05$ .

\* Fraction of initial fluorescence quenched at saturation could not be estimated precisely by curve-fitting, and so was taken to fall somewhere between the maximum observed and the maximum possible, making the uncertainty in the L<sub>0.5</sub> values quite large.

<sup>c</sup> Measured in the presence of 0.2mM oxaloacetate.

<sup>d</sup> Measured in the presence of 0.2mM coenzyme A.

<sup>e</sup> ND = not determined.

<sup>f</sup> Measured in the presence of 0.2mM coenzyme A; calculated from the effect on K<sub>D</sub> for oxaloacetate. For the wild type enzyme, and most mutants, 0.4mM  $\alpha$ -ketoglutarate was present; but for the two mutants: CS226H $\rightarrow$ Q and CS229H $\rightarrow$ Q, 5mM was used.

oxaloacetate effect, and apparent dissociation constants for oxaloacetate and  $\alpha$ -ketoglutarate, in the presence of 0.2mM coenzyme A, were calculated (Table 6). Binding of oxaloacetate to the His-229 mutant in the presence of 0.2mM coenzyme A was so weak that no change in fluorescence was detected unless very large amounts of oxaloacetate were added. Such concentrations, 5mM and above, caused a net increase in fluorescence which did not become saturated over the concentration range tested, and this effect is regarded as an unexplained artifact.

## CS305H→A and CS314R→L

Determination of the three-dimensional structure of pig heart citrate synthase, both alone and as a complex with the product, citrate, has led to the suggestion that an important feature of the catalytic mechanism is the polarization of the carbonyl of oxaloacetate by a polar interaction with the side chain of His-320 (Wiegand & Remington, 1986). Also, nearby is Arg-329, which has been shown to interact with the corresponding hydroxyl group of citrate (see Introduction), so that it could likewise play a role in polarization. The fact that oxaloacetate does undergo carbonyl polarization when it binds to the pig heart enzyme has been demonstrated by Kurz *et al.* (1985). *E. coli* citrate synthase has residues homologous to His-320 and Arg-329, His-305 and Arg-314 respectively (Ner *et al.*, 1983), which are shown in Figure 27. To confirm that the same roles are being played by these conserved residues in the *E. coli* enzyme, two mutants have been created; one with His-305 changed to alanine, and the other with Arg-314 mutated to leucine.

The plasmid encoding the His-305 mutant, CS305<sup>H→A</sup>, supported the growth of the *E. coli* strain MOB154, on minimal medium in the absence of glutamate, at a rate much less than the wild type plasmid, while that encoding the Arg-314 mutant, CS314<sup>R→L</sup>, did not sustain growth under these conditions. This was the first indication that the mutated *gltA* genes in these plasmids were, in one case only marginally sufficient, and in the other case inadequate to supply the normal cellular requirements for citrate synthase. The proteins could be purified in the usual way, however, with comparable amounts of protein produced to the wild type case; and each gave a single band of molecular weight about 48,000 g/mole on an SDS gel. The circular dichroism spectra of both mutant proteins were the same as that of the wild type enzyme, indicating that the mutations had not led to a substantial rearrangement of the secondary structure.

### Steady State Kinetic Studies:

As stated previously, both enzymes possessed extremely low specific activities: 0.004U/mg for CS305<sup>H→A</sup> and 0.032U/mg for CS314<sup>R→L</sup>, in the standard assay. Table 7 shows the kinetic parameters for the forward citrate synthase reaction. As can be seen, the most dramatic effect caused by each of the two mutations was on  $k_{cat}$ , the turnover number for the enzyme (Table 7). There were smaller effects on  $K_{OAA}$ , the Michaelis constant for oxaloacetate in the presence of saturating amounts of acetyl-CoA, and  $K_{iOAA}$ , the dissociation constant of the enzyme-OAA complex in the absence of bound acetyl-CoA. Precise determination of these parameters for CS305<sup>H→A</sup> was not possible, since only a narrow range of acetyl-CoA concentrations provided useful data for steady state kinetic analysis, because of sigmoid saturation at concentrations of acetyl-CoA less than 0.3mM and substrate inhibition at levels above 0.75mM. The Michaelis constant for acetyl-CoA in the presence of saturating oxaloacetate,  $K_{AcCoA}$ , is actually slightly lower for both mutant enzymes than for the wild type (Table 7). The ratios  $k_{cat}/K_{OAA}$  and  $k_{cat}/K_{AcCoA}$ , which are equal to the rate constants for association of oxaloacetate and acetyl-CoA with the enzyme, are much lower than for the wild type, suggesting that catalytically active complexes are formed with much more difficulty in the mutants. It is also of interest that the  $K_i$  for  $\alpha$ -ketoglutarate, an oxaloacetate analogue which has been shown to bind at the active site (see Results for CS226<sup>H→Q</sup> and CS229<sup>H→Q</sup>; Anderson & Duckworth, 1988), showed only a small loss of affinity in the His-305 mutant and was practically unchanged from the wild type value in the Arg-314 mutant.

As for the mutants CS226<sup>H→Q</sup> and CS229<sup>H→Q</sup>, the sensitivity to activation by KCl for CS314<sup>R→L</sup> was comparable to that of the wild type enzyme (Table 7). At the standard substrate concentrations of 0.1mM each, in the absence of KCl, the activity of CS305<sup>H→A</sup> was too low to measure. Therefore, KCl activation had to be measured at the higher substrate concentrations of 0.35mM acetyl-CoA and 0.40mM oxaloacetate

Table 7. Steady State Kinetic Parameters for Wild Type Citrate Synthase and Mutants CS305H $\rightarrow$ A and CS314R $\rightarrow$ L.

Parameter	Wild Type	CS305H $\rightarrow$ A	CS314R $\rightarrow$ L
$k_{cat}$ , sec $^{-1}$	81 $\pm$ 6 <sup>c</sup>	0.054 $\pm$ 0.016	0.032 $\pm$ 0.006
$K_{AcCoA}$ , $\mu$ M	120 $\pm$ 20	34 $\pm$ 18	26 $\pm$ 16
$K_{OAA}$ , $\mu$ M	26 $\pm$ 5	$\leq$ 55 $\pm$ 21	54 $\pm$ 21
$K_{iOAA}$ , $\mu$ M	33 $\pm$ 7	$\geq$ 950 $\pm$ 320	500 $\pm$ 400
$K_{i, \alpha-KG}$ , $\mu$ M	93 $\pm$ 18	240 $\pm$ 70 <sup>e</sup>	115 $\pm$ 18
KCl Activation Ratio <sup>a</sup>	39 $\pm$ 3 (7.4 $\pm$ 0.2) <sup>d</sup>	78 $\pm$ 4 <sup>d</sup>	34 $\pm$ 3
$K_M^a$ , KCl, mM	28 $\pm$ 4 (10 $\pm$ 1) <sup>d</sup>	25 $\pm$ 3 <sup>d</sup>	52 $\pm$ 19
% Inhibition by 100 $\mu$ M NADH <sup>b</sup>	99 $\pm$ 1	98 $\pm$ 1 <sup>d,f</sup>	70 $\pm$ 3 <sup>f</sup>

<sup>a</sup> KCl activation data, expressed as increases in reaction rate as a function of [KCl], were fitted to the Michaelis-Menten equation by the GENLSS program (See Methods section). Parameters quoted are  $K_M$  (the apparent Michaelis constant for KCl) and "Activation Ratio", the ratio of the limiting catalytic rate at saturating KCl to the rate obtained without KCl. All measurements were in Tris buffer, pH 7.8, with oxaloacetate and acetyl-CoA each at 0.1 mM. Data at [KCl] up to 100 mM were used, because of inhibition at concentrations higher than this.

<sup>b</sup> Determined by measuring activities, in the presence and absence of 100 $\mu$ M NADH, in a discontinuous assay. See Methods section for further details.

<sup>c</sup> For the method of calculation and the significance of the errors see the Methods section.

<sup>d</sup> Measured at [OAA] = 0.40mM and [AcCoA] = 0.35mM, rather than at the standard 0.1mM of each substrate.

<sup>e</sup> Measured at [AcCoA] = 0.35mM due to very low activity at the standard [AcCoA] of 0.1mM. Note that  $K_{i, \alpha-KG}$  for wild type citrate synthase is 93 $\pm$ 14  $\mu$ M at [AcCoA] = 0.35mM (i.e. the same as at [AcCoA] = 0.1mM).

<sup>f</sup> Special blanks had to be prepared due to the very large amounts of enzyme required to make these measurements.

for this mutant. The corresponding wild type control sample, measured at these higher substrate concentrations gave a substantially lower KCl activation ratio, than that measured for the same enzyme at the standard substrate concentrations (Table 7). The higher concentration of acetyl-CoA probably helped to shift the wild type enzyme towards R, the active state, so that further addition of KCl had less of an activating effect. The KCl activation of the His-305 mutant, measured at increased substrate concentrations, was considerably higher than for the corresponding control wild type sample (Table 7). Since the activity of CS305<sup>H→A</sup> could not be measured at the standard substrate concentrations in the absence of KCl, while the activity of CS314<sup>R→L</sup>, a mutant with comparable substrate affinities in the presence of 0.1M KCl (Table 7), could be measured under these conditions, the binding of substrates to CS305<sup>H→A</sup> seems to be more dependent on KCl than in the CS314<sup>R→L</sup> mutant. This is the most noteworthy difference between these two mutant enzymes.

The inhibition by NADH (Table 7) and the binding of that ligand (Table 8) to CS305<sup>H→A</sup> were normal. As noted previously in the Methods section, it was difficult to measure NADH inhibition because the amount of enzyme needed to obtain significant activity in the absence of KCl was very large, and considerable blank reaction with DTNB had to be evaluated and subtracted from the experimental values to get actual inhibitions for both mutants. At 100 $\mu$ M NADH, CS314<sup>R→L</sup> exhibited about 70% inhibition, compared to 99% for the wild type enzyme. Even though the binding of NADH to the Arg-314 mutant (Table 8) was normal, it is difficult to be certain that the inhibition remained unchanged by the mutation because of the large corrections involved in its determination. The fact that NADH inhibition persists in these two mutants is a further confirmation of earlier observations, that the molecule is an allosteric inhibitor of *E. coli* citrate synthase, so that mutations in the active site leave the NADH binding site intact.

Table 8. NADH Binding for Wild Type Citrate Synthase and Mutants CS305<sup>H→A</sup> and CS314<sup>R→L</sup>.

K <sub>D</sub> measured in the presence of:	Wild Type	CS305 <sup>H→A</sup>	CS314 <sup>R→L</sup>
—	1.94±0.07 <sup>a</sup> (0.42-0.74) <sup>b,c</sup>	1.70±0.04 (0.71±0.01) <sup>b</sup>	2.66±0.05 (0.82±0.01) <sup>b</sup>
0.1M KCl	3.68±0.05 (0.53±0.03)	3.64±0.13 (0.69±0.01)	4.62±0.29 (0.66±0.02)
0.2M KCl	6.87±0.16 (0.49±0.01)	5.34±0.14 (0.62±0.01)	9.03±0.24 (0.68±0.01)
0.3M KCl	11.8±0.5 (0.43±0.01)	9.42±0.12 (0.65±0.01)	19.5±0.3 (0.73±0.01)
0.5mM AcCoA	3.09±0.16 (0.50±0.01)	2.15±0.04 (0.63±0.01)	4.94±0.04 (0.83±0.01)
1.0mM AcCoA	6.69±0.41 (0.57±0.02)	3.19±0.07 (0.65±0.01)	9.38±0.51 (0.72±0.01)
1.5mM AcCoA	6.79±0.33 (0.54±0.02)	4.31±0.07 (0.66±0.01)	17.4±3.2 (0.99±0.11)
0.1mM OAA	1.91±0.17 (0.56±0.02)	1.63±0.07 (0.72±0.01)	2.62±0.08 (0.75±0.01)
1 mM NAD <sup>+</sup>	5.47±0.54 (0.65±0.03)	1.74±0.05 (0.66±0.01)	4.85±0.08 (0.80±0.01)

<sup>a</sup> For the method of calculation and the significance of the errors see the Methods section.

<sup>b</sup> Quantities in brackets are the numbers of NADH sites occupied per enzyme subunit at saturation.

<sup>c</sup> Range of values found with different preparations.

Measurements of Ligand Binding by ANS Displacement:

The same properties were measured for the His-305 and Arg-314 mutants as for wild type citrate synthase (Table 9). Coenzyme A, and to a lesser extent, acetyl-CoA, both caused a saturable decrease in the fluorescence of ANS-citrate synthase mixtures. The binding of these related ligands improved in the presence of 0.1M KCl, as evidenced by decreases in their respective  $L_{0.5}$  values. As well, oxaloacetate (0.2mM), when added alone, caused a reduction in the  $L_{0.5}$  value for coenzyme A, which was further lowered by the addition of 0.1M KCl (Table 9). Although the mutants showed similar trends to the wild type enzyme, the ability of acetyl-CoA and coenzyme A to displace ANS from their respective ANS-enzyme complexes was not as great, especially in the case of CS305<sup>H→A</sup>, regardless of whether KCl (0.1M) and/or oxaloacetate (0.2mM) was also present.

Table 9. Parameters for Ligand Binding to Wild Type Citrate Synthase and Mutants CS305H→A and CS314R→L, as Measured by ANS-Displacement.

Parameter	Wild Type		CS305H→A		CS314R→L	
	no KCl	0.1M KCl	no KCl	0.1M KCl	no KCl	0.1M KCl
$L_{0.5}$ , AcCoA, $\mu\text{M}$	260±40 <sup>a</sup> (*) <sup>b</sup>	60±3 (0.64)	2000±1400 (*)	740±170 (*)	360±120 (*)	152±3 (0.69)
$L_{0.5}$ , CoA, $\mu\text{M}$	270±40 (*)	53±3 (0.57)	1240±640 (*)	480±30 (*)	280±70 (*)	120±3 (0.68)
$L_{0.5}$ , CoA, $\mu\text{M}$ <sup>c</sup>	73±3 (0.78)	47±5 (0.38)	710±190 (*)	360±30 (*)	175±6 (0.69)	115±2 (0.66)
$K_D$ , OAA, $\mu\text{M}$ <sup>d</sup>	25±1 (0.54)	ND <sup>e</sup>	18±2 (0.67)	ND	24±2 (0.09)	ND
$K_D$ , $\alpha$ -KG, $\mu\text{M}$ <sup>f</sup>	76±11	ND	1480±240	ND	370±50	ND

<sup>a</sup> For the method of calculation and the significance of the errors see the Methods section.

<sup>b</sup> Quantities in brackets are the fractions of initial fluorescence of ANS-citrate synthase complex quenched by saturating amounts of ligand; in all cases the uncertainties are no more than  $\pm 0.05$ .

\* Fraction of initial fluorescence quenched at saturation could not be estimated precisely by curve-fitting, and so was taken to fall somewhere between the maximum observed and the maximum possible, making the uncertainty in the  $L_{0.5}$  values quite large.

<sup>c</sup> Measured in the presence of 0.2mM oxaloacetate.

<sup>d</sup> Measured in the presence of 0.2mM coenzyme A.

<sup>e</sup> ND = not determined.

<sup>f</sup> Measured in the presence of 0.2mM coenzyme A; calculated from the effect on  $K_D$  for oxaloacetate.

## Attempts to Locate the NADH Binding Site

## CS188R→L, CS217R→L, CS221R→L and CS217R→L/221R→L

Chemical modification of Cys-206 with a bulky fluorescent substituent, monobromobimane, has been found to eliminate allosteric inhibition by NADH, but has only a small effect on enzyme activity (Duckworth *et al.*, 1987). In addition, various adenylic acid derivatives, including NADH, all partially protect this cysteine from modification (Talgoy & Duckworth, 1979). These findings have led to the suggestion that Cys-206 may be in or near the NADH binding site itself (Figure 30). If it does mark a portion of the allosteric binding site, a nearby arginine residue might well form another feature of the site, since an arginine is frequently (Eklund *et al.*, 1976a, 1976b; Birkoft *et al.*, 1982), though not always (Biesecker *et al.*, 1977) found to form an ion pair interaction with the pyrophosphate portion of NAD, in enzymes which bind that nucleotide. In the *E. coli* citrate synthase model (Duckworth *et al.*, 1987), there are only three arginines reasonably close to Cys-206: Arg-188, Arg-217 and Arg-221 (Figure 30). Each of these arginines has been changed to leucine individually, and a double mutant, in which both Arg-217 and Arg-221 were converted to leucines, has also been prepared. There are no equivalent arginine residues in any of the non-allosteric citrate synthases of pig heart (Bloxham *et al.*, 1981) or yeast (Suissa *et al.*, 1984; Rosenkrantz *et al.*, 1986), but all three of these arginines are also present in the amino acid sequences of two other NADH-sensitive citrate synthases, those of *Acinetobacter anitratum* (Donald & Duckworth, 1987) and *Pseudomonas aeruginosa* (Donald *et al.*, in preparation). Of these, Arg-188 is predicted to be in the corner between the I and J helices of the *E. coli* citrate synthase model (Figure 30). The precise location of Arg-188 is uncertain, however, since there is little homology between the pig heart and *E. coli* sequences in this region of the model. Arg-217 and Arg-221 are both predicted to be on the solvent surface of the K helix.

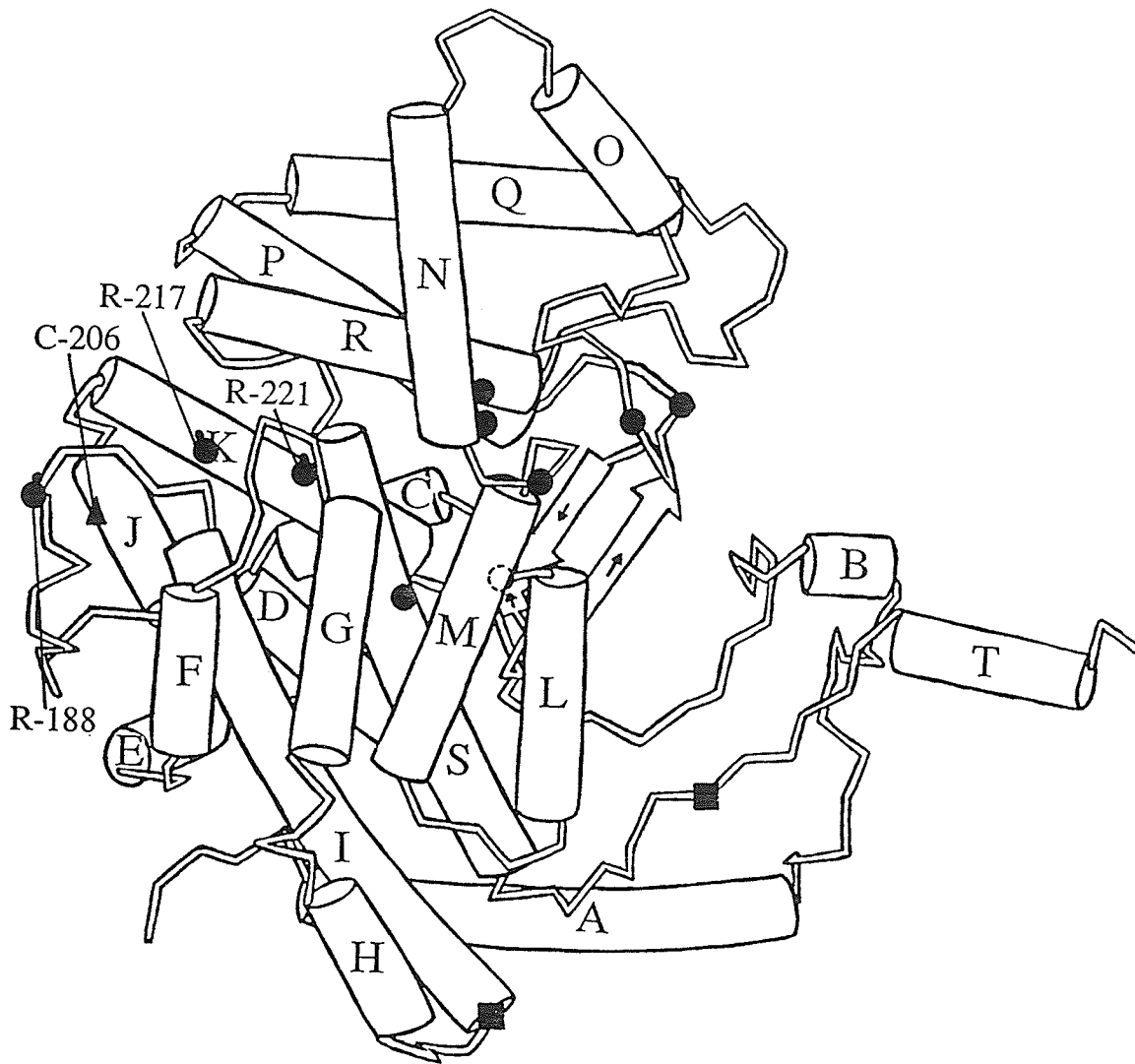


Figure 30. Model of an *E. coli* citrate synthase subunit showing the location of Cys-206 (▲) and the residues involved in mutagenesis experiments (●): Arg-188, Arg-217 and Arg-221.

The three point mutants, CS188<sup>R→L</sup>, CS217<sup>R→L</sup> and CS221<sup>R→L</sup>, and the double mutant, CS217<sup>R→L</sup>/221<sup>R→L</sup>, were all prepared by the usual method and the corresponding enzymes tested for sensitivity to NADH both in crude extracts and after purification. It should be noted that the single mutation of Arg-217 and Arg-221, as well as the double mutation of these two arginines, resulted in proteins which were retained on the DEAE cellulose column about 15% longer than the wild type or any other mutant protein described in this thesis during the KCl gradient step, normally used to elute citrate synthase from the column. This is most likely due to the removal of positively charged side chains on the enzyme surface, effectively making these mutant proteins more negative, so that they would have a somewhat higher affinity for the anion exchange resin. Each of the four mutant proteins described here behaved normally on a Sephadex G-200 column, resulting in pure enzyme which gave a single band of molecular weight about 48,000 g/mole on an SDS polyacrylamide gel.

Despite the fact that these arginine residues are conserved among the bacterial citrate synthases which are also sensitive to NADH inhibition, their mutation had no effect on the ability of NADH to inhibit enzyme activity (Table 10). The binding of NADH to these mutants was also normal (Table 11). KCl activation ratios for mutants CS217<sup>R→L</sup> and CS221<sup>R→L</sup> are notably higher than wild type values (Table 10), while the corresponding ratios for CS188<sup>R→L</sup> and CS217<sup>R→L</sup>/221<sup>R→L</sup> are as found previously for mutant enzymes in Table 4. Steady state kinetic parameters for these mutants show increased Michaelis constants for oxaloacetate and acetyl-CoA, as well as a higher affinity for the competitive inhibitor  $\alpha$ -ketoglutarate, compared to wild type citrate synthase (Table 10).

Most  $L_{0.5}$  values, determined by ANS displacement (Table 12), showed some variation from the wild type values, but no change was considered significant.

Table 10. Steady State Kinetic Parameters for Wild Type Citrate Synthase and Mutants CS188R→L, CS217R→L, CS221R→L and CS217R→L/221R→L.

Parameter	Wild Type	CS188R→L	CS217R→L	CS221R→L	CS217R→L/221R→L
$k_{cat}$ , sec <sup>-1</sup>	81±6 <sup>b</sup>	103±3	78±3	98±9	55±5
$K_{AcCoA}$ , μM	120±20	66±6	74±8	67±19	81±18
$K_{OAA}$ , μM	26±5	10±1	3.6±0.6	12±3	18±3
$K_{IOAA}$ , μM	33±7	16±2	11±2	54±14	46±9
$K_i$ , α-KG, μM	93±18	44±6	49±7	55±5	70±10
KCl Activation Ratio <sup>a</sup>	39±3	69±3	121±7	115±11	64±5
$K_M^a$ , KCl, mM	28±4	24±2	36±5	42±8	54±7
$K_i$ , NADH, μM	3.3±0.1	1.47±0.04	3.2±0.1	1.4±0.1	4.0±0.4
Maximum % Inhibition by NADH	99±1	97±1	93±2	95±2	92±4

<sup>a</sup> KCl activation data, expressed as increases in reaction rate as a function of [KCl], were fitted to the Michaelis-Menten equation by the GENLSS program (See Methods section). Parameters quoted are  $K_M$  (the apparent Michaelis constant for KCl) and "Activation Ratio", the ratio of the limiting catalytic rate at saturating KCl to the rate obtained without KCl. All measurements were in Tris buffer, pH 7.8, with oxaloacetate and acetyl-CoA each at 0.1 mM. Data at [KCl] up to 100 mM were used, because of inhibition at concentrations higher than this.

<sup>b</sup> For the method of calculation and the significance of the errors see the Methods section.

Table 11. NADH Binding for Wild Type Citrate Synthase and Mutants CS188R→L, CS217R→L, CS221R→L, CS217R→L/221R→L.

K <sub>D</sub> measured in the presence of:	Wild Type	CS188R→L	CS217R→L	CS221R→L	CS217R→L/221R→L
—	1.94±0.07 <sup>a</sup> (0.42-0.74) <sup>b,c</sup>	1.43±0.06 (0.78±0.01) <sup>b</sup>	1.62±0.05 (0.71±0.01) <sup>b</sup>	1.39±0.05 (0.83±0.01) <sup>b</sup>	1.64±0.11 (0.57±0.01) <sup>b</sup>
0.1M KCl	3.68±0.05 (0.53±0.03)	3.32±0.09 (0.70±0.01)	3.10±0.09 (0.59±0.01)	2.28±0.09 (0.69±0.01)	3.15±0.16 (0.45±0.01)
0.2M KCl	6.87±0.16 (0.49±0.01)	7.01±0.13 (0.69±0.013)	7.49±0.73 (0.66±0.04)	4.99±0.21 (0.66±0.01)	5.83±0.26 (0.42±0.01)
0.3M KCl	11.8±0.5 (0.43±0.01)	13.21±0.6 (0.61±0.02)	14.0±1.2 (0.61±0.04)	7.86±0.36 (0.50±0.01)	11.9±0.7 (0.35±0.01)
0.5mM AcCoA	3.09±0.16 (0.50±0.01)	2.23±0.02 (0.79±0.01)	2.75±0.04 (0.71±0.01)	2.19±0.13 (0.81±0.02)	2.57±0.12 (0.48±0.01)
1.0mM AcCoA	6.69±0.41 (0.57±0.02)	3.02±0.19 (0.79±0.01)	4.89±0.13 (0.72±0.01)	4.07±0.11 (0.85±0.01)	4.05±0.16 (0.51±0.01)
1.5mM AcCoA	6.79±0.33 (0.54±0.02)	4.64±0.53 (0.80±0.03)	9.10±0.19 (0.75±0.01)	7.23±0.33 (0.87±0.02)	6.10±0.25 (0.15±0.01)
0.1mM OAA	1.91±0.17 (0.56±0.02)	0.97±0.11 (0.75±0.02)	1.47±0.09 (0.66±0.01)	1.15±0.05 (0.76±0.01)	1.44±0.08 (0.46±0.01)
1 mM NAD <sup>+</sup>	5.47±0.54 (0.65±0.03)	2.68±0.24 (0.72±0.02)	2.41±0.12 (0.61±0.01)	3.58±0.27 (0.85±0.03)	4.41±0.62 (0.54±0.03)

<sup>a</sup> For the method of calculation and the significance of the errors see the Methods section.

<sup>b</sup> Quantities in brackets are the numbers of NADH sites occupied per enzyme subunit at saturation.

<sup>c</sup> Range of values found with different preparations.

Table 12. Parameters for Ligand Binding to Wild Type Citrate Synthase and Mutants: CS188R→L, CS217R→L, CS221R→L and CS217R→L/221R→L, as Measured by ANS-Displacement.

Parameter	Wild Type			CS188R→L		CS217R→L	
	no KCl	0.1M KCl	no KCl	no KCl	0.1M KCl	no KCl	0.1M KCl
$L_{0.5}$ , AcCoA, $\mu\text{M}$	260±40 <sup>a</sup> (*) <sup>b</sup>	60±3 (0.64)	510±310 (*)	87±4 (0.57)	310±130 (*)	80±4 (0.64)	
$L_{0.5}$ , CoA, $\mu\text{M}$	270±40 (*)	53±3 (0.57)	350±160 (*)	70±3 (0.58)	270±100 (*)	70±3 (0.63)	
$L_{0.5}$ , CoA, $\mu\text{M}^c$	73±3 (0.78)	47±5 (0.38)	85±1 (0.72)	26±1 (0.36)	84±2 (0.78)	28±1 (0.49)	
$K_D$ , OAA, $\mu\text{M}^d$	25±1 (0.54)	ND <sup>e</sup>	77±4 (0.67)	ND	70±5 (0.54)	ND	
$K_D$ , $\alpha$ -KG, $\mu\text{M}^f$	76±11	ND	1000±160	ND	1160±170	ND	

Parameter	Wild Type		CS221R→L		CS217R→L/221R→L	
	no KCl	0.1M KCl	no KCl	0.1M KCl	no KCl	0.1M KCl
L <sub>0.5</sub> , AcCoA, $\mu\text{M}$	260±40 <sup>a</sup> (* <sup>b</sup> )	60±3 (0.64)	410±130 (* <sup>b</sup> )	98±5 (0.66)	560±320 (* <sup>b</sup> )	116±7 (0.50)
L <sub>0.5</sub> , CoA, $\mu\text{M}$	270±40 (* <sup>b</sup> )	53±3 (0.57)	310±120 (* <sup>b</sup> )	91±4 (0.64)	420±190 (* <sup>b</sup> )	115±4 (0.53)
L <sub>0.5</sub> , CoA, $\mu\text{M}$ <sup>c</sup>	73±3 (0.78)	47±5 (0.38)	120±5 (0.81)	23±1 (0.59)	131±6 (0.65)	35±2 (0.52)
K <sub>D</sub> , OAA, $\mu\text{M}$ <sup>d</sup>	25±1 (0.54)	ND <sup>e</sup>	151±9 (0.46)	ND	90±6 (0.36)	ND
K <sub>D</sub> , $\alpha$ -KG, $\mu\text{M}$ <sup>f</sup>	76±11	ND	190±60	ND	380±90	ND

<sup>a</sup> For the method of calculation and the significance of the errors see the Methods section.

<sup>b</sup> Quantities in brackets are the fractions of initial fluorescence of ANS-citrate synthase complex quenched by saturating amounts of ligand; in all cases the uncertainties are no more than  $\pm 0.05$ .

\* Fraction of initial fluorescence quenched at saturation could not be estimated precisely by curve-fitting, and so was taken to fall somewhere between the maximum observed and the maximum possible, making the uncertainty in the L<sub>0.5</sub> values quite large.

<sup>c</sup> Measured in the presence of 0.2mM oxaloacetate.

<sup>d</sup> Measured in the presence of 0.2mM coenzyme A.

<sup>e</sup> ND = not determined.

<sup>f</sup> Measured in the presence of 0.2mM coenzyme A; calculated from the effect on K<sub>D</sub> for oxaloacetate.

Mutants which Affect the Allosteric Equilibrium  
of *E. coli* Citrate Synthase



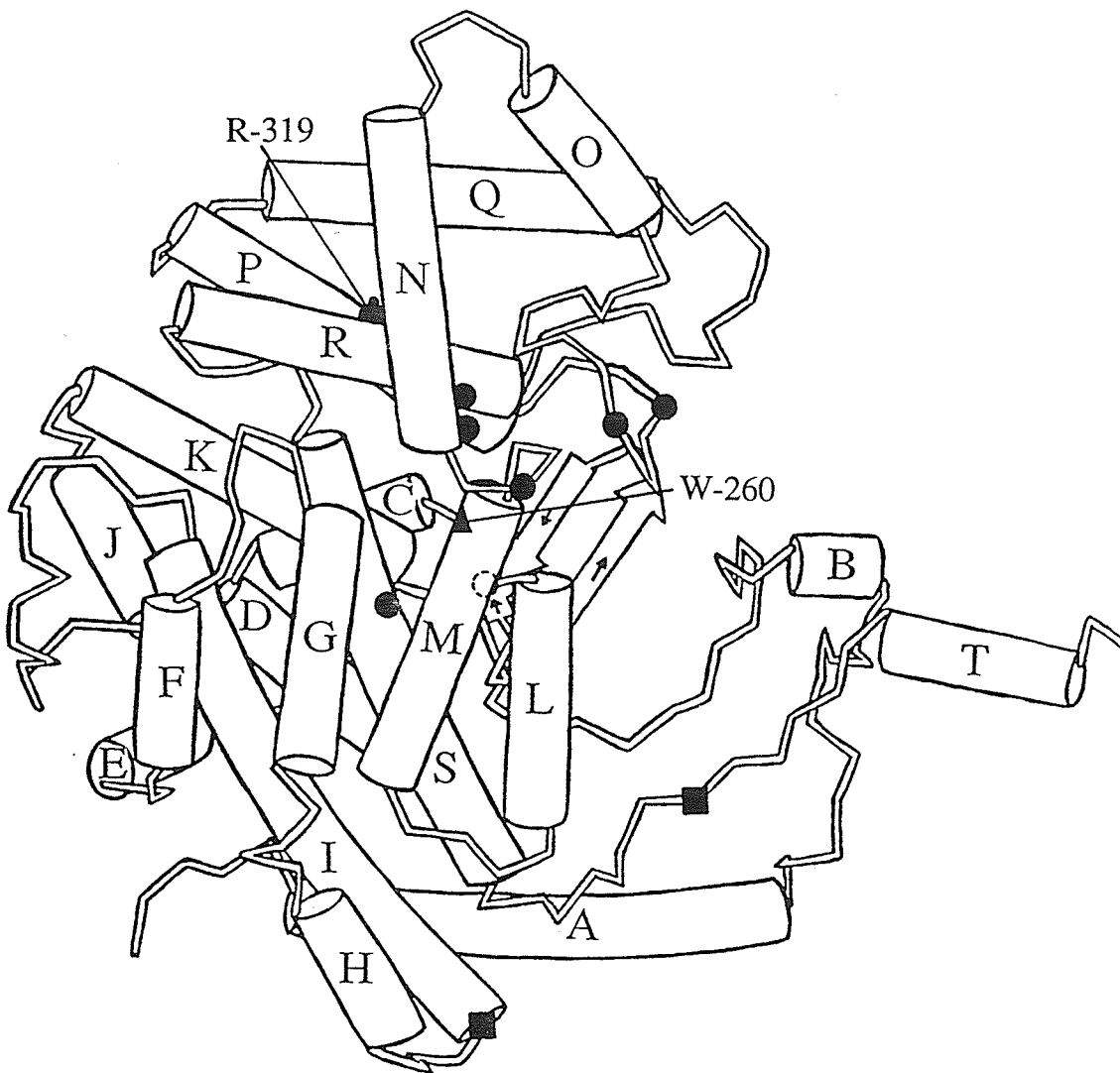


Figure 32. Model of an *E. coli* citrate synthase subunit showing the location of Trp (W)-260 (▲), and Arg-319 (●).

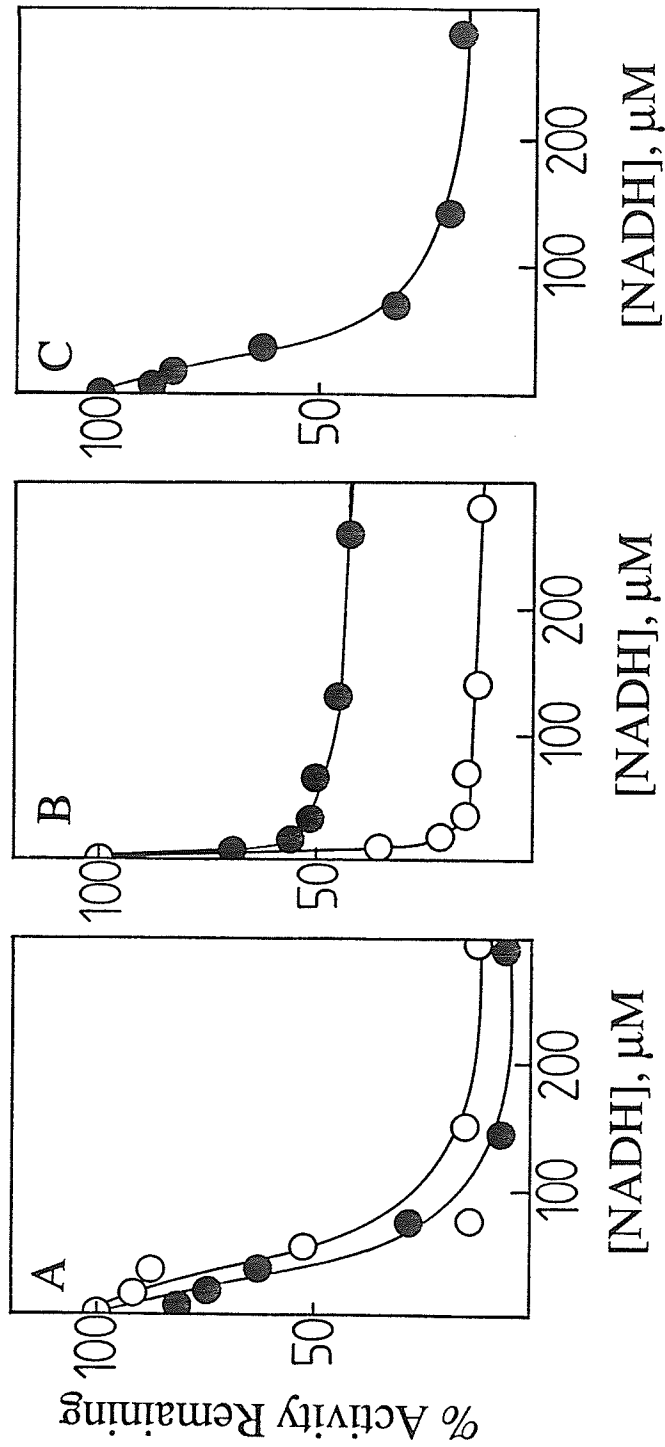


Figure 33. NADH saturation curves for wild type (O) and CS260 W→A (●). A) crude enzyme extracts, B) enzymes purified using the standard method, C) CS260 W→A purified using ammonium sulfate precipitation followed by a Sephadex G-200 chromatography step.

of NADH oxidase in these extracts, which oxidizes NADH to NAD<sup>+</sup>. *E. coli* citrate synthase has a very weak affinity for NAD<sup>+</sup> ( $K_D = 1100\mu\text{M}$ ) compared to that for NADH ( $K_D = 1.6\mu\text{M}$ ) (Duckworth & Tong, 1976), so NAD<sup>+</sup> does not affect enzyme activity at low concentrations. After the typical purification procedure, wild type citrate synthase exhibits a hyperbolic NADH saturation curve, which was also observed for CS260<sup>W→A</sup>, except that roughly half the activity was not sensitive to NADH inhibition (Figure 33, Panel B). Interestingly, if crude enzyme extract was added to this partially NADH-insensitive, purified enzyme, which has been designated CS260<sup>W→A(I)</sup>, full inhibition by NADH was restored (Table 13).

Table 13. Restoration of normal NADH sensitivity to partially insensitive, purified CS260<sup>W→A(I)</sup>, upon addition of crude extract.

	pure CS260 <sup>W→A(I)</sup>	crude extract CS260 <sup>W→A</sup>	combined pureCS260 <sup>W→A(I)</sup> & crude extract CS260 <sup>W→A</sup>
Activity in absence of NADH (U/mL)	0.1199	0.1149	0.2160
Activity in presence of 250 $\mu\text{M}$ NADH (U/mL)	0.0813	0.0069	0.0064
% Activity remaining in presence of 250 $\mu\text{M}$ NADH	67.8%	6.0%	3.0%

So it seems that something present in the crude extract allows this citrate synthase mutant to regain complete sensitivity to NADH. No attempt has been made to identify

or purify the factor which confers full NADH sensitivity on CS260<sup>W→A</sup> (I), but adding various fractions from the DEAE cellulose column to this NADH-insensitive enzyme would be the obvious place to begin this investigation. Since this partial desensitization arose during the purification procedure, a variation of this standard purification method was employed. Crude extract was simply concentrated and slightly enriched by taking the fraction which precipitates between 55 and 70% saturation in ammonium sulfate, and then passed through a Sephadex G-200 column as usual. This resulted in a mutant enzyme which demonstrated sigmoid saturation and complete inhibition by NADH, and has been designated CS260<sup>W→A</sup>(S) (Figure 33, Panel C). Although this simpler purification procedure omitted the DEAE cellulose chromatography step normally used, SDS polyacrylamide gel electrophoresis showed that the enzyme preparation was better than 80% pure.

This modified purification procedure was repeated several times in an attempt to obtain more of the NADH-sensitive form of CS260<sup>W→A</sup>, but all subsequent attempts were unsuccessful, yielding only the NADH-insensitive form of the mutant. The inability to purify further preparations of CS260<sup>W→A</sup> which retained their NADH-sensitivity, placed serious limitations on the amount of information gathered about this unusual mutant form.

CS260<sup>W→A</sup>(I) was found to have a molar extinction coefficient of 43700, while the wild type protein has a value of 46800. The difference is not unexpected, since the mutant has one of its three tryptophan residues mutated to alanine.

Both the "sensitive", CS260<sup>W→A</sup>(S) and "insensitive", CS260<sup>W→A</sup>(I), enzymes were submitted to the usual tests, consisting of NADH binding and ANS displacement studies; and steady state kinetic analysis. As well, further experiments were performed in an attempt to understand more fully the effect of this point mutation. In spite of the fact that these two mutant enzyme forms show such a difference in their kinetic inhibition by NADH (Table 14), their ability to bind NADH, as measured by

Table 14. Steady State Kinetic Parameters for Wild Type Citrate Synthase and Mutants CS260<sup>W→A</sup>(I) and CS260<sup>W→A</sup>(S).

Parameter	Wild Type	CS260 <sup>W→A</sup> (I)	CS260 <sup>W→A</sup> (S)
$k_{\text{cat}}$ , sec <sup>-1</sup>	81±6 <sup>b</sup>	86±14	7.9±0.1
$K_{\text{AcCoA}}$ , μM	120±20	260±70	100±10
$K_{\text{OAA}}$ , μM	26±5	71±28	35±11
$K_{\text{iOAA}}$ , μM	33±7	130±30	120±30
$K_{\text{i, } \alpha\text{-KG}}$ , μM	93±18	120±10	110±10
KCl Activation Ratio <sup>a</sup>	39±3	56±17	68±8
$K_{\text{M}}^{\text{a}}$ , KCl, mM	28±4	54±17	44±8
$K_{\text{i}}$ , NADH, μM	3.3±0.1	20±8	120±20
Maximum % Inhibition by NADH	99±1	55±14	85±10

<sup>a</sup> KCl activation data, expressed as increases in reaction rate as a function of [KCl], were fitted to the Michaelis-Menten equation by the GENLSS program (See Methods section). Parameters quoted are  $K_{\text{M}}$  (the apparent Michaelis constant for KCl) and "Activation Ratio", the ratio of the limiting catalytic rate at saturating KCl to the rate obtained without KCl. All measurements were in Tris buffer, pH 7.8, with oxaloacetate and acetyl-CoA each at 0.1 mM. Data at [KCl] up to 100 mM were used, because of inhibition at concentrations higher than this.

<sup>b</sup> For the method of calculation and the significance of the errors see the Methods section.

fluorescence enhancement, is approximately equal (Table 15). Although NADH binding by CS260<sup>W→A(S)</sup> was inhibited by KCl, acetyl-CoA and NAD<sup>+</sup>, just as with CS260<sup>W→A(I)</sup> and the wild type enzyme, it showed a remarkable effect with oxaloacetate, even small amounts, like 10–100μM, abolished the fluorescence associated with nucleotide binding altogether. In fact, when NADH was added to mixtures of CS260<sup>W→A(S)</sup> and oxaloacetate (>10μM), the fluorescence observed was less than that found for free NADH in the absence of enzyme. Thus, not only was there no NADH fluorescence enhancement effect in the presence of enzyme and oxaloacetate, but a quenching effect was observed. This unusual result will be discussed further in the Discussion.

Previous work has shown that *E. coli* citrate synthase is inactivated by incubation with high concentrations of urea, but that if the incubation includes 0.5mM NADH or 0.1M KCl, the enzyme is more resistant to urea denaturation (Morse & Duckworth, 1980). Figure 34 shows the amount of enzyme activity remaining after incubation of the wild type enzyme and each of the two forms of the Trp-260 mutant for one hour in urea solutions of different concentrations. The wild type enzyme is quite resistant to this treatment and about 6.5M urea causes the loss of about half the activity in one hour. For the "sensitive" and "insensitive" forms of the mutant, the amount of urea needed to cause a 50% loss in activity in one hour were 5.25 and 5.75M, respectively. The effects of the presence of 0.5mM NADH and 0.1M KCl on enzyme stability were also examined by including these factors in the Tris-urea-enzyme incubation mixture, and are also shown in Figure 34. For all three enzymes, 0.1M KCl affords each some protection from urea denaturation. The presence of 0.5mM NADH, on the other hand, has different effects: for the wild type enzyme it appears to give the same, or even slightly more stability to the enzyme as did 0.1M KCl; for CS260<sup>W→A(S)</sup> the addition of NADH has no apparent effect; while for

Table 15. NADH Binding for Wild Type Citrate Synthase and Mutants CS260<sup>W→A(I)</sup> and CS260<sup>W→A(S)</sup>.

K <sub>D</sub> measured in the presence of:	Wild Type	CS260 <sup>W→A(I)</sup>	CS260 <sup>W→A(S)</sup>
—	1.94±0.07 <sup>a</sup> (0.42-0.74) <sup>b,c</sup>	1.71±0.14 (0.72±0.02) <sup>b</sup>	1.89±0.22 (0.37±0.01) <sup>b</sup>
0.1M KCl	3.68±0.05 (0.53±0.03)	4.46±0.15 (0.64±0.01)	4.91±0.33 (0.34±0.01)
0.2M KCl	6.87±0.16 (0.49±0.01)	8.67±0.31 (0.67±0.01)	10.6±1.7 (0.35±0.04)
0.3M KCl	11.8±0.5 (0.43±0.01)	16.1±0.7 (0.70±0.02)	12.0±1.1 (0.29±0.02)
0.5mM AcCoA	3.09±0.16 (0.50±0.01)	3.84±0.20 (0.66±0.02)	4.72±0.58 (0.39±0.02)
1.0mM AcCoA	6.69±0.41 (0.57±0.02)	5.47±0.12 (0.68±0.01)	5.05±0.23 (0.37±0.01)
1.5mM AcCoA	6.79±0.33 (0.54±0.02)	9.25±0.31 (0.71±0.01)	6.27±0.23 (0.32±0.01)
0.1mM OAA	1.91±0.17 (0.56±0.02)	1.98±0.04 (0.61±0.01)	d
1 mM NAD <sup>+</sup>	5.47±0.54 (0.65±0.03)	2.80±0.09 (0.65±0.01)	2.19±0.23 (0.28±0.01)

<sup>a</sup> For the method of calculation and the significance of the errors see the Methods section.

<sup>b</sup> Quantities in brackets are the numbers of NADH sites occupied per enzyme subunit at saturation.

<sup>c</sup> Range of values found with different preparations.

<sup>d</sup> As little as 10 μM oxaloacetate abolished the fluorescence associated with NADH binding, altogether.

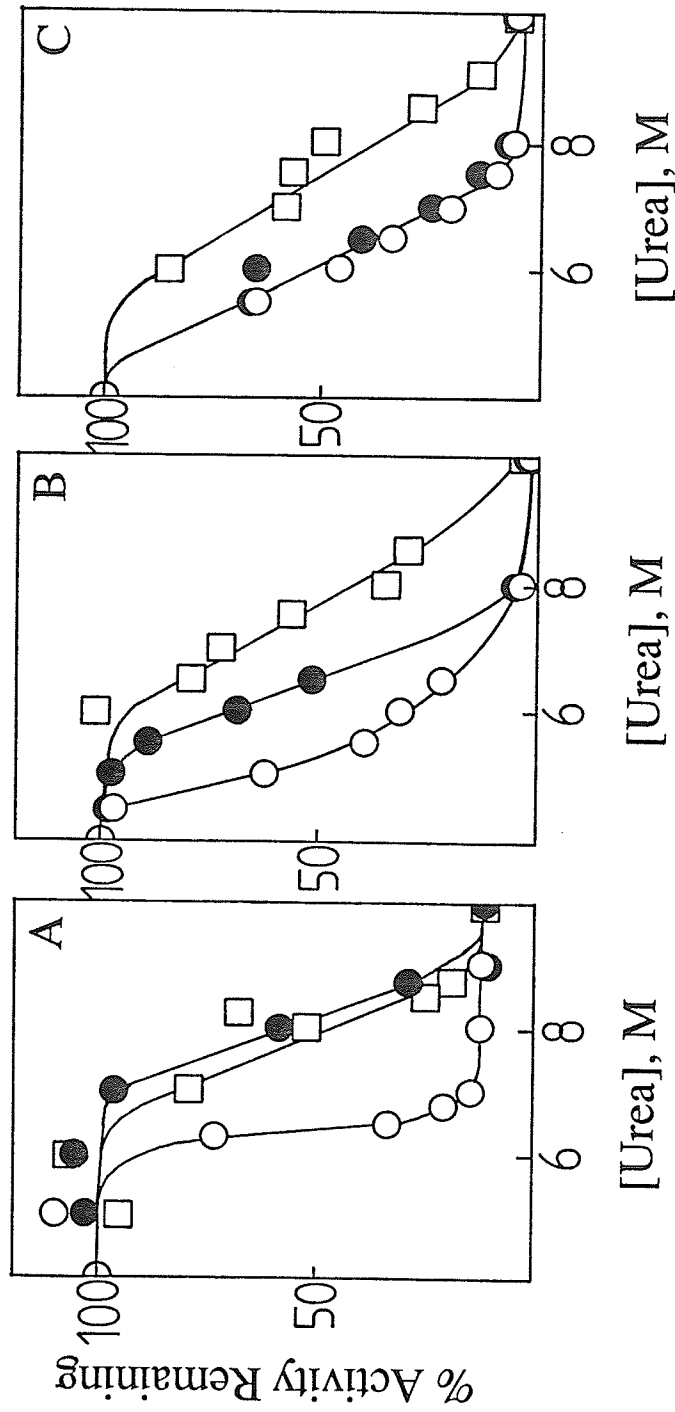


Figure 34. Effect of urea incubation on wild type citrate synthase (A) and the Trp-260 mutant forms, CS260<sup>W→A(I)</sup> (B) and CS260<sup>W→A(S)</sup> (C). Samples (10 $\mu$ L-aliquots) of incubation mixtures were assayed in 1.0mL final volumes of the standard assay solution. Enzyme in Tris buffer with urea concentration as shown (O); in Tris-urea plus 0.5mM NADH ( $\bullet$ ); and in Tris-urea plus 0.1M KCl ( $\square$ ). Incubations were for one hour at 23°C.

CS260<sup>W→A</sup>(I), its inclusion has an intermediate beneficial effect, between those seen for the other two enzymes.

Steady State Kinetic Studies and Measurements of Ligand Binding by ANS Displacement:

The kinetic parameters for these two enzyme forms are quite similar to each other as well as to the wild type enzyme in most respects (Table 14). The most noteworthy differences are in the significantly lower turnover number ( $k_{cat}$ ) for CS260<sup>W→A</sup>(S) and the somewhat reduced affinity of CS260<sup>W→A</sup>(I) for both substrates.

Unlike the case for wild type protein, ANS displacement measurements for the two forms of CS260<sup>W→A</sup>, gave lower  $L_{0.5}$  values when titrating ANS-citrate synthase mixtures with coenzyme A as compared to acetyl-CoA, indicating that coenzyme A is better able to displace ANS from ANS-enzyme complexes (Table 16). Addition of 0.2mM oxaloacetate to the coenzyme A titration of either form of the mutant did not displace more ANS, again contrary to the wild type case. Although the wild type enzyme shows a decrease in each of its  $L_{0.5}$  values upon addition of 0.1M KCl, only the "insensitive" form of CS260<sup>W→A</sup> shows this effect in the titration with acetyl-CoA (Table 16). The remaining  $L_{0.5}$  values show substantial increases from those measured in the absence of KCl, indicative of enzymes with poorer affinities for these ligands in the presence of 0.1M KCl.

This marked disparity between the effect of KCl on CS260<sup>W→A</sup>(S) and CS260<sup>W→A</sup>(I), and wild type citrate synthase, prompted further kinetic measurements to be made in the absence of KCl. Unfortunately, the lack of sufficient quantities of the "sensitive" form of CS260<sup>W→A</sup>, and the inability of several attempts to produce more of the Trp-260 mutant, which still retains its sensitivity to NADH, has prevented further study of this enzyme form. Steady state kinetic parameters were measured for

Table 16. Parameters for Ligand Binding to Wild Type Citrate Synthase and Mutants CS260W→A(T) and CS260W→A(S), as Measured by ANS-Displacement.

Parameter	Wild Type			CS260W→A(T)		CS260W→A(S)	
	no KCl	0.1M KCl	no KCl	0.1M KCl	no KCl	0.1M KCl	
L <sub>0.5</sub> , AcCoA, μM	260±40 <sup>a</sup> (* <sup>b</sup> )	60±3 (0.64)	380±40 (0.30)	250±20 (0.20)	250±30 (0.19)	740±110 (0.30)	
L <sub>0.5</sub> , CoA, μM	270±40 (* <sup>c</sup> )	53±3 (0.57)	150±10 (0.22)	580±140 (0.32)	158±7 (0.22)	1290±130 (0.41)	
L <sub>0.5</sub> , CoA, μM <sup>c</sup>	73±3 (0.78)	47±5 (0.38)	148±5 (0.49)	600±80 (0.46)	158±6 (0.34)	500±20 (0.26)	
K <sub>D</sub> , OAA, μM <sup>d</sup>	25±1 (0.54)	ND <sup>e</sup>	45±3 (0.14)	ND	58±3 (0.25)	ND	
K <sub>D</sub> , α-KG, μM <sup>f</sup>	76±11	ND	220±30	ND	180±40	ND	

<sup>a</sup> For the method of calculation and the significance of the errors see the Methods section.

<sup>b</sup> Quantities in brackets are the fractions of initial fluorescence of ANS-citrate synthase complex quenched by saturating amounts of ligand; in all cases the uncertainties are no more than ±0.05.

\* Fraction of initial fluorescence quenched at saturation could not be estimated precisely by curve-fitting, and so was taken to fall somewhere between the maximum observed and the maximum possible, making the uncertainty in the L<sub>0.5</sub> values quite large.

<sup>c</sup> Measured in the presence of 0.2mM oxaloacetate.

<sup>d</sup> Measured in the presence of 0.2mM coenzyme A.

<sup>e</sup> ND = not determined.

<sup>f</sup> Measured in the presence of 0.2mM coenzyme A; calculated from the effect on K<sub>D</sub> for oxaloacetate.

CS260<sup>W→A(I)</sup> and wild type citrate synthase in the absence of KCl (Table 17). Both these enzymes show improved turnover numbers and acetyl-CoA binding in the presence of 0.1M KCl. The binding of oxaloacetate in the wild type enzyme was rather indifferent to the presence of KCl, while the "insensitive" form of the mutant seemed to bind oxaloacetate somewhat better in the absence of KCl, especially in the presence of saturating amounts of acetyl-CoA ( $K_{OAA}$ ) (Table 17).

Table 17. Steady State Kinetic Parameters for Wild Type Citrate Synthase and Mutant CS260<sup>W→A(I)</sup>, in the presence and absence of KCl.

Parameter	Wild Type		CS260 <sup>W→A(I)</sup>	
	no KCl	0.1M KCl	no KCl	0.1M KCl
$k_{cat}$ , sec <sup>-1</sup>	44±5 <sup>a</sup>	81±6	24±5	86±14
$K_{AcCoA}$ , μM	750±200	120±20	8900±1100	260±70
$K_{OAA}$ , μM	11±6	26±5	6.8±4.0	71±28
$K_{iOAA}$ , μM	36±11	33±7	58±7	130±30

<sup>a</sup> For the method of calculation and the significance of the errors see the Methods.

## CS319R→L

Arg-319 (see Figure 32 for location) is a residue which is not thought to be part of the active site, although it must have some role in enzyme function, as a positively charged residue, since it is conserved in all seven citrate synthases sequenced to date. To determine the importance of this arginine residue, a mutant enzyme was produced, CS319R→L, in which Arg-319 was changed to leucine.

### Steady State Kinetic Studies:

CS319R→L was purified in the usual way and gave a single band of molecular weight about 48,000 g/mole on an SDS gel. Its specific activity in the standard assay was 48U/mg, compared with 36U/mg for wild type citrate synthase. The mutant binds NADH normally, except that the binding shows some weakening in the presence of 0.1mM oxaloacetate, whose inhibitory effect is enhanced by the addition of 0.1mM CoA, unlike the wild type enzyme which does not show this effect (Table 18). The maximum inhibition observed at saturating concentrations of NADH for CS319R→L has been found to be dependent on the concentration of oxaloacetate present in the assay (Figure 35). At the standard concentration of oxaloacetate (0.1mM), only about 25% inhibition by NADH is achieved (Figure 35, Panel B; Table 19), but at 0.02mM oxaloacetate or less, the observed NADH inhibition is about 80% (Figure 35B). NADH inhibition of wild type citrate synthase does not show this oxaloacetate concentration dependence (Figure 35A).

Typical steady state kinetic measurements were made on CS319R→L in the presence of 0.1M KCl, and it was found to have a somewhat lower  $k_{cat}$  value than the wild type enzyme, but a higher affinity for both substrates (Table 19). Furthermore, the dissociation constant for  $\alpha$ -ketoglutarate,  $K_{i,\alpha-KG}$ , is significantly larger for the mutant than for wild type citrate synthase.

Table 18. NADH Binding for Wild Type Citrate Synthase and Mutant CS319<sup>R→L</sup>.

$K_D$ measured in the presence of:	Wild Type	CS319 <sup>R→L</sup>
—	1.94±0.07 <sup>a</sup> (0.42-0.74) <sup>b,c</sup>	1.56±0.03 (0.47±0.01) <sup>b</sup>
—	1.50±0.05 <sup>d</sup> (0.81±0.01)	1.89±0.05 <sup>d</sup> (0.56±0.01)
0.1M KCl	3.68±0.05 (0.53±0.03)	3.03±0.10 (0.42±0.01)
0.2M KCl	6.87±0.16 (0.49±0.01)	4.22±0.23 (0.33±0.01)
0.3M KCl	11.8±0.5 (0.43±0.01)	6.42±0.54 (0.24±0.01)
0.5mM AcCoA	3.09±0.16 (0.50±0.01)	2.62±0.05 (assume 0.47) <sup>e</sup>
1.0mM AcCoA	6.69±0.41 (0.57±0.02)	5.49±0.33 (assume 0.47) <sup>e</sup>
1.5mM AcCoA	6.79±0.33 (0.54±0.02)	8.93±0.75 (assume 0.47) <sup>e</sup>
0.1mM OAA	1.91±0.17 (0.56±0.02)	7.71±0.46 (0.43±0.02)
1 mM NAD <sup>+</sup>	5.47±0.54 (0.65±0.03)	3.03±0.11 (0.37±0.01)
0.1mM CoA	1.66±0.10 (0.89±0.01)	1.86±0.05 (0.60±0.01)
0.1mM OAA	1.32±0.07 <sup>d</sup> (0.93±0.01)	4.35±0.18 <sup>d</sup> (0.66±0.01)
0.1mM CoA +0.1mM OAA	1.56±0.09 (0.90±0.01)	13.8±0.6 (0.73±0.02)

<sup>a</sup> For the method of calculation and the significance of the errors see the Methods section.

<sup>b</sup> Quantities in brackets are the numbers of NADH sites occupied per enzyme subunit at saturation.

<sup>c</sup> Range of values found with different preparations.

<sup>d</sup> These values were measured subsequent to the above set of data, and show typical fluctuations in the repeated measurements.

<sup>e</sup> These plots were quite curved, so the number of NADH sites occupied at saturation was assumed to be the same as in the absence of any competing ligands, i.e. 0.47.

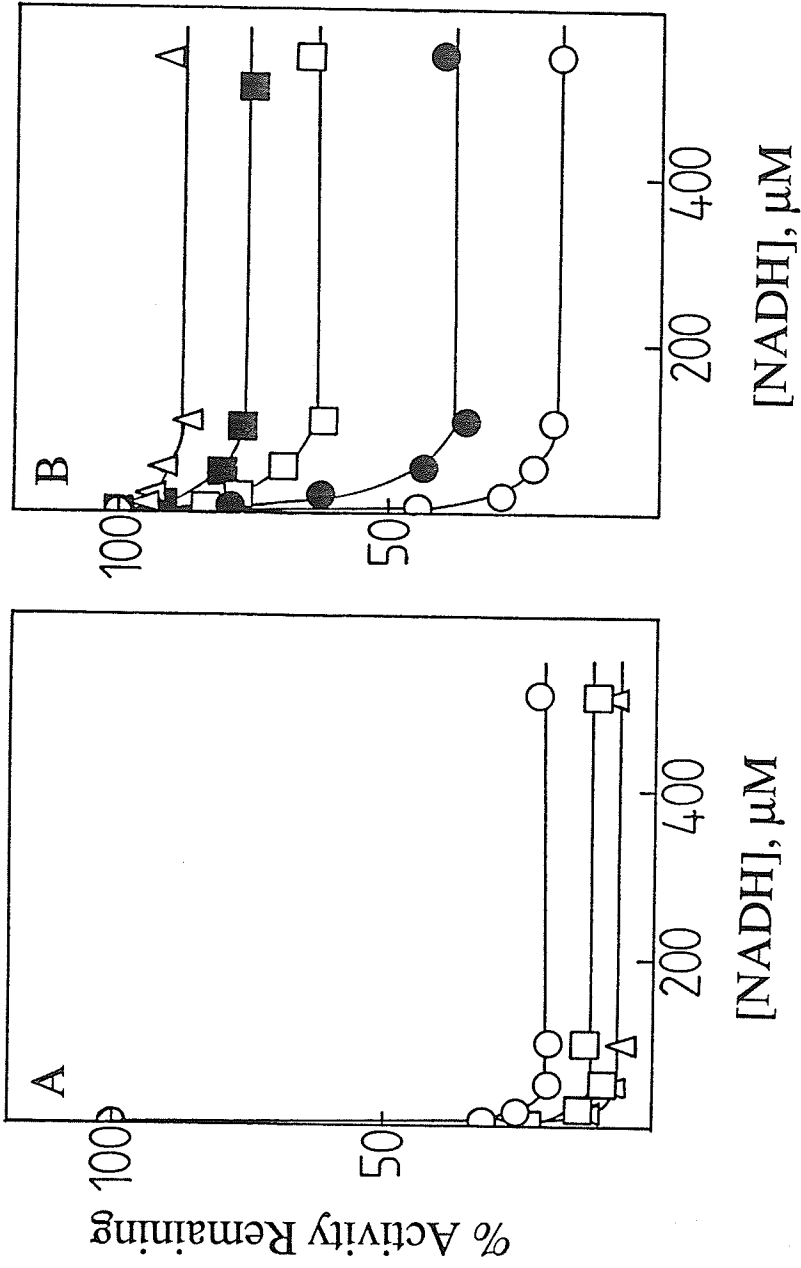


Figure 35. Effect of oxaloacetate concentration on NADH saturation curves for wild type citrate synthase (A) and CS319R→L (B). Concentrations of oxaloacetate were 0.02mM (O), 0.04mM (●), 0.08mM (□), 0.10mM (■) and 0.16mM (Δ).

Table 19. Steady State Kinetic Parameters for Wild Type Citrate Synthase and Mutant CS319R→L.

Parameter	Wild Type		CS319R→L	
	no KCl	0.1M KCl	no KCl	0.1M KCl
$k_{cat}$ , sec <sup>-1</sup>	44±5	81±6	23±5	48±3
$K_{AcCoA}$ , μM	750±200	120±20	190±60	25±4
$K_{OAA}$ , μM	11±6	26±5	72±24	4.4±1.0
$K_{iOAA}$ , μM	36±11	33±7	52±12	5.1±2.4
$K_{i, \alpha-KG}$ , μM	93±18		390±70	
KCl Activation Ratio <sup>a</sup>	39±3		3.67±0.08	
$K_M^a$ , KCl, mM	28±4		4.4±0.7	
$K_i$ , NADH, μM	3.3±0.1		75±19	
Maximum % Inhibition by NADH	99±1		25±6 <sup>c</sup>	

<sup>a</sup> KCl activation data, expressed as increases in reaction rate as a function of [KCl], were fitted to the Michaelis-Menten equation by the GENLSS program (See Methods section). Parameters quoted are  $K_M$  (the apparent Michaelis constant for KCl) and "Activation Ratio", the ratio of the limiting catalytic rate at saturating KCl to the rate obtained without KCl. All measurements were in Tris buffer, pH 7.8, with oxaloacetate and acetyl-CoA each at 0.1 mM. Data at [KCl] up to 100 mM were used, because of inhibition at concentrations higher than this.

<sup>b</sup> For the method of calculation and the significance of the errors see the Methods section.

<sup>c</sup> Varies with oxaloacetate concentration (see Figure 35, and text).

The mutant enzyme is only activated 3.7-fold by addition of 0.1M KCl, in contrast to 39-fold for the wild type enzyme. This point is clearly illustrated in Figure 36, which shows the effect of increasing KCl concentrations on the specific activities of the Arg-319 mutant and the wild type enzyme, at the standard substrate concentrations of 0.1mM each. At these non-saturating substrate concentrations, the turnover number ( $k_{cat}$ ) observed at saturating concentrations of KCl is higher for the mutant than for the wild type enzyme. The converse is observed at saturating substrate concentrations and 0.1M KCl (Table 19), where the  $k_{cat}$  value for CS319<sup>R→L</sup> is lower than the corresponding wild type value. Therefore in the presence of 0.1M KCl, CS319<sup>R→L</sup> has a higher turnover number at low substrate concentrations than the wild type enzyme, presumably because it also has a higher affinity for both substrates. At saturating substrate concentrations, however, the wild type enzyme turns over substrates to products more quickly than the Arg-319 mutant.

Some of these kinetic parameters have also been measured in the absence of KCl (Table 19). For the wild type enzyme, 0.1M KCl causes a doubling of the turnover number and about a 7.5-fold decrease in the  $K_M$  for acetyl-CoA. The same effects were observed for CS319<sup>R→L</sup>. While the increased ionic strength has little or no effect on the  $K_M$  for oxaloacetate ( $K_{OAA}$ ) or its dissociation constant ( $K_{iOAA}$ ) for wild type citrate synthase, both these parameters showed substantial decreases in the presence of 0.1M KCl for CS319<sup>R→L</sup>; about 16 times for  $K_{OAA}$ , and about 10 times for  $K_{iOAA}$ . Since KCl shifts wild type *E. coli* citrate synthase from T to R state, and substantially improves the binding of acetyl-CoA, it appears that in the Arg-319 mutant the T↔R allosteric equilibrium is shifted towards R, the active state (Figure 37), since it already shows improved binding of both substrates and a lower KCl activation ratio. Note that in the Arg-319 mutant, KCl also appears to improve the binding of the other substrate, oxaloacetate.

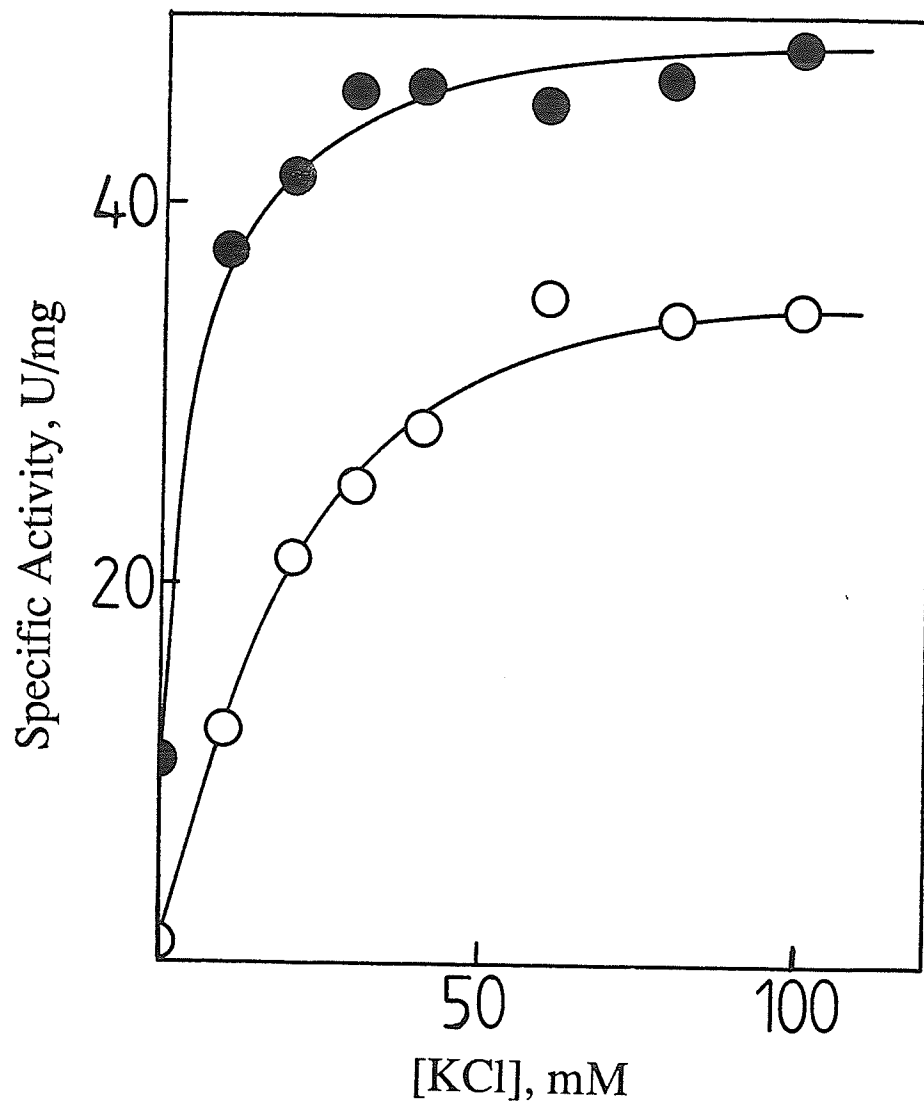


Figure 36. KCl saturation for wild type citrate synthase (O), and CS319<sup>R→L</sup> (●).

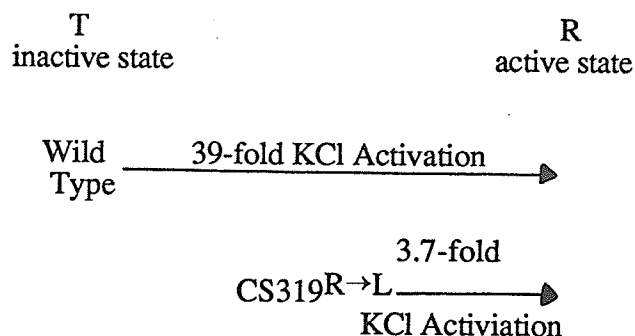


Figure 37. CS319<sup>R→L</sup> appears to have its allosteric equilibrium shifted towards R state.

Several methods were used to try to show that CS319<sup>R→L</sup> had in fact adopted a different conformational state, distinct from that of the wild type protein. Since the absorption spectrum and fluorescence emission spectrum of the wild type enzyme are different in the presence and absence of 0.1M KCl, the corresponding spectra were measured for the Arg-319 mutant. The mutant was found to have the same properties as the wild type. Modification of wild type citrate synthase with DTNB has also been shown to vary in the presence and absence of 0.1M KCl (Talgoy & Duckworth, 1979; Talgoy *et al.*, 1979). At a molar ratio of about five DTNB molecules to one enzyme subunit, approximately one sulfhydryl group on each enzyme subunit was modified (Talgoy & Duckworth, 1979). In the presence of 0.1M KCl, the modification reaction proceeds much more quickly than in its absence. CS319<sup>R→L</sup> was modified with DTNB (in 5-fold excess), both in the presence and absence of 0.1M KCl, and showed the same effects as the wild type enzyme. Circular dichroism spectra of *E. coli* citrate synthase are unaffected by KCl, and again were the same for both enzymes. The amount of enzyme activity remaining after incubation of both the wild type (Figure 34A) and CS319<sup>R→L</sup> enzymes for one hour in urea solutions of increasing concentration gave the same results; and addition of 0.5mM NADH or 0.1M KCl had the same effects for both the mutant and the wild type enzymes.

Measurements of Ligand Binding by ANS Displacement:

Like the wild type enzyme, CS319<sup>R→L</sup> showed a saturable decrease in the fluorescence of ANS-citrate synthase mixtures upon addition of acetyl-CoA and coenzyme A, from which  $L_{0.5}$  values were calculated (Table 20). Each enzyme showed a decrease in its respective  $L_{0.5}$  value in the presence of 0.1M KCl. Oxaloacetate (0.2mM) also decreased the  $L_{0.5}$  value for coenzyme A, in both ANS-citrate synthase mixtures, but the combination of oxaloacetate and KCl, only caused a further decrease in the wild type enzyme; for CS319<sup>R→L</sup>, this combination increases the  $L_{0.5}$  parameter. Although oxaloacetate alone did not cause a substantial decrease in the fluorescence of ANS-wild type enzyme mixtures, an  $L_{0.5}$  value with a large uncertainty was obtained (Table 20). Mixtures of ANS and the Arg-319 enzyme give much lower  $L_{0.5}$  values when titrated with oxaloacetate than the corresponding wild type value (Table 20). This is not surprising in light of the increased affinity of this mutant for oxaloacetate, already demonstrated by the steady state kinetic studies above. Also shown in Table 20, are the indirect effects of 0.5mM coenzyme A on the  $L_{0.5}$  values of oxaloacetate. The combination of coenzyme A and oxaloacetate decreased the  $L_{0.5}$  value for oxaloacetate alone, but again, while KCl caused a further decrease in  $L_{0.5}$  value for ANS-citrate synthase mixtures of the wild type enzyme, it had the opposite effect on that of CS319<sup>R→L</sup>.

From the indirect effect of oxaloacetate on coenzyme A binding, oxaloacetate saturation of the wild type enzyme and the Arg-319 mutant were measured, in the presence and absence of  $\alpha$ -ketoglutarate. The apparent dissociation constants for oxaloacetate and  $\alpha$ -ketoglutarate, measured in the presence of 0.2mM coenzyme A, could then be determined (Table 20). This ANS-displacement method shows an increased dissociation constant for  $\alpha$ -ketoglutarate in the Arg-319 mutant compared to that of the wild type enzyme, similar to what was observed in the steady state kinetic studies.

Table 20. Parameters for Ligand Binding to Wild Type Citrate Synthase and Mutant CS319<sup>R→L</sup> as Measured by ANS-Displacement.

Parameter	Wild Type		CS319 <sup>R→L</sup>	
	no KCl	0.1M KCl	no KCl	0.1M KCl
L <sub>0.5</sub> , AcCoA, μM	260±40 <sup>a</sup> (* <sup>b</sup> )	60±3 (0.64)	100±20 (0.48)	91±5 (0.38)
L <sub>0.5</sub> , CoA, μM	270±40 (* <sup>b</sup> )	53±3 (0.57)	135±9 (0.57)	93±3 (0.41)
L <sub>0.5</sub> , CoA, μM <sup>c</sup>	73±3 (0.78)	47±5 (0.38)	35±2 (0.49)	130±10 (0.46)
K <sub>D</sub> , OAA, μM <sup>d</sup>	25±1 (0.54)	ND <sup>e</sup>	14±1 (0.41)	ND
K <sub>D</sub> , α-KG, μM <sup>f</sup>	76±11	ND	770±70	ND
L <sub>0.5</sub> , OAA, μM	850±450 (0.22)	490±80 (0.87)	33±2 (0.64)	4.4±0.2 (0.41)
L <sub>0.5</sub> , OAA, μM <sup>g</sup>	42±2 (0.49)	24±2 (0.17)	5.0±0.3 (0.41)	6.2±0.9 (0.10)

<sup>a</sup> For the method of calculation and the significance of the errors see the Methods section.

<sup>b</sup> Quantities in brackets are the fractions of initial fluorescence of ANS-citrate synthase complex quenched by saturating amounts of ligand; in all cases the uncertainties are no more than ±0.05.

\* Fraction of initial fluorescence quenched at saturation could not be estimated precisely by curve-fitting, and so was taken to fall somewhere between the maximum observed and the maximum possible, making the uncertainty in the L<sub>0.5</sub> values quite large.

<sup>c</sup> Measured in the presence of 0.2mM oxaloacetate.

<sup>d</sup> Measured in the presence of 0.2mM coenzyme A.

<sup>e</sup> ND = not determined.

<sup>f</sup> Measured in the presence of 0.2mM coenzyme A; calculated from the effect on K<sub>D</sub> for oxaloacetate.

<sup>g</sup> Measured in the presence of 0.5mM coenzyme A.

## **DISCUSSION**

## Active Site Mutants

## CS $\Delta$ (264–287)

The 24 amino acids deleted in CS $\Delta$ (264–287) are predicted (from the model of *E. coli* citrate synthase), to correspond to all of the N helix, the N–O corner and a few residues of the O helix (Figure 22). In addition, the remainder of the O helix may well be distorted to compensate for the 24 missing amino acids, thus reducing the  $\alpha$ -helical secondary structure of the mutant even further. Using circular dichroism, the deletion mutant was found to contain about 9% less  $\alpha$ -helical content than the wild type protein, a number which indicates that the mutant has also lost the remaining  $\alpha$ -helical structure of the O helix. In addition, it seems probable that the dimeric contact surface of CS $\Delta$ (264–287) has remained intact, since sedimentation equilibrium measurements show the mutant to have a similar quaternary structure to the wild type enzyme. The M helix is one of the helices involved in the dimeric contact surface, and is very close to the region deleted in CS $\Delta$ (264–287) (Figure 22). Thus, in order for the mutant to maintain its basic tertiary structure at the dimeric contact surface, the rest of the O helix and the random coil between the O and P helices must be distorted. The amino acid residues between the O and P helices are involved in binding citrate (or oxaloacetate) (His–305) and CoA (Lys–309), and also form the adenine recognition loop (Arg–299, Leu–300, Met–301, Gly–302, Phe–303 and Gly–304) (see Table 1 in the Introduction). Since this region makes major contributions to the active site, any distortion of its tertiary structure would seriously affect the ability of the enzyme to bind acetyl-CoA and catalyze the condensation reaction. Further, among the 24 amino acid residues deleted from CS $\Delta$ (264–287) is His–264, a residue believed to be vitally involved in catalysis (Figure 7). Given this information, it is not unexpected that the mutant protein was inactive.

In spite of its inactivity, CS $\Delta$ (264–287) could, however, be purified by the method used for the wild type enzyme, using an immunological method to assay

fractions. The preparations, though not completely pure, were still suitable for the experiments which were performed. The deletion mutant  $CS\Delta(264-287)$  was created to obtain a mutant in which the active site had been destroyed, but the allosteric NADH binding site remained intact. Such a mutant would provide information about the binding of ligands to the NADH site, without the possibility of heterotropic interactions, observed when the active and allosteric sites compete for the same ligand. As expected, NADH binding was retained in this mutant, and the  $K_D$  values obtained for this process were actually smaller (that is, the binding was tighter) than those measured with the wild type enzyme (Figure 24). The number of binding sites was low, possibly because of the greater, and perhaps less organized, aggregation of the subunits of the deletion protein, which could have the result of "burying" binding sites. Still, the number of sites did increase as pH was lowered, in a manner qualitatively like the effect on the wild type enzyme. This binding was also weakened by KCl or acetyl-CoA, just as is the case with the wild type enzyme.

The fact that acetyl-CoA inhibits NADH binding is most readily explained by assuming that acetyl-CoA binds at the allosteric site, since the deletion almost certainly would destroy normal binding at the active site. To confirm this, the method of ANS displacement was used to measure the effects of KCl and oxaloacetate on coenzyme A binding to  $CS\Delta(264-287)$ . The interaction of ANS with this protein was different from that with the wild type, in that 0.1M KCl increased the fluorescence of the complex by about 25%, whereas it decreased the fluorescence of the wild type complex by about 50% (Figure 26). This difference, which must have arisen from rearrangements in the protein as a result of the deletion, was not really a complication, since changes in fluorescence could still be measured and used to monitor ligand binding. Acetyl-CoA or coenzyme A displaced very little ANS from the deletion protein, and this weak effect was not enhanced by oxaloacetate (Figure 26). The ability of coenzyme A binding to improve in the presence of oxaloacetate, in the wild type protein (Table 6), is an

indication that this binding occurs at the active site. Because coenzyme A binding to CS $\Delta$ (264–287) was unresponsive to oxaloacetate, it appears that coenzyme A derivatives do not bind to the damaged active site of this mutant, and the small amount of ANS displacement from the deletion mutant can be attributed to binding of these derivatives at the allosteric NADH binding site. Binding of acetyl–CoA to the NADH site could allow this ligand to activate acetyl–CoA binding at the active site, as ADP–ribose, 5'–AMP, and NADPH seem to do (Talgoy & Duckworth, 1979). Such an effect would contribute to the sigmoid saturation of *E. coli* citrate synthase which acetyl–CoA shows at low salt concentration (Faloona & Sreere, 1969).

## CS226H→Q and CS229H→Q

These two mutations were chosen because the two histidines are conserved in all seven citrate synthases whose sequences are known. Further, in the pig heart enzyme His-238 (the equivalent of *E. coli* His-229) is directly involved in the binding of citrate, and probably oxaloacetate, to the active site, while His-235 (the equivalent of *E. coli* His-226) forms a "reverse charge relay system" through a water molecule with a vital catalytic residue, Asp-375 (the pig heart equivalent of *E. coli* Asp-362) (Remington *et al.*, 1982). His-226 and His-229 of *E. coli* citrate synthase have each been changed to glutamine because this amino acid has been found to play a partial role in binding as an alternative to histidine. In one study, for instance, it was found that replacing His-48 in *Bacillus stearothermophilus* tyrosyl-tRNA synthetase by glutamine increased  $K_M$  for ATP by a factor of 13 and decreased  $k_{cat}$  to 7% of the wild type value. If asparagine was introduced at this position instead, little or no change in the kinetics was found (Lowe *et al.*, 1985). Refinement of the pig heart citrate synthase structure has led Wiegand and Remington (1986) to conclude that His-238 forms either a hydrogen bond or an ion pair with a carboxylate anion of citrate and oxaloacetate, while they make no further speculation about the role of His-235. In view of the high degree of amino acid sequence homology between the *E. coli* and pig heart sequences, particularly around the active site, similar roles should be played by His-229 and His-226 in the *E. coli* enzyme.

Although almost all the kinetic parameters in Table 4 were changed to some extent by the mutations in CS226H→Q and CS229H→Q, the only large effects were on constants which measure the affinity of the enzyme for oxaloacetate and  $\alpha$ -ketoglutarate. In the case of CS226H→Q, the estimated value for  $K_{iOAA}$ , which is interpreted as the dissociation constant for the binary enzyme-oxaloacetate complex, was four times that for the wild type enzyme, while the  $K_{i,\alpha-KG}$  for  $\alpha$ -ketoglutarate

inhibition was nine times that for the wild type—the binding strengths for the two  $\alpha$ -keto acids both decreased. With CS229<sup>H→Q</sup>, the  $K_{iOAA}$  was more than 50 times that for wild type. No  $\alpha$ -ketoglutarate inhibition was detected for this mutant (Figure 29), but if  $K_{i,\alpha-KG}$  for this inhibition increased in proportion, the value would be about 5mM, well above the lower limit of 2mM which was estimated for this parameter (Table 4).

These kinetic measurements were confirmed in large part by static measurements made with the citrate synthase-ANS complex (Table 6). The  $K_D$  values for oxaloacetate reported in Table 6 are not strictly comparable to the  $K_{iOAA}$  values in Table 4, since those in Table 6 were determined from the ability of oxaloacetate to enhance the binding of coenzyme A and therefore were measured in the presence of 0.2mM coenzyme A. Binding of oxaloacetate or  $\alpha$ -ketoglutarate to CS229<sup>H→Q</sup> was too weak to measure by this method, but even this result shows that the binding of the  $\alpha$ -keto acids to this mutant is very weak, as expected from the kinetic data.

In the kinetic equation for the Ordered Bisubstrate mechanism (see Methods), the second order rate constant for formation of the catalytically productive enzyme-oxaloacetate complex,  $k_1$ , is given by  $k_{cat}/K_{OAA}$ , while the rate constant for the dissociation of this complex,  $k_2$ , is given by  $(k_{cat} \cdot K_{iOAA})/K_{OAA}$  (Cleland, 1963). These values have been calculated for the wild type and mutant enzymes, and are given in Table 21. These calculations have rather large errors, but they suggest that the CS226<sup>H→Q</sup> mutant binds oxaloacetate less strongly than wild type enzyme because the complex forms at a normal rate but dissociates more easily. More striking, the CS229<sup>H→Q</sup> mutant forms the enzyme-oxaloacetate complex far more slowly than the wild type and CS226<sup>H→Q</sup> enzymes do. The very weak binding of oxaloacetate to CS229<sup>H→Q</sup>, relative to the wild type and CS226<sup>H→Q</sup> enzymes (see  $K_{iOAA}$  values in Table 4), would appear to arise entirely from the low rate of formation of this complex. These findings are consistent with the conclusion of the crystallographic studies on pig

heart citrate synthase, that His-238 (the equivalent of His-229 in the *E. coli* enzyme) is directly involved in oxaloacetate binding, but that His-235 (the equivalent of *E. coli* His-226) is farther removed from the active site, interacting indirectly through a water molecule.

Table 21. Association ( $k_1$ ) and dissociation ( $k_2$ ) constants for oxaloacetate binding to wild type and mutant forms of citrate synthase.

Parameter	Wild Type	CS226 <sup>H→Q</sup>	CS229 <sup>H→Q</sup>
$k_1, M^{-1} s^{-1}$	$(3.1 \pm 0.6^a) \times 10^6$	$(5.8 \pm 4.5) \times 10^6$	$(0.020 \pm 0.013) \times 10^6$
$k_2, s^{-1}$	$100 \pm 30$	$810 \pm 650$	$36 \pm 25$

<sup>a</sup> Uncertainties were calculated according to Shoemaker and Garland (1962).

In the wild type enzyme, a bound water molecule appears to be polarized by His-226, and also interacts with Asp-362, which is in van der Waals' contact with a carboxyl group of citrate, and probably oxaloacetate. In this system, a water molecule is used to relay the positive charge from His-226 to Asp-362, and thereby helps oxaloacetate to assume the correct orientation by maintaining the general integrity of the active site (Remington *et al.*, 1982). Thus CS226<sup>H→Q</sup>, which lacks the interaction between the positively charged His-226 side chain and water, which in turn may make the enzyme less structured at the active site, could be expected to show a somewhat poorer affinity for oxaloacetate, as is observed. The binding of  $\alpha$ -ketoglutarate is even more strongly affected by this mutation than that of oxaloacetate, presumably because  $\alpha$ -ketoglutarate is even more poorly accommodated by the slight rearrangements at the active site.

Mutation of histidine to glutamine in CS229<sup>H→Q</sup> had a profound effect on  $\alpha$ -keto acid binding; the rate of formation of the complex with oxaloacetate was slower by 2 orders of magnitude (Table 21), and binding of  $\alpha$ -ketoglutarate was not detectable at all (Figure 29). Removal of one of the normal points of attachment of oxaloacetate in the active site might also be expected to affect the catalytic rate to some extent, since the full distortion of substrate in the direction of the transition state should be harder than usual, and indeed a 10-fold decrease in  $k_{\text{cat}}$  was measured with CS229<sup>H→Q</sup> (Table 4).

The principal reason for making and studying these two mutants was to test whether factors which weaken oxaloacetate binding would weaken binding of the inhibitor  $\alpha$ -ketoglutarate in a parallel fashion. This is clearly the case, and therefore it seems that  $\alpha$ -ketoglutarate exerts its inhibition on *E. coli* citrate synthase not through a specific allosteric site but by a special kind of interaction at the active site. Its binding to the active site can occur only in the absence of KCl (which desensitizes the enzyme to  $\alpha$ -ketoglutarate) (Wright *et al.*, 1967), presumably because KCl induces a conformational adjustment at the active site which makes the site discriminate among  $\alpha$ -keto acids more precisely. This adjustment would also be the reason why KCl substantially activates *E. coli* citrate synthase (Table 4).

## CS305<sup>H→A</sup> and CS314<sup>R→L</sup>

The *E. coli* citrate synthase mutations CS305<sup>H→A</sup> and CS314<sup>R→L</sup> were chosen because the equivalent positively charged residues in pig heart citrate synthase have been implicated in the polarization of the carbonyl group of oxaloacetate. The carbon-13 NMR (Kurz *et al.*, 1985) and infra-red (Kurz & Drysdale, 1987) spectra of oxaloacetate bound in the active site of pig heart citrate synthase indicate that the bond order of the carbonyl group of oxaloacetate is substantially reduced when this substrate is bound to the enzyme. The crystal structure of pig heart citrate synthase shows His-320 hydrogen bonded to the carbonyl oxygen of oxaloacetate in an ideal position to protonate the oxygen as the condensation reaction occurs (Wiegand & Remington, 1986). Also hydrogen bonded to the equivalent oxygen atom of citrate is Arg-329, so that it could likewise play a role in polarization. Both of these active site residues have also been shown to form hydrogen bonds with carboxylate groups in citrate, and probably oxaloacetate (Remington *et al.*, 1982), so that they may also be important in oxaloacetate binding. His-320 hydrogen bonds with the carboxylate oxygen of citrate, designated O-1 (that is, the same oxygen which His-238 interacts with), and Arg-329 forms an important hydrogen bond or salt bridge with O-5 (Figure 9A). Both of these residues are absolutely conserved in all citrate synthases sequenced to date. In *E. coli* citrate synthase, the corresponding residues are His-305 and Arg-314. Each of these residues has been mutated separately, His-305 to alanine, and Arg-314 to leucine, to verify that the same roles are being played in the *E. coli* enzyme.

A similar mutagenesis experiment was done by Handford *et al.* (1988) to confirm the role of Asp-362 of *E. coli* citrate synthase, whose homologous pig heart residue (Asp-375) is believed to be vital in the formation of a mixed anhydride intermediate during the break down of citryl-CoA to form citrate and CoA (see Introduction). The mutant enzyme contained a glycine in place of Asp-362, and was

still able to bind NADH and oxaloacetate as the wild type enzyme. The mutant did, however, possess an activity less than 2% of the wild type value, which was found to be due to the mutant enzyme's poorer affinity for acetyl-CoA and reduced ability to catalyze the condensation reaction.

Under conditions selective for an active citrate synthase gene, in the *gltA*-*E. coli* host strain MOB154, the two plasmids encoding mutant citrate synthases, CS305<sup>H→A</sup> and CS314<sup>R→L</sup>, showed different effects on cell growth. The plasmid encoding CS305<sup>H→A</sup> sustained cell growth at a rate much less than the wild type plasmid, while that encoding CS314<sup>R→L</sup> did not support growth of this citrate synthase defective cell line at all. The ability of CS305<sup>H→A</sup> to supplement MOB154 cells with citrate synthase activity sufficient for cell propagation, while CS314<sup>R→L</sup> did not, may be because of the somewhat higher turnover number ( $k_{cat}$ ) measured for CS305<sup>H→A</sup> (Table 7). Thus CS314<sup>R→L</sup>, whose turnover number is only about 60% as large as that for CS305<sup>H→A</sup>, is inadequate to supply the minimum cellular requirements for citrate synthase in the MOB154 cell line, while CS305<sup>H→A</sup> may barely be adequate to provide for the cell's needs.

As mentioned previously, kinetic measurements for the His-305 and Arg-314 mutants were run with blanks, in which oxaloacetate was omitted from the reaction, since their extremely low specific activities required very large quantities of enzyme to obtain measurable activities, particularly in the absence of KCl. Although both mutants showed similar affinities for the two substrates in the presence of 0.1M KCl (Table 7), the activity of CS305<sup>H→A</sup> could not be measured in the absence of KCl unless the substrate concentrations were increased above the standard 0.1mM each. At substrate concentrations of 0.35mM acetyl-CoA and 0.40mM oxaloacetate, the KCl activation ratio for CS305<sup>H→A</sup> is much greater than for the corresponding wild type enzyme (Table 7). Since CS314<sup>R→L</sup> does not show an increased KCl activation ratio, and the substrate affinities in the presence of 0.1M KCl are the same for both mutants, the

binding of substrates to CS305<sup>H→A</sup> seems to be more dependent on KCl than in the Arg-314 mutant. It is possible, therefore, that KCl tightens up the active site of both mutants, as well as the wild type enzyme, but that in the absence of KCl the His-305 mutant has a much less structured active site than the Arg-314 mutant and wild type citrate synthase, so that KCl has more of an activating effect.

Table 22. Kinetic parameters for wild type citrate synthase and two active site mutants, CS305<sup>H→A</sup> and CS314<sup>R→L</sup>.

Parameter	Wild Type	CS305 <sup>H→A</sup>	CS314 <sup>R→L</sup>
$k_1, M^{-1}s^{-1}$	$(3.1 \pm 0.6^c) \times 10^6$	$\geq (9.8 \pm 4.7) \times 10^2$	$(5.9 \pm 2.5) \times 10^2$
$k_2, s^{-1}$	$100 \pm 30$	$\geq 0.93 \pm 0.55$	$0.30 \pm 0.27$
$k_3^a, M^{-1}s^{-1}$	$(6.8 \pm 1.2) \times 10^5$	$(1.6 \pm 1.0) \times 10^3$	$(1.2 \pm 0.8) \times 10^3$
$\Delta G_{OAA}^b$ kcal mole <sup>-1</sup>	—	$\geq -4.7 \pm 2.4$	$-5.0 \pm 2.3$

<sup>a</sup>  $k_3 = (k_{cat}/K_{AcCoA}) \cdot (1 + k_4/k_5)$ ; assuming  $k_5 \gg k_4$ ,  $k_3 = k_{cat}/K_{AcCoA}$ .

<sup>b</sup>  $\Delta G_{OAA} = RT \cdot \ln \{ (k_{cat}/K_{OAA})_{mutant} / (k_{cat}/K_{OAA})_{wild\ type} \}$ .

<sup>c</sup> Uncertainties were calculated according to Shoemaker and Garland (1962).

The association ( $k_1$ ) and dissociation ( $k_2$ ) constants for the enzyme-oxaloacetate complex have been calculated for these two mutants (Table 22). In addition, if the dissociation constant for the product CoA ( $k_5$ ) is assumed to be much larger than the dissociation constant for acetyl-CoA ( $k_4$ ), then the association constant for acetyl-CoA ( $k_3$ ) can also be calculated. Oxaloacetate associates with these mutant enzymes about 3000 and 5000 times more slowly for the His-305 and Arg-314 mutants, respectively. Their respective dissociation constants for the enzyme-oxaloacetate complex are also

lower than the wild type value, but only by factors of about 100 and 300. Similarly, the association constant for acetyl-CoA to these citrate synthase mutants is about 400 times lower for CS305<sup>H→A</sup> and about 600 times lower for CS314<sup>R→L</sup>. The lower association constants for acetyl-CoA to the mutants may be the reason for the reduced ability of acetyl-CoA and CoA to displace ANS from ANS-citrate synthase complexes. Of these three results, by far the largest single factor which would contribute to the minute  $k_{\text{cat}}$  values measured for these two citrate synthase mutants appears to be the extremely low rate of formation of the enzyme-oxaloacetate complex. Of course, the fact that His-305 and Arg-314 are probably involved in the formation of the transition state, since they are believed to polarize the carbonyl group of oxaloacetate making it more susceptible to attack by the enol form of acetyl-CoA (Figure 38, Panel A), would also manifest itself as a reduced  $k_{\text{cat}}$  value in mutants which lack these polarizing groups. Figure 38A shows a closeup view of the active site of *E. coli* citrate synthase during the first stage of catalysis and clearly illustrates the importance of various side chains in the binding of oxaloacetate and catalysis.

The contributions ( $\Delta G$ ) of the missing amino acid side chains in these two mutants to the binding energy of the enzyme-transition state complexes may be calculated by comparing  $k_{\text{cat}}/K_M$  for the mutant and wild type enzymes (Wilkinson *et al.*, 1983).  $\Delta G_{\text{OAA}}$  values have been calculated for each of the His-305 and Arg-314 mutants, and are shown in Table 22. These  $\Delta G$  values are negative due to the loss of a favorable interaction between the enzyme and oxaloacetate, upon deletion of each of these side chains. The size of the  $\Delta G$  value is an indication of the nature of the interaction between the enzyme and the substrate. If the deleted side chain formed a hydrogen bond with an uncharged group on oxaloacetate, and was only important in binding the substrate, a  $\Delta G$  value of 0.5-1.5 kcal mole<sup>-1</sup> would be expected (Fersht *et al.*, 1985). If, however, the missing side chain had formed a hydrogen bond with oxaloacetate involving a charged group, a significantly larger  $\Delta G$  value of 3.5-4.5 kcal

mole<sup>-1</sup> would be typical. The magnitude of the  $\Delta G$  values in Table 22 is even larger than this value, suggesting that not only do charged forms of His-305 and Arg-314 normally form hydrogen bonds with oxaloacetate, but that they are also important in helping to form the transition state. This agrees with the X-ray data for the homologous pig heart citrate synthase residues and their proposed roles (Remington *et al.*, 1982; Wiegand & Remington, 1986).

Other differences between CS305<sup>H→A</sup> and CS314<sup>R→L</sup> which should be noted are the dissociation constants for oxaloacetate ( $K_{iOAA}$ ) and  $\alpha$ -ketoglutarate ( $K_{i,\alpha-KG}$ ) (Table 7). CS314<sup>R→L</sup> has a higher dissociation constant for oxaloacetate, but the same dissociation constant for  $\alpha$ -ketoglutarate, compared to wild type citrate synthase. CS305<sup>H→A</sup> shows reduced affinity for both these  $\alpha$ -keto acids, but the effect on  $\alpha$ -ketoglutarate binding is much smaller than that on the binding of oxaloacetate. Note that both Arg-314 and His-305, as well as interacting with the carbonyl oxygen, also are involved in hydrogen bonding two separate carboxyl groups of oxaloacetate: His-305 forms a hydrogen bond with the 4-carboxyl group of oxaloacetate, while Arg-314 hydrogen bonds to its 1-carboxyl group (Figure 38A). The parallel loss of affinity for oxaloacetate and  $\alpha$ -ketoglutarate previously shown by CS229<sup>H→Q</sup> (His-229 hydrogen bonds to the 4-carboxyl group of oxaloacetate), suggests that both these  $\alpha$ -keto acids are bound in much the same way in this region of the active site. Since His-305 interacts with the same carboxyl group as His-229, a mutant lacking His-305 may be expected to show reduced affinity for both oxaloacetate and  $\alpha$ -ketoglutarate, just as CS229<sup>H→Q</sup> did.  $\alpha$ -Ketoglutarate may well fit into the active site in place of oxaloacetate as shown in Figure 38, Panel B. It would therefore allow analogous interactions between its 5-carboxyl group and Arg-407' (from the second subunit), His-229 and His-305, similar to those found between these same amino acid side chains and the 4-carboxyl group of oxaloacetate. However, the additional  $-\text{CH}_2-$  group located in the middle of the  $\alpha$ -ketoglutarate molecule, would likely move the

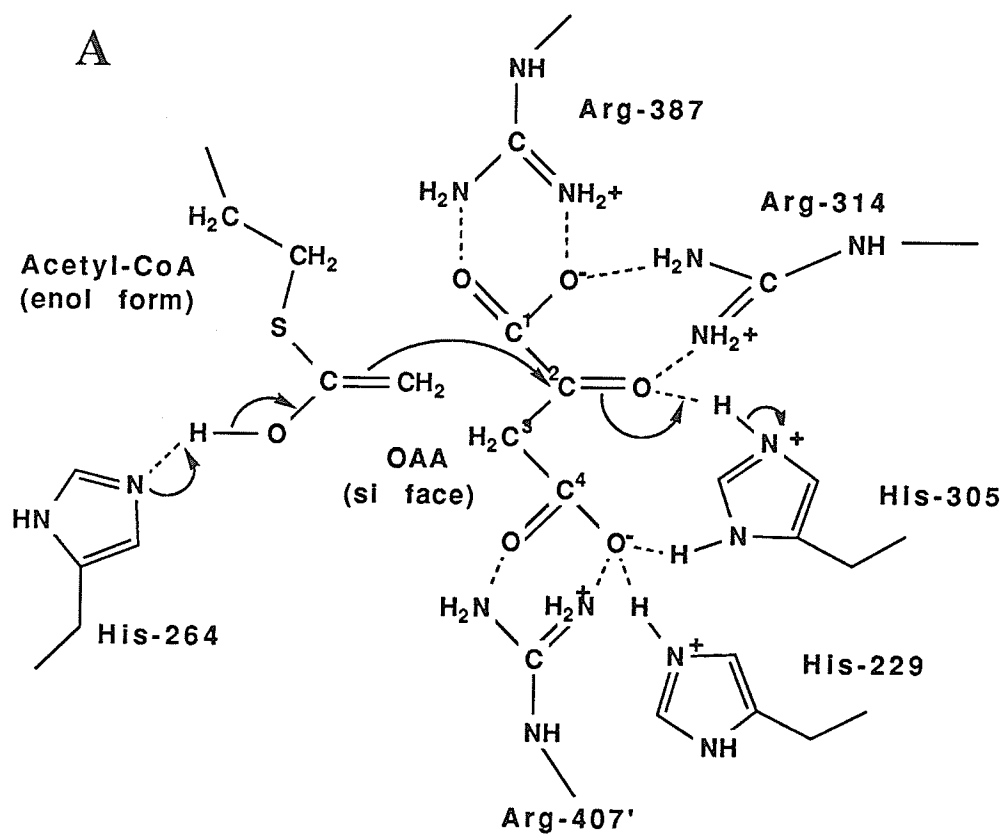
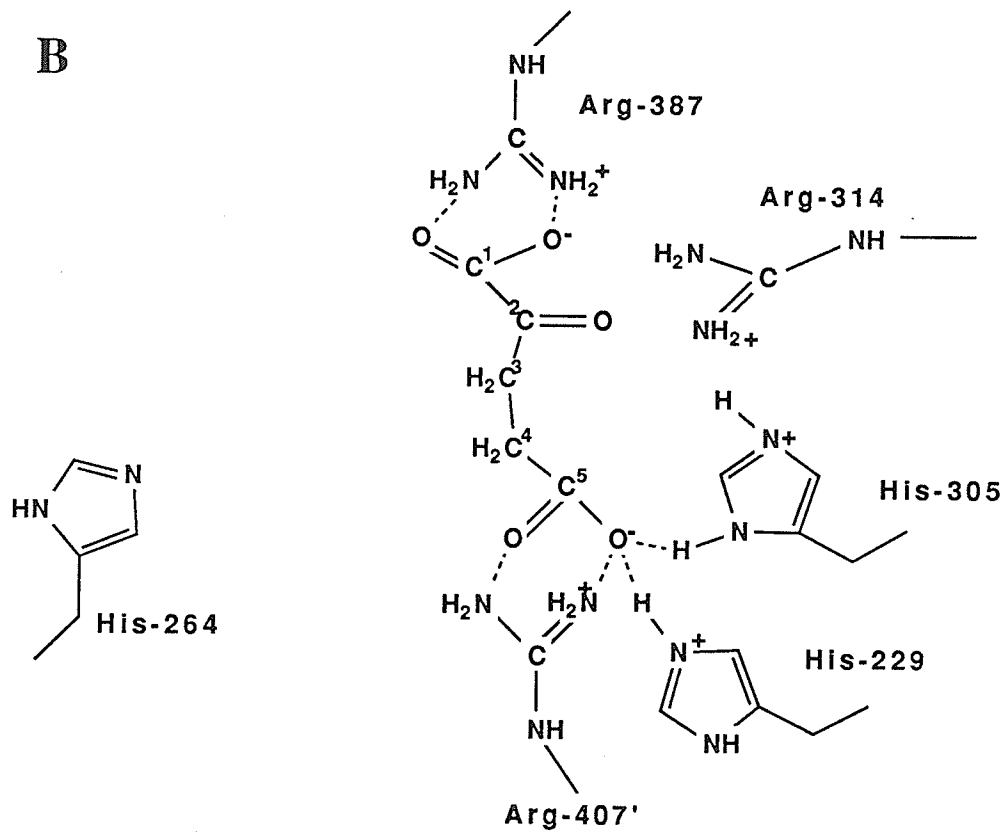


Figure 38. Active site of *E. coli* citrate synthase, A) showing the residues involved in binding oxaloacetate (OAA) and initiating the formation of the transition state.



B) Active site of *E. coli* citrate synthase, showing how  $\alpha$ -ketoglutarate may fit into the active site in place of oxaloacetate. See text for discussion of important features.

1-carboxyl group away from Arg-314, which form hydrogen bonds with the corresponding 1-carboxyl group in oxaloacetate (Figure 38). This would explain why  $\alpha$ -ketoglutarate binding was unaffected by the Arg-314 mutation and showed only a small change for the His-305 mutation. Note in Figure 38B, that the carbonyl group of  $\alpha$ -ketoglutarate is too far away to interact significantly with those groups which polarize the carbonyl of oxaloacetate (His-305 and Arg-314), which may explain why this inhibitor is not a substrate for citrate synthase (Srere, 1972).

To confirm the importance of His-305 and Arg-314 of *E. coli* citrate synthase in the polarization of the carbonyl group of oxaloacetate, Linda Kurz's research group at Washington University School of Medicine in St. Louis Missouri, will be measuring the carbon-13 NMR spectra of wild type *E. coli* citrate synthase, CS305<sup>H→A</sup> and CS314<sup>R→L</sup> with oxaloacetate, in the presence and absence of the acetyl-CoA enolate analogue, carboxymethyl-CoA. Similar measurements with pig heart citrate synthase indicate some carbonyl polarization in the enzyme-oxaloacetate complex, but with the addition of carboxymethyl-CoA, the chemical shift of the carbonyl carbon indicates a much stronger polarization of the carbonyl bond or protonation of the carbonyl oxygen (Kurz *et al.*, 1985). Comparison of the analogous carbon-13 NMR spectra of wild type *E. coli* citrate synthase with that for the His-305 and Arg-314 mutants, should confirm the importance of these active site residues in the polarization of the carbonyl of oxaloacetate.

## Attempts to Locate the NADH Binding Site

## CS188R→L, CS217R→L, CS221R→L and CS217R→L/221R→L

Chemical modification of one cysteine per subunit of *E. coli* citrate synthase by DTNB has been shown to abolish allosteric inhibition by NADH, but cause only a small loss of enzyme activity (Danson & Weitzman, 1973). More recently the fluorescent alkylating agent, monobromobimane has been found to produce the same effects (Duckworth *et al.*, 1987). The bimane labelled peptide has been isolated and sequenced, and the modified residue was found to be Cys-206. Since various adenylic acid derivatives, including NADH, all partially protect this cysteine from modification, it has been suggested that Cys-206 is at or near the NADH binding site itself (Talgoy & Duckworth, 1979). Unfortunately, the absence of any direct three-dimensional information about a citrate synthase enzyme which is NADH-sensitive, has hindered the search for the NADH binding site in the *E. coli* enzyme.

Three-dimensional information about interactions between various dehydrogenase enzymes and NAD have shown an arginine residue to be involved in nucleotide binding (Eklund *et al.*, 1976a, 1976b; Birktoft *et al.*, 1982), although this has not always been found to be the case (Biesecker *et al.*, 1977). In examples where an arginine residue is involved in nucleotide binding, it forms an ion pair interaction with the pyrophosphate portion of NAD.

The three-dimensional model of one subunit of *E. coli* citrate synthase places Cys-206 some distance from the active site, in a region containing little sequence homology with the pig heart enzyme. The *E. coli* enzyme contains three arginines very close to Cys-206: Arg-188, Arg-217 and Arg-221 (Figures 30 and 39). Each of these arginines has been mutated to leucine individually, to remove the positive charge from the amino acid side chain. Since Arg-217 and Arg-221 are located on the same face of the K helix separated by one  $\alpha$ -helical turn, a double mutant which has both Arg-217

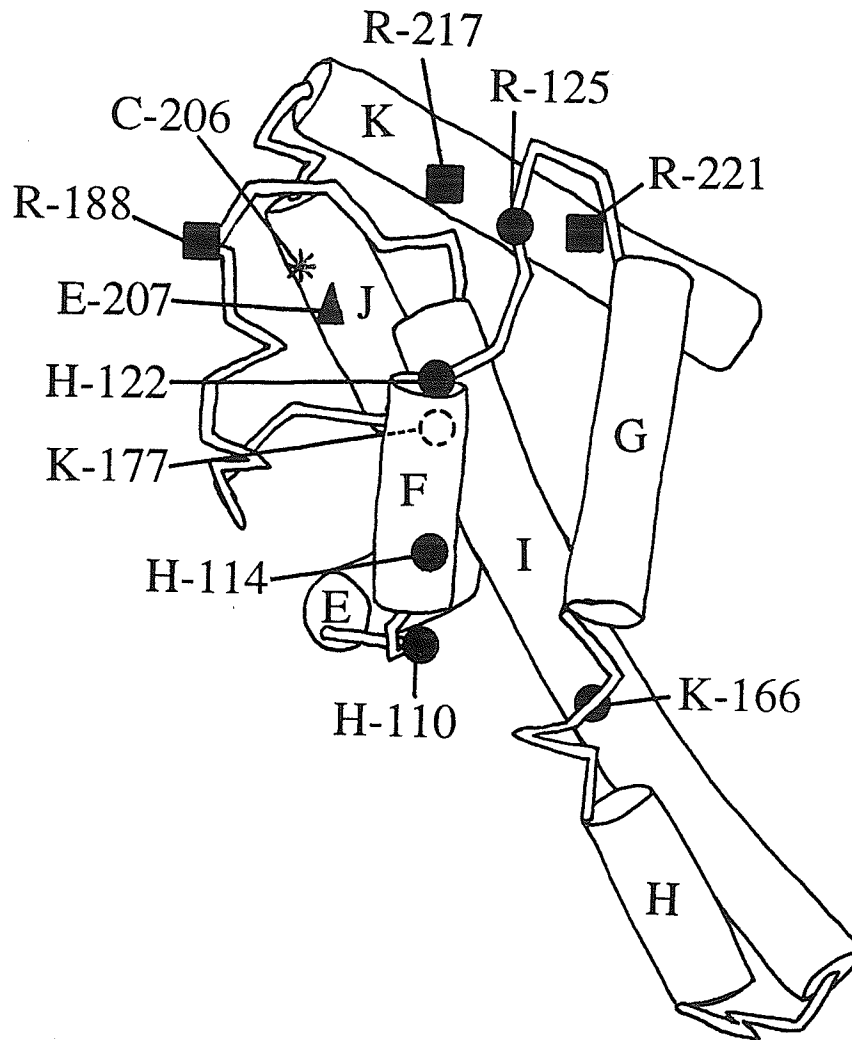


Figure 39. Region of *E. coli* citrate synthase model near Cys-206 (\*), showing the location of amino acid residues potentially involved in NADH binding. The three arginine residues already mutated: Arg (R)-188, Arg-217, and Arg-221 are indicated by "■". The other positively charged residues in this region: Arg-125, Lys (K)-167, His-110, His-114, and His-122 are shown as "●", except Lys-177 which is concealed in the diagram behind helix F on helix I, and is shown as "○". A negatively charged residue, Glu (E)-207, thought to form a hydrogen bond with the 2'-hydroxyl group of the ribose of NADH, is shown as "▲".

and Arg-221 changed to leucine was also prepared, to exclude the possibility that one residue could simply substitute for the other. In spite of the fact that these three arginine residues are conserved in the 3 bacterial citrate synthases which are also sensitive to NADH inhibition (except Arg-217, whose homologous residue is lysine in *P. aeruginosa*) (Table 23), their mutation had no effect on the ability of NADH to bind to these mutants (Table 11), or inhibit enzyme activity (Table 10).

Although none of the three arginines mutated appear to be involved in NADH binding, there are several other positively charged residues in the vicinity of Cys-206 which may form an ion pair with the pyrophosphate portion of NADH (Table 23). Three histidine residues are included in this table, since they can be positively charged, depending on the pH of the local environment. This fact makes a histidine residue particularly attractive for this role, since NADH binding shows some dependence on pH (Figure 24; Duckworth & Tong, 1976). The locations of all of these residues are shown in Figure 39. Although the sequences of the three citrate synthases from the Gram-negative bacteria are very homologous around Cys-206, they do not share this homology with the pig heart enzyme, on which the *E. coli* citrate synthase model was based (Figure 8). For this reason, the locations of the amino acid residues in Figure 39 may not be precisely as shown. The diagram does, however, provide information about residues which have the potential to be important in NADH binding.

Table 23 shows the amino acid residues in each of the citrate synthase sequences, in the homologous positions to those for the *E. coli* enzyme. It seems feasible that any residue involved in binding NADH should be conserved in all enzymes which are sensitive to NADH inhibition; this includes the three Gram-negative bacterial citrate synthases. Therefore, His-122 in *E. coli* citrate synthase would probably not be particularly well-suited for a role in NADH binding, since it is not conserved in either the *A. anitratum* or *P. aeruginosa* sequences (Table 23). One can only speculate as to whether or not a residue involved in NADH binding would be maintained in sequences

Table 23. Homology between amino acid residues potentially involved in NADH binding, near Cys-206 of *E. coli* citrate synthase and the corresponding sequences of the six other citrate synthases.

Enzyme	Residues involved in mutagenesis experiments	Positively charged residues potentially involved in NADH binding	d
NADH-sensitive			
<i>E. coli</i> <sup>a</sup>	R-188 R-217 R-221	R-125 K-167 K-177 H-110 H-114 H-122	E-207
<i>A. anitratum</i> <sup>a</sup>	R R R	R K K H H N	D
<i>P. aeruginosa</i> <sup>a</sup>	R K R	R K K H H N	E
<i>R. prowazekii</i> <sup>b</sup>	D K K	C K K H N Q	T
NADH-insensitive			
pig heart <sup>c</sup>	A E L	P K R R P D	Q
yeast 1 <sup>c</sup>	S D L	P K R R P D	D
yeast 2 <sup>c</sup>	E D L	P K R R P D	D

<sup>a</sup> Gram-negative bacteria

<sup>b</sup> Parasitic bacterium

<sup>c</sup> Eukaryotic

<sup>d</sup> Acidic side chain which may form a hydrogen bond with the 2'-hydroxyl of the adenine ribose of NADH.

of enzymes which are not sensitive to NADH. Lys-167 is identical in all seven sequences, while Lys-177 and His-110 of *E. coli* citrate synthase have identical residues in the three other bacteria (including *R. prowazekii*), and arginines in the eukaryotic sequences. Intuitively, it would seem that enzymes which are not sensitive to NADH, should not be expected to maintain amino acid residues homologous to those involved in NADH binding. Therefore, Arg-125 and His-114 of *E. coli* citrate synthase would be the most suitable choices for future mutagenesis experiments in the effort to locate the allosteric NADH binding site, because only the three NADH-sensitive enzymes have identical residues at these positions, with no analogous residues in the corresponding positions of the NADH-insensitive enzymes.

A comparison of a portion of the *E. coli* citrate synthase sequence with five nucleotide binding regions from five proteins of known sequence and structure is shown in Figure 40. The "known structures" are of the NAD binding regions of glyceraldehyde-3-phosphate dehydrogenase (GPDH), lactate dehydrogenase (LDH) and alcohol dehydrogenase (ADH), and the FAD binding regions of glutathione reductase (GR) and *p*-hydroxybenzote hydroxylase (PHB) (Sternberg & Taylor, 1984). These five sequences all contain the sequence Gly-X-Gly-X-X-Gly (where X is any amino acid residue) (Figure 40). The role of these glycine residues has been described by Wierenga and Hol (1983). The first glycine of this sequence is required for the binding of the ribose group to the enzyme because it allows an acidic residue (as will be discussed shortly) to interact with the ribose group of the nucleotide. The second glycine enables the close approach of the negatively charged pyrophosphate group to the positively charged N-terminus of the dipole created by the  $\alpha$ -helix (Hol *et al.*, 1978), while both the first and third glycines enable the chain to make a sharp turn between  $\beta$ -strand 1 and the  $\alpha$ -helix (Figure 40). A second important feature is the presence of a conserved acidic side chain (Asp(D) or Glu(E)), which forms a hydrogen bond with the 2'-hydroxyl of the adenine ribose (Sternberg & Taylor, 1984).



Although the *E. coli* citrate synthase sequence does not contain the precise Gly-X-Gly-X-X-Gly sequence, it does have the sequence Gly-X-Pro-X-X-X-Pro shortly before Cys-206, a potential marker for the NADH binding site (Figure 40). Interestingly, the acidic amino acid residue, located a short distance from these Gly- (or Pro-)rich sequences, is conserved in the *E. coli* sequence (Figure 40), and also in the other NADH-sensitive citrate synthases (Table 23) (as well as both yeast sequences). Thus, Gly-207 of *E. coli* citrate synthase may hydrogen bond with the 2'-hydroxyl on the ribose (of NADH), as analogous acidic side chains of the other nucleotide binding enzymes were found to do. This possibility could be tested by mutating Glu-207 to an uncharged residue like alanine, and studying the resulting mutants' ability to bind NADH. In addition, since the first glycine of the conserved Gly-rich sequence is also present in the *E. coli* citrate synthase sequence as well as the acidic amino acid residue, it is tempting to speculate that the *E. coli* enzyme may bind the ribose group like these other nucleotide binding enzymes, with a glycine allowing an acidic side chain to hydrogen bond with the 2'-hydroxyl group of ribose. The fact that two proline residues are found in the *E. coli* sequence, at positions nearly corresponding to the glycines in the sequences of the "known structures", indicates that they may be important for the maintenance of a secondary structure which allows the binding of the ribose, since, like glycine, they are considered to be helix breaking amino acid residues. However, in the "known structures" the second glycine is also required to allow the interaction between the negatively charged pyrophosphate group of the nucleotide and the positively charged N-terminus of the dipole created by the  $\alpha$ -helix (Hol *et al.*, 1978), so that in *E. coli* citrate synthase, where the homologous residue is proline, this interaction is unlikely.

The absence of any three-dimensional information about NADH-sensitive citrate synthases specifically, makes further experiments aimed at locating the allosteric NADH binding site difficult to plan; unless, of course, a mutation is made which has a specific

detrimental effect on NADH binding. If the NADH binding site is formed upon association of three-dimers into a hexamer, the model of a single subunit of *E. coli* citrate synthase currently available provides only a fraction of the potential amino acid residues which may be involved in nucleotide binding. Extension of the model to a dimer may improve some aspects of citrate synthase study, such as examination of the active site (since the active site has contributions from both subunits of the dimer), but unless information becomes available about how the three-dimers fit together to form a hexamer, characterization of the allosteric NADH binding site of *E. coli* citrate synthase will be an arduous task.

Mutants which Affect the Allosteric Equilibrium  
of *E. coli* Citrate Synthase

## CS260W → A

Allosteric citrate synthases, like *E. coli*, have a conserved tryptophan residue in the homologous position to the alanine residue conserved in non-allosteric citrate synthases. Since the allosteric and non-allosteric enzymes have very similar sequences around these tryptophan and alanine residues (Figure 31), it was thought that this single amino acid difference might be important in giving these enzymes their distinct properties; therefore, Trp-260 of *E. coli* citrate synthase was mutated to alanine. More recently, the sequence of the non-allosteric *R. prowazekii* enzyme has also been determined, and unlike the other non-allosteric citrate synthases, it has a tryptophan residue in the corresponding position (Figure 31). As noted in the Introduction, although the citrate synthase of *R. prowazekii* is non-allosteric, like its eukaryotic counterparts, its amino acid sequence is far more homologous to the allosteric Gram-negative class of enzymes. For this reason, Wood *et al.* (1987) have suggested that comparison of this unusual enzyme with the *E. coli* and pig heart enzymes may establish the location and extent of changes required to convert one class of citrate synthases to the other. Given this new sequence information, Trp-260 of the *E. coli* enzyme by itself could not be sufficient to confer allosteric properties on a given citrate synthase enzyme, rather, it may be one of several residues which act together to give the enzyme its allosteric nature.

Trp-260 of *E. coli* citrate synthase is located on the M helix, one of the four helices (F, G, and L are the others) involved in intersubunit contacts between monomers in the formation of a dimer (Figure 32). Figure 41 is a stereodiagram of the model of *E. coli* citrate synthase (from the bottom looking up with respect to the view in Figure 32). The four helices which form the dimeric contact surface are shown at the top of this diagram, looking down the axis of the helices F, G, M and L. The side chain of

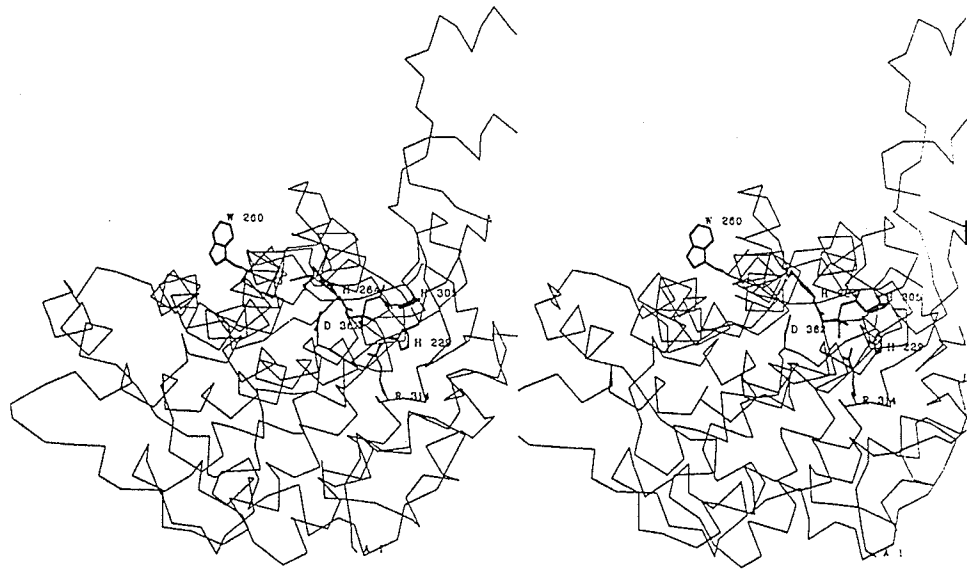


Figure 41. Stereodiagram of the model of *E. coli* citrate synthase, showing the projection of Trp-260 into the dimeric contact surface. The view is from "the bottom" as compared to the standard view of the model shown previously.

Trp-260 is also shown in this figure, projecting from the dimeric contact surface of this subunit into the region where the second subunit of the dimer would be—the helix F interacting with F', G with G', M with M', and L with L' (where ' indicates the second subunit). Trp-260 is also very close to the catalytically important active site residue His-264 (Figures 32 and 41). Given its proximity to these two essential regions of the enzyme, mutation of Trp-260 to alanine could be expected to have diverse effects on the properties of the enzyme.

Two forms of the Trp-260 mutant enzyme were prepared, using slightly different purification procedures (see Results), yielding an enzyme form which had lost about half its sensitivity to NADH inhibition, CS260<sup>W→A(I)</sup>, and a form which retains full sensitivity to NADH inhibition, CS260<sup>W→A(S)</sup> (Table 14). As discussed in Results, some difficulties were encountered in obtaining the CS260<sup>W→A(S)</sup> form; in fact, only one such preparation successfully retained full sensitivity to NADH inhibition, despite several attempts to repeat the method. In view of this fact, and considering that addition of crude extract was able to restore NADH sensitivity to samples of the NADH-insensitive CS260<sup>W→A(I)</sup> (Table 13), this one sensitive preparation, which was found to be about 80% pure, probably still contained a factor present in crude enzyme extracts which conferred complete NADH sensitivity on CS260<sup>W→A(I)</sup>. Identification of this factor may help to explain this unusual effect.

Although the kinetic inhibition by NADH was very different for these two mutant forms, both forms bound that nucleotide normally, with one exception (Table 15). Unlike the case for wild type citrate synthase and CS260<sup>W→A(I)</sup>, as little as 10 $\mu$ M oxaloacetate reduced the fluorescence of the NADH-CS260<sup>W→A(S)</sup> mixture to less than that observed for NADH alone, that is, oxaloacetate seemed to cause CS260<sup>W→A(S)</sup> to quench the fluorescence of NADH in the mixture. No explanation could be found for this curious effect.

It is not surprising that the kinetic parameters for the two mutant enzyme forms are similar (Table 14) since they contain the same mutation. The variation in their turnover numbers and Michaelis constants may reflect slight rearrangements at the active site which probably took place during the two different purification procedures used. The standard method of citrate synthase purification uses a DEAE chromatography step, which subjects the enzyme to buffers containing high concentrations of KCl over a period of several days. In the presence of KCl, wild type enzyme undergoes a conformational shift to R state, causing rearrangements which seem to tighten up the active site (see Results; Anderson & Duckworth, 1988). In wild type citrate synthase, the interconversion between T and R state is totally reversible, so that in the absence of KCl, the enzyme returns to T state; this is evidenced by its hyperbolic saturation curve for NADH, and the effect of KCl on acetyl-CoA saturation curves (see Introduction). CS260<sup>W→A(I)</sup>, which was purified like the wild type enzyme, could be expected to show some of these same rearrangements upon addition of KCl, except where the mutation of Trp-260 to alanine prohibited them. It is possible though, since NADH can inhibit only about half the enzyme activity, that the rearrangements induced by KCl during purification may not be entirely normal and/or reversible in this case. Suppose that deletion of the large Trp-260 side chain has been compensated for in CS260<sup>W→A(I)</sup> by a conformational rearrangement, resulting in a higher  $k_{cat}$  value at the expense of the ability of the enzyme to bind both of the substrates, and this has left the enzyme unable to respond normally to bound NADH. CS260<sup>W→A(S)</sup>, on the other hand, which was not subjected to these high ionic strength buffers during purification, presumably did not undergo any compensatory rearrangements, which is why it had a lower  $k_{cat}$ , normal substrate affinities, and could be completely inhibited by NADH (Table 14). The adverse effects of KCl, particularly on the affinity of both mutant enzyme forms for oxaloacetate (observed in ANS displacement experiments for both mutant forms (Table 16), and in steady state kinetic data measured for

CS260<sup>W→A(I)</sup>, both in the presence and absence of 0.1M KCl (Table 17)), supports this theory.

## CS319R→L

Arg-319 is located on the P helix, a short distance from the active site (Figure 32). It is a positively charged residue, whose homologous residue in the three eukaryotic sequences is also arginine, and whose equivalent residue in the three other bacterial sequences is lysine. In order to determine the functional importance of this highly conserved positively charged side chain, Arg-319 of *E. coli* citrate synthase has been mutated to leucine.

CS319R→L binds NADH normally, except that the binding shows some inhibition by 0.1mM oxaloacetate (Table 18). This is consistent with the fact that the extent of NADH inhibition was found to be dependent upon the concentration of oxaloacetate present in the assay, and at 0.1mM oxaloacetate only about 25% inhibition by NADH was observed (Figure 35B).

In the presence of 0.1M KCl, the Arg-319 mutant shows a somewhat lower  $k_{cat}$  value than the wild type enzyme, but it has a higher affinity for both substrates (Table 19). In the absence of KCl, CS319R→L again has a lower  $k_{cat}$  and a substantially higher affinity for acetyl-CoA, but has a lower affinity for both oxaloacetate and  $\alpha$ -ketoglutarate than wild type citrate synthase.

The effects of KCl on substrate association and dissociation constants for wild type citrate synthase and CS319R→L have been calculated and are shown in Table 24. The association constant of oxaloacetate ( $k_1$ ) to the Arg-319 mutant is 3.5-fold higher than that to the wild type enzyme in the presence of 0.1M KCl, but in the absence of KCl, it is 12.5-fold lower. Once the enzyme-oxaloacetate complex is formed in the Arg-319 mutant enzyme, it dissociates ( $k_2$ ) more slowly than the complex involving the wild type enzyme, particularly in the absence of KCl. So the Arg-319 mutant seems to have more difficulty in orienting the oxaloacetate molecule in the active site in the absence of KCl than the wild type enzyme, but once oxaloacetate is bound to the

enzyme, it also has more difficulty leaving the active site. Both in the presence and absence of 0.1M KCl, acetyl-CoA associates ( $k_3$ ) more quickly to the enzyme-oxaloacetate complex in CS319<sup>R→L</sup> as compared to the wild type enzyme, and in general, seems to be far better at orienting itself in the active site of both enzymes in the presence of 0.1M KCl (Table 24). Moreover, addition of 0.1M KCl activates the Arg-319 mutant enzyme only 3.7-fold, compared to 39-fold for the wild type enzyme (Table 19); this is because the "baseline" value, in the absence of KCl, is already about 10-fold higher than for the wild type case (Figure 36).

Table 24. Effect of 0.1M KCl on kinetic parameters for wild type citrate synthase and mutant CS319<sup>R→L</sup>.

Parameter	Wild Type		CS319 <sup>R→L</sup>	
	no KCl	0.1M KCl	no KCl	0.1M KCl
$k_1, M^{-1}s^{-1}$	$(4.0 \pm 2.2^b) \times 10^6$	$(3.1 \pm 0.6) \times 10^6$	$(0.32 \pm 0.13) \times 10^6$	$(11 \pm 3) \times 10^6$
$k_2, s^{-1}$	$140 \pm 90$	$100 \pm 30$	$17 \pm 8$	$56 \pm 30$
$k_3^a, M^{-1}s^{-1}$	$(0.59 \pm 0.17) \times 10^5$	$(6.8 \pm 1.2) \times 10^5$	$(1.2 \pm 0.5) \times 10^5$	$(19 \pm 3) \times 10^5$

<sup>a</sup>  $k_3 = (k_{cat}/K_{AcCoA}) \cdot ((1 + k_4/k_5))$ ; assuming  $k_5 \gg k_4$ ,  $k_3 = k_{cat}/K_{AcCoA}$ .

<sup>b</sup> Uncertainties were calculated according to Shoemaker and Garland (1962).

These results indicate that the Arg-319 mutant is altered in the T↔R allosteric equilibrium, shifted towards R or active state. This shift is dramatic enough to allow oxaloacetate to have some effect on NADH binding, and in some way "decouples" the NADH binding from its inhibitory activity. Note that compared to wild type citrate synthase, CS319<sup>R→L</sup> has a poorer affinity for α-ketoglutarate, which is precisely what would be expected if a conformational shift towards R state had taken place, since R state is better able to discriminate between the true substrate, oxaloacetate and

$\alpha$ -ketoglutarate, a substrate analogue and competitive inhibitor of oxaloacetate (Anderson & Duckworth, 1988). Upon addition of KCl, which presumably makes the conformational change to R state more highly organized, the binding of oxaloacetate, as well as the second substrate acetyl-CoA, actually becomes tighter in the Arg-319 mutant than that observed in the wild type enzyme. The fact that in this mutant the substrates have Michaelis constants well below those for wild type enzyme, approaching values found for the non-allosteric pig heart enzyme (Johansson & Pettersson, 1974), shows that the active site of *E. coli* citrate synthase has all of the apparatus needed to bind both substrates effectively, and that the lower affinity of the wild type enzyme is not due to a lack of one or more particular groups. This suggestion had been made earlier (Ner *et al.*, 1983), on the basis of the fact that the *E. coli* enzyme is apparently missing a residue equivalent to Arg-46 of the pig heart enzyme, which is believed to make an acetyl-CoA binding contact in the crystalline form of this enzyme (Wiegand & Remington, 1986). As was pointed out in the Introduction, however, the *R. prowazekii* citrate synthase also lacks this homologous residue (as well as an Arg-164 equivalent), and yet shows the same high affinity as the pig heart enzyme for acetyl-CoA (Wood *et al.*, 1987).

Physical studies on CS319<sup>R→L</sup>, with comparisons to the wild type enzyme, have so far failed to show any useful probe for the allosteric state of the enzyme. KCl induces an ultraviolet light difference spectrum in wild type citrate synthase (Faloona & Srere, 1969), which might correlate with the transition from T to R state, but the same difference spectrum is obtained when KCl is added to the CS319<sup>R→L</sup> mutant, although the mutant is believed to be largely in R state already. Similarly, KCl slightly increases the reactivity of wild type citrate synthase towards DTNB (Talgoy *et al.*, 1979), but the same effect is found with the Arg-319 mutant. No difference has been found between wild type and CS319<sup>R→L</sup> citrate synthase in circular dichroism spectrum, tryptophan fluorescence spectrum, or sensitivity to urea denaturation, in the absence or presence of

KCl. Thus, the Arg-319 mutant allows us to eliminate certain KCl-dependent changes in physical properties as probes for conformational change, but the evidence for the conformational change itself remains simply the interpretation of ligand binding and substrate saturation curves.

In previous work, Weitzman and co-workers (Danson *et al.*, 1979) isolated a regulatory mutant of *E. coli* citrate synthase, whose kinetic properties were similar to those of CS319<sup>R→L</sup>, in that it showed an increased affinity for both substrates. The mutation leading to this change in properties has not been identified, and that mutant enzyme was not obtained completely pure, but it was established that the mutant had a lower molecular weight than the hexameric wild type enzyme, and was probably a dimer. Thus the loss of allostery, in that case, seems to have been the result of a substantial change in quaternary structure. CS319<sup>R→L</sup>, on the other hand, has the same molecular weight as wild type citrate synthase, and so its mutation must have a more subtle effect on the structure.

Removal of the positive charge of Arg-319 could lead to a conformational shift towards the active conformational state of the enzyme much in the same way as KCl affects this transition. Since addition of KCl to assay solutions shifts the enzyme into R state, it is almost certain that Arg-319 makes an ionic interaction, either attractive or repulsive, which helps to stabilize the T or inactive state. An attractive interaction, that is an ion pair or salt bridge, would be like those which Perutz (1970) has shown to be critical in stabilizing the deoxy or T state of hemoglobins. Similarly, Valdez *et al.* (1988) have found an analogous arginine residue in *Bacillus stearothermophilus* phosphofructokinase, except that it specifically stabilizes the R state of that enzyme. Mutation of this arginine residue to alanine resulted in an enzyme with a high affinity for its allosteric inhibitor, and a 2000-fold decrease in its substrate affinity.

Such an interaction, of course, requires a negative charge somewhere nearby. Careful examination of the model of an *E. coli* citrate synthase subunit has revealed that

Glu-343 is in a good position to interact with Arg-319, though, since the model does not provide information about the unknown differences between T and R states, it is not obvious how the interaction would stabilize the T state specifically. Figure 42 shows a close-up view of the interaction between Arg-319 (on the P helix), and Glu-343 (on the Q helix). To confirm this interaction, the glutamate could be mutated (to remove its negative charge) instead of the arginine, to see if the resulting mutant showed properties similar to those of CS319<sup>R→L</sup>. If this was in fact the case, further confirmation would be provided by the exchange of arginine and glutamate residues by mutating Arg-319 to glutamate, and Glu-343 to arginine.

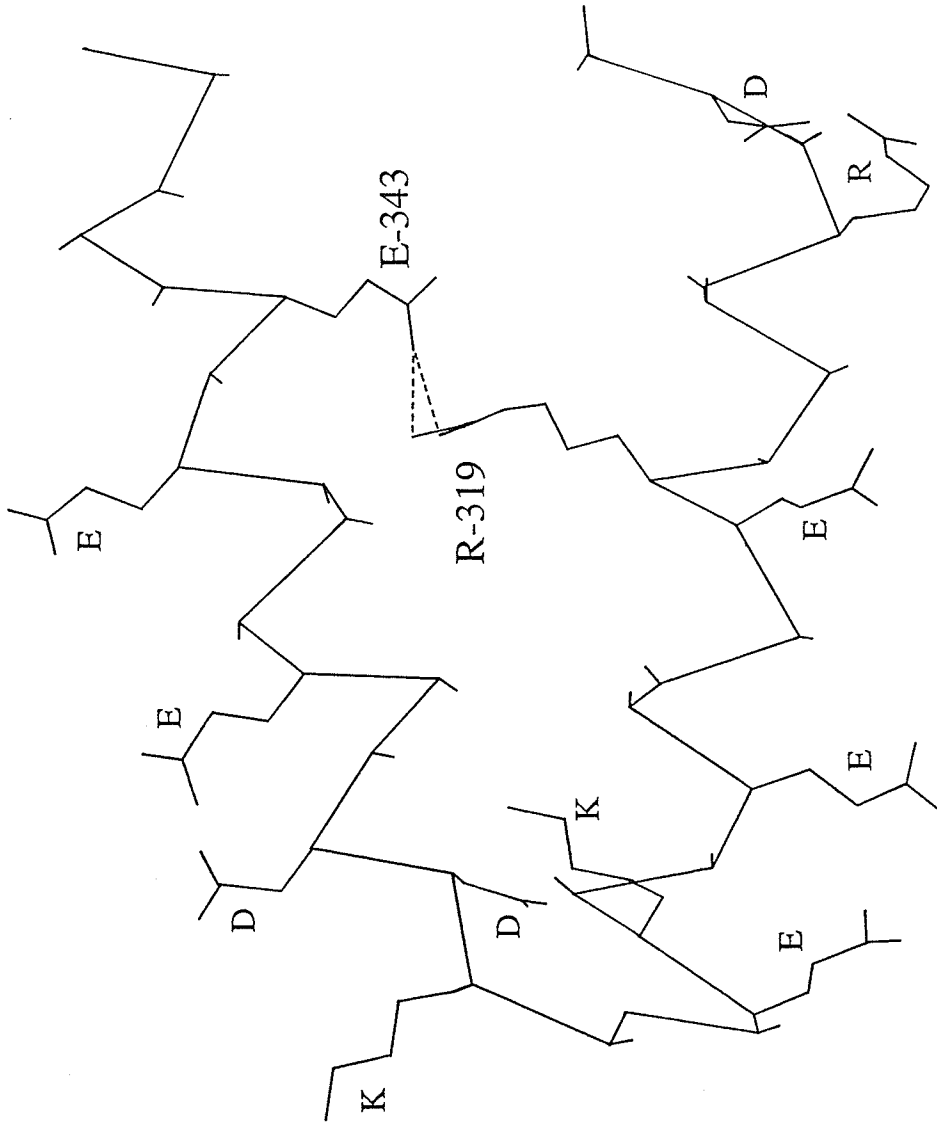


Figure 42. Close-up view of the interaction between R-319 and E-343 in the *E. coli* citrate synthase model. All positively and negatively charged side chains in this region are also shown (R = Arg, E = Glu, K = Lys, and D = Asp). The remaining side chains are those of hydrophobic residues and have not been included for the sake of clarity.

## Conclusions

In these experiments *in vitro* mutagenesis techniques are used to manipulate the structure of the citrate synthase enzyme of *E. coli*, in order to determine the functions of various amino acid residues. Although no direct three-dimensional information is available for the *E. coli* citrate synthase enzyme, a model of one of its subunits has been constructed using the known X-ray structure of the pig heart enzyme and the sequence homology between the two enzymes. Mutations of active site residues of the *E. coli* enzyme (His-226, His-229, His-305 and Arg-314) have confirmed the predicted roles of residues which are homologous to those in the pig heart enzyme. The fact that analogous roles appear to be played by analogous amino acid residues is strong evidence for the idea that the individual subunits of the non-allosteric (pig heart) and allosteric (*E. coli*) citrate synthases are very similar. Mutation of non-active site residues, conserved between the two sequences, may also provide useful information about the relationship between the structure and function of a protein. In the case of Arg-319 of *E. coli* citrate synthase, mutation of this residue to leucine specifically destabilized the T state conformation of the enzyme, presumably by removing the charged interaction between Arg-319 and Glu-343.

The regions of the *E. coli* model with little sequence homology to the pig heart enzyme can also provide useful information about the structural features of the sequence which may be responsible for the different properties of the enzymes—in particular, the allosteric nature of *E. coli* citrate synthase, and the location of its NADH binding site. Examination of the sequences of the *E. coli* and pig heart enzymes, as well as those of other citrate synthases both allosteric and non-allosteric, led to the selection of several residues for mutagenesis. One residue which sequence comparisons have brought to light is Trp-260 of *E. coli* citrate synthase. This tryptophan residue is conserved in the allosteric class of citrate synthases and is also present in the *R. prowazekii* enzyme

sequence, in spite of the fact that the *R. prowazekii* enzyme is non-allosteric. Mutation of Trp-260 to alanine had effects on both enzyme activity and sensitivity to NADH inhibition. Thus, although it clearly cannot be the only residue involved in giving the *E. coli* enzyme its allosteric properties since it is also present in the non-allosteric *R. prowazekii* enzyme, it may be one of several residues which act together to give the enzyme its allosteric nature. Several arginine residues (Arg-188, Arg-217 and Arg-221) which are unique to the allosteric class of citrate synthases, are located very close to Cys-206, a possible marker for the NADH binding site, making them likely candidates for involvement in NADH binding. Mutation of these arginines had no effect on the ability of NADH to bind to these mutant enzymes, or inhibit enzyme activity; however, there are other residues in the region of Cys-206 which have yet to be investigated, and it is possible that one or more of these may be involved in binding NADH.

These experiments illustrate the power of oligonucleotide-directed *in vitro* mutagenesis for creating specific mutant enzymes, in order to manipulate the structure of proteins in a controlled way. It is the present day tool of protein chemists and enzymologists, and will be used to reveal the details of catalysis, and the conformational change associated with allosteric enzymes—limited only by the ingenuity of the experimentalist!

## **BIBLIOGRAPHY**

## BIBLIOGRAPHY

- Alam, T., D. Finkelstein & P. A. Srere (1982) *J. Biol. Chem.* **257**, 11181-11185
- Amarasingham, C. R. & B. D. Davis (1965) *J. Biol. Chem.* **240**, 3664-3668
- Amersham, "Oligonucleotide-directed *in vitro* mutagenesis system" handbook (1987), pp. 1-48
- Anderson, D. H. & H. W. Duckworth (1988) *J. Biol. Chem.* **263**, 2163-2169
- Bell, A. W., V. Bhayana & H. W. Duckworth (1983) *Biochemistry* **22**, 3400-3405
- Bhayana, V. & H. W. Duckworth (1984) *Biochemistry* **23**, 2900-2905
- Biesecker, G. & A. J. Wonacott (1977) *Biochem. Soc. Trans.* **5**, 647-652
- Birktoft, J. J., R. T. Fernley, R. A. Bradshaw & L. J. Banaszak (1982) *Proc. Natl. Acad. Sci., USA* **79**, 6166-6170
- Birnboim, H. C. & J. Doly (1979) *Nucl. Acids Res.* **7**, 1513-1523
- Bloxham, D. P., D. C. Parmelee, S. Kumar, R. D. Wade, L. H. Ericsson, H. Neurath, K. A. Walsh & K. Titani (1981) *Proc. Natl. Acad. Sci., USA* **78**, 5381-5385
- Bloxham, D. P., D. C. Parmelee, S. Kumar, K. A. Walsh & K. Titani (1982) *Biochemistry* **21**, 2028-2036
- Buehner, M., G. C. Ford, D. Moras, K. W. Olsen & M. G. Rossmann (1975) In: *The Enzymes*, Vol. 11A, 191-292
- Buehner, M., G. C. Ford, D. Moras, K. W. Olsen & M. G. Rossmann (1976) *J. Mol. Biol.* **102**, 27-59
- Carter, P., H. Bedouelle & G. Winter (1985) *Nucl. Acids Res.* **13**, 4431-4443
- Chen, Y. H., J. T. Yang & H. M. Martinez (1972) *Biochemistry* **11**, 4120-4131
- Cleland, W. W. (1963) *Biochim. Biophys. Acta* **67**, 104-137
- Danson, M. J. & P. D. J. Weitzman (1973) *Biochem. J.* **135**, 513-524
- Danson, M. J., S. Harford & P. D. J. Weitzman (1979) *Eur. J. Biochem.* **101**, 515-521

- Detar, D. F. (1972) *Comput. Programs Chem.* **4**, 71-123
- Donald, L. J. & H. W. Duckworth (1987) *Biochem. Cell Biol.* **65**, 930-938
- Duckworth, H. W., D. H. Anderson, A. W. Bell, L. J. Donald, A. L. Chu & G. D. Brayer (1987) *Biochem. Soc. Symp.* **54**, 83-92
- Duckworth, H. W. & A. W. Bell (1982) *Can. J. Biochem.* **60**, 1143-1147
- Duckworth, M. L., M. J. Gait, P. Goelet, G. F. Hong, M. Singh & R. C. Timas (1981) *Nucl. Acids Res.* **9**, 1691-1706
- Duckworth, H. W. & E. K. Tong (1976) *Biochemistry* **15**, 108-114
- Eklund, H., C. -I. Brändén & H. Jörnvall (1976a) *J. Mol. Biol.* **102**, 61-73
- Eklund, H., B. Nordström, E. Zeppezauer, G. Söderlund, I. Ohlsson, T. Boiwe, B. -O. Söderberg, O. Tapia, C. -I. Brändén & Å. Åkeson (1976b) *J. Mol. Biol.* **102**, 27-59
- Fairbanks, G., T. L. Steck & D. F. H. Wallach (1971) *Biochemistry* **10**, 2606-2617
- Faloon, G. R. & P. A. Srere (1969) *Biochemistry* **8**, 4497-4503
- Fersht, A. R., J.-P. Shi, J. Knill-Jones, D.M. Lowe, A. J. Wilkinson, D. M. Blow, P. Brick, P. Carter, M. M. Y. Waye & G. Winter (1985) *Nature (London)* **314**, 235-238
- Guest, J. R. (1981) *J. Gen. Microbiol.* **124**, 17-23
- Handford, P. A., S. S. Ner, D. P. Bloxham & D. C. Wilton (1988) *Biochim. Biophys. Acta* **953**, 232-240
- Harmey, M. A. & W. Neupert (1979) *FEBS Lett.* **108**, 385-389
- Higa, A. I. & J. J. Cazzulo (1976) *Experientia* **32**, 1373-1374
- Hill, A. V. (1910) *J. Physiol. (London)* **40**, 190-224
- Hol., W. G. J., P. Th. Van Duijnen & H. J. C. Berendsen (1978) *Nature (London)* **273**, 443-446
- Holbrook, J. J., A. Liljas, S. J. Steindel & M. G. Rossmann (1975) in: "The Enzymes", vol 11A, 191-292

- Johansson, C. -J. & G. Pettersson (1974) *Eur. J. Biochem.* **46**, 5-11
- Juan, S. M., J. J. Cazzulo & E. L. Segura (1977) *J. Parasitol.* **63**, 921-922
- Koeller, W. & H. Kindl (1977) *Arch. Biochem. Biophys.* **181**, 236-248
- Kramer, W., K. Schughart & H. -J. Fritz (1982) *Nucl. Acids Res.* **10**, 6475-6485
- Krebs, H. A. & J. M. Lowenstein (1960) The tricarboxylic acid cycle. In *Metabolic Pathways*. Edited by D. M. Greenberg. New York: Academic Press Vol. 1, pp. 129-203
- Kunkel, T. A. (1985) *Proc. Natl. Acad. Sci., USA* **82**, 488-492
- Kurz, L. C., J. J. H. Ackerman & G. R. Drysdale (1985) *Biochemistry* **24**, 452-457
- Kurz, L. C. & G. R. Drysdale (1987) *Biochemistry* **26**, 2623-2627
- Laemmli, U. K. (1970) *Nature (London)* **227**, 680-685
- Lesk, A. M. & C. Chothia (1984) *J. Mol. Biol.* **174**, 175-191
- Lewin, Benjamin (1983) What is a Gene? A Biochemical View. In *Genes*. Edited by M. Dana. New York: John Wiley & Sons, p. 45
- Lill, U., A. Schreil, A. Henschen & H. Eggerer (1984) *Eur. J. Biochem.* **143**, 205-212
- Lowe, D. M., A. R. Fersht, A. J. Wilkinson, P. Carter & G. Winter (1985) *Biochemistry* **24**, 5106-5109
- Lowry, O. H., N. J. Rosebrough, A. L. Farr & R. J. Randall (1951) *J. Biol Chem.* **193**, 265-275
- Maniatis, T., E. F. Fritsch & J. Sambrook (1982) *Molecular Cloning: A Laboratory Manual*, Cold Spring Harbor Laboratory, Cold Spring Harbor, NY
- Massarini, E. & J. J. Cazzulo (1974) *FEBS Lett.* **39**, 252-254
- Massarini, E. & J. J. Cazzulo (1975) *FEBS Lett.* **57**, 134-138
- Messing, J. (1983) *Meth. Enzymol.* **101**, 20-78
- Monod, J., J. Wyman & J. P. Changeux (1965) *J. Mol. Biol.* **12**, 88-118
- Morse, D. & H. W. Duckworth (1980) *Can. J. Biochem.* **58**, 696-706

- Nakamaye, K. & F. Eckstein (1986) *Nucl. Acids Res.* **14**, 9679-9698
- Ner, S. S., V. Bhayana, A. W. Bell, I. G. Giles, H. W. Duckworth & D. P. Bloxham  
(1983) *Biochemistry* **22**, 5243-5249
- Ouchterlony, O. (1953) *Acta Path. Microbiol. Scand.* **32**, 231-236
- Perutz, M. F. (1970) *Nature (London)* **228**, 726-734
- Porter, J. S. & B. E. Wright (1977) *Arch. Biochem. Biophys.* **181**, 155-163
- Remington, S. J., G. Wiegand & R. Huber (1982) *J. Mol. Biol.* **158**, 111-152
- Rosenkrantz, M., T. Alam, K. -S. Kim, B. J. Clark, P. A. Srere & L. P. Guarente  
(1986) *Mol. Cell. Biol.* **6**, 4509-4515
- Sanchez-Pescador, R. & M. S. Urdea (1984) *DNA* **3**, 339-343
- Sanger, F., A. R. Coulson, B. G. Barrell, A. J. H. Smith & B. A. Roe (1981) *J. Mol.  
Biol.* **143**, 161-178
- Sanger, F., S. Nicklen & A. R. Coulson (1977) *Proc. Natl. Acad. Sci., USA* **74**,  
5463-5467
- Shoemaker, D. P., & C. W. Garland (1962) Treatment of Experimental Data,  
Propagation of Errors. In *Experiments in Physical Chemistry*. 2nd Ed.  
New York: McGraw-Hill, Inc., pp. 30-34
- Smith, M. (1985) *Ann. Rev. Genet.* **19**, 423-462
- Solomon, M. & P. D. J. Weitzman (1983) *FEBS Lett.* **155**, 157-160
- Srere, P. A. (1972) *Curr. Top. Cell. Regul.* **5**, 229-283
- Srere, P. A., H. Brazil & L. Gonen (1963) *Acta Chem. Scand.* **17**, S129-S134
- Sternberg, M. J. E. & W. R. Taylor (1984) *FEBS Lett.* **175**, 387-392
- Suissa, M., K. Suda & G. Schatz (1984) *EMBO J.* **3**, 1773-1781
- Talгой, M. M., A. W. Bell & H. W. Duckworth (1979) *Can. J. Biochem.* **57**,  
822-833
- Talгой, M. M. & H. W. Duckworth (1979) *Can. J. Biochem.* **57**, 385-395

- Tamarin, R. H. (1982) Mutation, DNA Repair and Recombination. In *Principles of Genetics*. Edited by R. S. van Leeuwen. Boston: Prindle, Weber and Schmidt, pp. 505-523
- Taylor, J.W., W. Schmidt, R. Cosstick, A. Okruszek & F. Eckstein (1985a) *Nucl. Acids Res.* **13**, 8749-8764
- Taylor, J.W., J. Ott, & F. Eckstein, (1985b) *Nucl. Acids Res.* **13**, 8764-8785
- Thieme, R., E. F. Pai, R. H. Schirmer & G. E. Schulz (1981) *J. Mol. Biol.* **152**, 763-782
- Tong, E. K. & H. W. Duckworth (1975) *Biochemistry* **14**, 235-241
- Valdez, B. C. , B. A. French, E. S. Youathan & S. H. Chang From: Abstracts of The FASEB Journal, Vol 2, Number 4, March 15 (1988), 72nd Annual Meeting, Abstract #1482
- Weijer, W. J. J. Hofsteenge, J. M. Vereijken, P. A. Jekel & J. J. Beinfema (1982) *Biochim. Biophys. Acta* **704**, 385-388
- Weitzman, P. D. J. (1966) *Biochim. Biophys. Acta* **128**, 213-215
- Weitzman, P. D. J. (1987) *Biochem. Soc. Symp.* **54**, 33-43
- Weitzman, P. D. J. & M. J. Danson (1976) *Curr. Top. Cell. Regul.* **10**, 161-204
- Weitzman, P. D. J. & P. Dunmore (1969) *FEBS Lett.* **3**, 265-267
- Weitzman, P. D. J. & D. Jones (1968) *Nature (London)* **219**, 270-272
- Wiegand, G. & S. J. Remington (1986) *Annu. Rev. Biophys. Biophys. Chem.* **15**, 97-117
- Wierenga, R. K. & W. G. J. Hol (1983) *Nature (London)* **302**, 842-844
- Wierenga, R. K., R. G. de Jong, K. H. Kalk, W. G. J. Hol & J. Drenth (1979) *J. Mol. Biol.* **131**, 55-73
- Wilkinson, A. J., A. R. Fersht, D. M. Blow & G. Winter (1983) *Biochemistry* **22**, 3581-3585

- Wood, D. O., L. R. Williamson, H. H. Winkler & D. C. Krause (1987) *J. Bacteriol.* **169**, 3564-3572
- Wright, J. A., P. Maeba & B. D. Sanwal (1967) *Biochem. Biophys. Res. Commun.* **29**, 34-38
- Wright, J. A. & B. D. Sanwal (1971) *J. Biol Chem.* **246**, 1689-1699
- Zoller, M. J. & M. Smith, (1982) *Nucl. Acids Res.* **10**, 6487-6500
- Zoller, M. J. & M. Smith, (1983) *Meth. Enzymol.* **100**, 468-500
- Zoller, M. J. & M. Smith, (1984) *DNA* **3**, 479-488